GJO 1635-1

110400-2-F

Final Report

MULTISPECTRAL PROCESSING OF ERTS-A (LANDSAT) DATA FOR URANIUM EXPLORATION IN THE WIND RIVER BASIN, WYOMING: A Visible Region Ratio to Enhance Surface Alteration Associated With Roll-Type Uranium Deposits

BETTE C. SALMON and WILLIAM W. PILLARS
Infrared and Optics Division

AUGUST 1975

Energy Research and Development Administration
P.O. Box 2567
Grand Junction, Colorado 81501
Contract No. AT (05-1)-1635
Technical Monitors: P. Dodd and D. Dahlem

ENVIRONMENTAL
RESEARCH INSTITUTE OF MICHIGAN
FORMERLY WILLOW RUN LABORATORIES, THE UNIVERSITY OF MICHIGAN
BOX 618 • ANN ARBOR • MICHIGAN 48107

TECHNICAL REPORT STANDARD TITLE PAGE

1. Report No.	2. Government Accession No.	3. Recipient's Catalog No.
110400-2-F		

4. Title and Subtitle	5. Report Date
MULTISPECTRAL PROCESSING OF ERTS-A (LANDSAT) DATA FOR URANIUM EXPLORATION IN THE WIND RIVER BASIN, WYOMING (A visible region ratio to enhance surface alteration associated with roll-type uranium deposits.)	July 1975
	6. Performing Organization Code

7. Author(s)	8. Performing Organization Report No.
Salmon, Bette C., and Pillars, William W.	110400-2-F

9. Performing Organization Name and Address	10. Work Unit No.
Environmental Research Institute of Michigan P. O, Box 618 Ann Arbor, Michigan 48107	11. Contract or Grant No. AT(05-1)-1635
	13. Type of Report and Period Covered Final Report June 1974 - July 1975
12. Sponsoring Agency Name and Address Energy Research and Development Administration P. O. Box 2567 Grand Junction, Colorado 81501	14. Sponsoring Agency Code

15. Supplementary Notes

Technical monitor: Philip Dodd
David Dahlem

16. Abstract

The purpose of this report is to document possible detection capabilities of the LANDSAT multispectral scanner data for use in exploration for uranium roll-type deposits. Spectral reflectivity, mineralogy, iron content, and color parameters were measured for twenty natural surface samples collected from a semiarid region. The relationships of these properties to LANDSAT response-weighted reflectances and to reflectance ratios are discussed. It was found that the single ratio technique of multispectral processing is likely to be sensitive enough to separate hematitic stain, but not limonitic. A combination of the LANDSAT $R_{5,4}$ and $R_{7,6}$ ratios, and a processing technique sensitive to vegetative cover is recommended for detecting areas of limonitic stain.

Digital level slicing of LANDSAT $R_{5,4}$ over the Wind River Basin, after geometric correction, resulted in adequate enhancement of Triassic redbeds and lighter red materials, but not for limonitic areas. No recommendations for prospects in the area were made. Information pertaining to techniques of evaluating laboratory reflectance spectra for remote sensing applications, ratio processing, and planimetric correction of LANDSAT data is presented qualitatively.

17. Key Words	18. Distribution Statement
uranium, multispectral, LANDSAT, geologic remote sensing, spectral reflectivity	

19. Security Classif. (of this report)	20. Security Classif. (of this page)	21. No. of Pages	22. Price
UNCLASSIFIED	UNCLASSIFIED	129	

PREFACE

This report explores the hypothesis that multispectral information collected by the Earth Resources Technology Satellite (now LANDSAT) over a semiarid region in the western United States can be used to detect surface alteration indicative of potential uranium deposits. Specifically, a test of LANDSAT data processed to enhance colors assumed to be characteristic of iron oxides was performed to test LANDSAT multispectral sensitivity to these materials. This detailed study was founded upon the results of an initial study funded by the National Aeronautics and Space Administration. Resources for this research were provided by the Atomic Energy Commission (now Energy Research and Development Administration) and allowed improved documentation and understanding of the capabilities of LANDSAT spectral ratios for mineral exploration. All of the work was done at the Environmental Research Institute of Michigan (ERIM).

The research described herein was performed under Contract No. AT(05-1)-1635, and covered a period between June, 1974, and June, 1975. Dr. Philip Dodd of Energy Research and Development Administration in Grand Junction, Colorado, was the technical monitor. The program was conducted by Bette C. Salmon, Principal Investigator and Research Assistant and William W. Pillars, Research Assistant at ERIM's Infrared and Optics Laboratory.

The work of the following staff members is greatly appreciated: Frederick J. Thomson, Jeanne E. Harris, Ross H. Hieber, and Nancy J. Moon. Also, a great deal of credit for development and research leading to the success of this work must go to Robert K. Vincent of Geospectra Corporation, Ann Arbor, Michigan. Section 5.3 is predominantly the contribution of Dr. Vincent as it was prepared for a previous LANDSAT report (Vincent, et al., 1975). Section 5.2 is substantively from Malila, Hieber, and McCleer (1973), with their permission.

A digital color map at 1:250,000 scale was provided to the sponsor as the formal data product to accompany this report.

SUMMARY

1. Hematitic alteration associated with roll-type uranium deposits is likely to be enhanced using only the LANDSAT $R_{5,4}$ allowing for simple processing techniques when assuming minimal vegetative influence.

2. Limonitic alteration associated with roll-type deposits, as is the case in the Gas Hills test site, is not unique in the $R_{5,4}$ ratio and is unlikely to be recognized in single ratio processing. However, when the strong yellow color used to visually identify limonitic alteration correlates with high concentrations of free ferric oxide content, the absorption bands in the infrared may be strong enough to allow improved recognition with the additional contribution of the $R_{7,6}$.

3. Munsell color designations of samples of natural surface materials appeared to correlate with iron content determinations for the eighteen samples tested.

4. Response-weighted reflectances of both LANDSAT and Skylab multispectral configurations correlated with Munsell hue, although their relationship was not the same as had been that of iron content.

5. Bulk mineralogy as it was determined here could not be definitively linked to features of the response-weighted reflectances.

6. Additional spectral features of seeming importance in limonite-rich surface materials were seen outside the LANDSAT MSS spectral region and may be of use in studies where other scanner data is available.

7. Response-weighted reflectances indicated that, all other considerations assumed optimal, at least five classes of color could be determined using LANDSAT $R_{5,4}$. Comparison of sample colors and the $R_{5,4}$ recognition map confirmed that these separations could be expected. With increased sophistication in treatment of vegetative differences and in-scene normalization, more precise determinations could be expected.

8. In agreement with laboratory results of the study, limonitic surface materials associated with known or suspected uranium deposits were not separated uniquely on the 1:250,000 digital recognition map. No recommendations for possible uranium prospects were made.

CONTENTS

FIGURES

TABLES

1
INTRODUCTION

1.1 BACKGROUND

Much can and has been said about the benefits to be gained from Earth Resource Satellite programs. In particular, there has been much speculation that the new remote sensing technology will bring us the discovery of new mineral and energy resources both in remote, inaccessible regions of the world and those which have been overlooked in more developed areas. In actuality, few real new discoveries have been reported. Demonstration cases for which the technology has been used have been selected carefully for their obvious promise where the location and conditions are already known. In truth, aside from recognition of important regional linears, which is a well established procedure, we do not know at this time the full potential of space-based remote sensing techniques for mineral exploration. The complexity of the interplay among spectra, natural variation, instrument response, and atmospheric effects makes most procedures used in exploration presently, by necessity, oversimplified. This does not imply pessimism, however, about the potential for such capabilities, which in this study and others is clearly indicated.

The regional perspective possible from space platforms is important to spectral studies, as it is for structural interpretation. Contrasts developed on a regional scale allow recognition of spectral

differences of importance-- separation of features from background spectral properties. However, increased altitude and decreased spatial resolution (compared to aircraft data) makes application of well formulated preprocessing techniques essential for quantitative spectral studies. The questions involving known sources of variation, such as atmospheric interference, vegetative cover, and natural mixing must be addressed. The limitations as well as the potential of individual multispectral scanners must be recognized. Herein lies the gap between theoretical possibilities and actual successes.

This study uses LANDSAT data in an empirical attempt to match remotely sensed scanner data collected over the Wind River Basin, Wyoming, with the theoretical potential for recognizing materials important in uranium exploration. Also, a preliminary look at the Skylab sensor configuration portends new opportunities which may be available with different response and band configuration.

Selection of targets must be made from those types of mineral deposits which first fit the basic criteria of possible spectral distinction and sufficiently large surficial expression. Then it must be determined that compositional differences which are important to discovery of the deposit have spectral characteristics strong enough for detection within scanner spectral resolution. Although the spectra of many surface materials we would like to differentiate are too similar over most of the available electro-

magnetic spectrum, some which are important for mineral exploration do have the potential for unique enhancement or recognition. Even at that, the capacity to detect these differences is not independent of background material and vegetation cover which may serve to obfuscate otherwise unique spectral signatures.

1.2 OBJECTIVES

The Wind River Basin, Wyoming, is a well known petroleum, natural gas, and uranium locality. Unoxidized deposits of uraninite in this basin and other Tertiary basins of Wyoming are known to have associated alteration products which are occasionally intersected by the present erosional surface. In a previous study (Vincent, 1975; Salmon and Vincent, 1974) there was preliminary indication that it may be possible to recognize on LANDSAT data some of these secondary minerals. The intent of this research was to document pertinent data needed to test a seemingly promising technique for multispectral processing of LANDSAT data. Do spectral ratios of LANDSAT data actually enhance features of interest in uranium exploration? The stated objectives were these:

1. To test the hypothesis that alteration associated with uranium deposits, if exposed at the surface in semiarid regions, could be enhanced by the ratio processing of LANDSAT data.

2. To test the relationship among mineralogy, Munsell color, and iron content of natural surface materials and compare them to response-weighted reflectances of LANDSAT bands to determine controlling factors recognized in remotely sensed data.
3. To determine whether color differences as they are used by exploration geologists can be reliably recognized with the wide-band configuration of the LANDSAT multispectral scanner; quantitatively, to determine the magnitude of reflectance differences needed for separation with LANDSAT data. In so doing, we hope to translate the multispectral approach into a form to which the geologic community can readily relate.
4. To produce a planimetrically corrected map display of the resultant data at a scale of 1:250,000 for comparison with gamma spectrometer contours collected by aircraft to see whether features enhanced in LANDSAT data correlate with known concentrations of uranium.

1.3 APPROACH

The emphasis in this study has been on multispectral information and not on structural interpretation. Measurement of the properties of actual surface materials was needed to test the rigor with which

these correspond to the spectral features of LANDSAT reflectances. Laboratory spectra, color, mineralogy, and iron content have been tested for correlation with a single LANDSAT ratio.

Response-weighted laboratory spectra of samples actually collected from the area have been compared with these properties as well as with actual LANDSAT data. Most of the samples were collected from well-exposed outcrops or from soils derived directly from the recognizable formation below; hence, they are similar in character but more representative of the scene as it is exposed to a satellite sensor. It is understood that the character of these will not necessarily correlate with samples collected for other geologic investigations, as it is usually standard procedure to collect the freshest sample with the least recent physical and chemical alteration. For remote sensing, materials exposed and weathered are precisely those of interest. Expectation for correlation between surface materials and mapped geologic formations is based on geologic interpretation and varies from place to place in the test site. Factors contributing to spectra variations such as topography, vegetation, and grain size of sediments, are treated qualitatively.

2

PREVIOUS WORK

Aside from the many geologic investigators using satellite and high altitude areal photography for structural interpretation, there are several groups actively struggling with the application and correlation of measured spectra to multispectral data. Salisbury and Hunt, et al. have provided, in their series of articles from 1970-74, a large collection of spectra for minerals as well as for separate rock types. In a review article (Salisbury and Hunt, 1974) summarizing the importance of particular chemical compounds to spectra, they concluded that the spectral detail of natural materials in the visible and near infrared region is provided by two chemical constituents--the transition metal Fe and the hydroxol or water molecule. As a result, it is apparent that general rock-type mapping is unlikely to be accomplished with just the use of this spectral region. As indicated by Salisbury and Hunt, minor constituents of the rock can often dominate the spectral characteristics. For example, in a study of possible lunar mineralogies, small percentages of titanium oxide were shown to disproportionately reduce the overall reflectivity of mixtures (Adams, 1974). Salmon and Vincent (1974) reported that even with small percentages of ferric oxide present in Triassic sedimentary rocks, ratios of red to green reflectivities were dominated by that ion's strong absorption

in the green. This domination may be used to advantage in some applications.

Rowan (1972) predicted the usefulness of iron absorption features in recognizing "mineralized areas where the ore distribution is either indirectly or directly related to the distribution of iron". A mineralized Tertiary breccia pipe in the New World Mining District, Montana, was used to illustrate the detectability of the infrared absorption active for iron on multispectral photography. The central ferrous-rich breccia pipe contrasted highly with the peripheral zone, which was characterized by the presence of limonite (ferric-rich) on the surface. The important spectral feature credited with this separation is the wavelength difference in the absorption of the two ions, i.e., ferric bands are centered at 0.70 μm, and 0.87 μm, while a strong ferrous band is located at 1.00 μm. The reflectance maximum of limonite at 0.80 allows particularly high contrast between the two spectral regions.

More recently, Rowan et al. (1974) used computer-enhanced LANDSAT images and ratio composites to discriminate rock types and detect hydrothermally altered areas in south-central Nevada. Using a qualitative color-additive method of superimposing color-keyed LANDSAT ratios, outcrops designated as likely to be altered were seen to coincide with known mining areas. Their success is most likely due to the strongly represented spectral properties of iron oxide minerals.

Pohn (1974) has reported what he calls "high reflectivity anomalies" in aircraft data collected by The University of Michigan multispectral scanner in the 1.0-1.4 μm region and the 2.0-2.6 μm region. These areas occur on Tertiary or younger rocks that are reddish and usually andesitic or more mafic in southern California. The features are ascribed to very fine grained iron oxide (less than 5 micron particle size), most likely hematite, which is thought to have been produced by "late eruptive oxidation of mafic minerals and by precipitation of sublimate during posteruptive fumerolic steaming." Pohn reports that, at the same time, no such high reflectivities are seen on the brick-red Aztec Sandstone, and none are seen on any of the data collected at wavelengths shorter than 1 μm. An important consideration emphasized is that factors independent of obvious colors can control the relative spectral reflectivity. In Pohn's article it is the grain size of hematite that he deems important to its recognition.

Vincent et al. (1971-1975) have worked extensively with the theoretical and practical applications of laboratory spectra in interpreting actual data collected by aircraft, LANDSAT, and Skylab. Use of response-weighted reflectances, reflectances corrected for the response functions of particular sensors, for quantitative comparison to remotely sensed data is an important contribution to remote sensing. This group has also tried to correlate absolute

values of spectral ratios from laboratory spectra to actual data through use of atmospheric corrections and in-scene normalization. These procedures are not yet established as operational tools, although some preliminary successes have been reported for both aircraft and satellite data (Dillman and Vincent, 1974; Salmon and Vincent, 1974).

The geologic literature contains many detailed studies of the alteration associated with roll-type uranium deposits, particularly since the discovery of the Luck Mc Mine, Gas Hills District, Wyoming, in 1953 (Anderson, 1969). Color photography as well as ground surveillance in search of the reds and yellows which may indicate such deposits have been used for a long time. Hellinger (1971) has reviewed the applications of remote sensing techniques and the possibilities for uranium exploration using LANDSAT or other satellite platform data. Of particular interest is the enhancement of important features outside the spectral region available from photographic techniques, in the reflective infrared, where additional information can be gained from spectral properties attributed to iron oxide minerals. A previous study (Vincent et al., 1975) indicated there may be potential in LANDSAT data for recognizing these features. Unfortunately, the wide band infrared configuration of LANDSAT bands prevented their use for best spectral separation. The two LANDSAT visible channels, however, showed a successful case of enhancement

using Vincent's processing techniques. More work with the spectra of natural surface materials and their correlation with remotely sensed data will lead to better evaluation of these techniques.

3

GEOLOGY

3.1 SELECTION OF TEST SITE

The Wind River Basin and the encompassing mountain ranges cover most of Fremont County and the western part of Natrona County in central Wyoming (Figure 1). The basin floor, ranging from 7,000 ft. above sea level in the northwest to 5,000 ft. above sea level in the southeast is sparsely vegetated due to the semiarid climate. The basin is not only a topographic low, but also a structural basin with Tertiary sediments directly underlying most of the interior. Quaternary sediments, also present in the central basin, are generally local deposits and are often found along present-day drainage courses. In general, the Quaternary deposits are more heavily vegetated than most of the Tertiary and Paleozoic areas.

Paleozoic and Mesozoic sediments are exposed at the perimeters of the basin and in local structural highs. These will not be treated specifically in this study, although it is important to recognize their contributions to Tertiary deposits as sources of sedimentary material reworked into younger deposits. Of particular interest in this respect are the Triassic redbeds which provided, during Early Tertiary time, a source of red sediment for redeposition as Tertiary clastics, such as in the Indian Meadows and Wind River Formations.

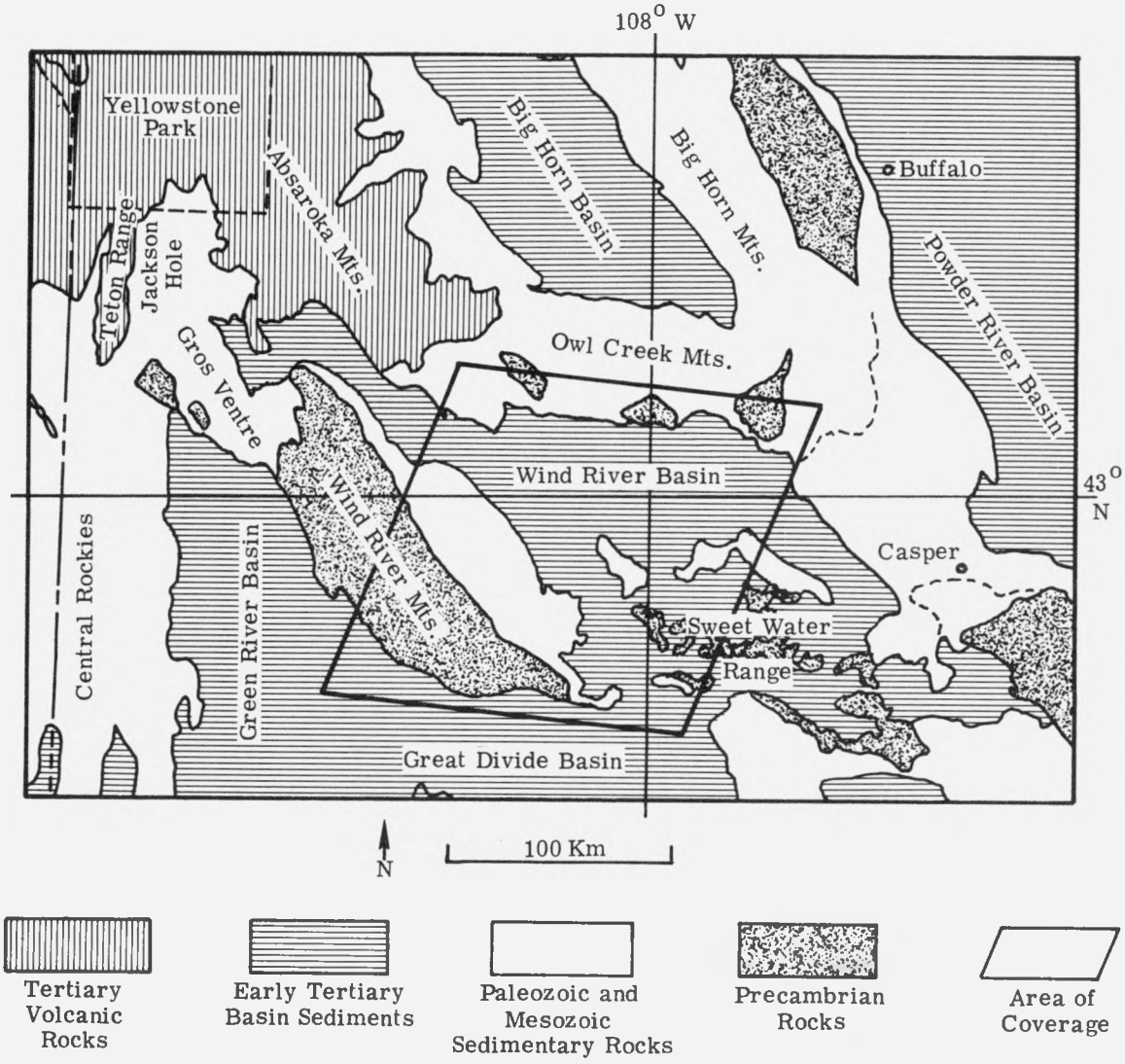

FIGURE 1. INDEX MAP OF WIND RIVER BASIN, WYOMING SHOWING THE AREA OF LANDSAT DATA COVERAGE

The mountains surrounding the Wind River Basin, such as the Wind River Range, the Granite Mountains, the Bighorn Mountains, and the Owl Creek Mountains, all have Precambrian granite cores. These granites are considered to be one possible provenance for the uranium found in younger sediments deposited in the basin. The Absarokas, the mountains limiting the basin to the northwest, are composed of Tertiary volcanics. These and the volcanics of the Rattlesnake Hills are also considered to be possible sources of uranium which was later leached and concentrated in the Tertiary arkosic sandstones.

The Wind River Basin combines favorable geographic characteristics with a geologic setting which is promising for mineral exploration by remote sensing. First, the sparse and fairly uniform vegetative cover of the basin provides minimum interference with geologic information to be acquired by multispectral coverage. Next, the relatively dry climate and high altitude reduce atmospheric effects which must be considered before quantitative work is possible. Third, the roll-type uranium deposits which are known here and in other locations are of sufficient areal extent that satellite spatial resolution should not be the limiting factor for their recognition. Finally, the alteration product characteristically found in association with these deposits, limonite, has distinctive characteristics in the spectral regions useful for remote sensing techniques and covered by LANDSAT spectral bands. Although the above features

are the important technical features for choosing this test site, it should be mentioned that the availability of data from a previous study, and the overlapping gamma spectrometer information provided by the sponsor, were also influential in the selection.

3.2 CHARACTERISTICS OF ROLL-TYPE DEPOSITS

Roll-type deposits were first recognized in the United States on the Colorado Plateau and are sometimes referred to as "Colorado plateau-type deposits". Later, they were discovered in many western intermontane basins. Current theory attributes the mobilization and concentration of uranium to supergene processes active mostly in Tertiary time. Alkaline groundwater carried uranyl complex ions and altered primary minerals of the Tertiary sediments until a reducing agent caused deposition near the leading edge of hydrologically controlled tongue-shaped features. Although the general geochemical scheme for transportation and concentration is the same for many of the deposits, the mineralogy and alteration products are somewhat specific to individual districts. Distinct color differences between the outer, unaltered sands and the inner, oxidized or bleached zone are, however, a universal characteristic for recognition of these deposits.

Formations from which uranium is now extracted were deposited when relief surrounding the basin reached a maximum in Early Eocene.

Precambrian granite cores of the uranium-rich granites surrounding the Wind River Basin, particularly the Granite Mountains to the southeast, were fully exposed. Alluvial fans of conglomerate, grading basinward into coarse akosic sandstone, were deposited in the basin from the Granite Mountains forming the Wind River Formation. Volcanic material both in the form of stream sediments and ash falls became available both from the Absaroka-Yellowstone volcanic province in late Early Eocene and the Rattlesnake Hills volcanic center during the Middle Eocene. The sediments of Oligocene through Pliocene time were fine-grained and even more filled with volcanic debris than those of the Eocene, making available what may have been an additional source of uranium to be later leached and concentrated in the Eocene rocks.

In the Gas Hills District, roll-type deposits are found in the arkosic sandstone member of the Lower Eocene Wind River Formation, which was named the Puddle Springs Arkose by Soister in 1966 (Armstrong, 1970), and the upper transition zone. Anderson (1969) described the host rock for uranium in the Gas Hills region as "yellowish-orange to yellowish-gray arkose, derived primarily from Precambrian gnessoid and granitoid rocks; it contains little clay, abundant calcium carbonates, and limonite cement". Most of the ore is found in the coarse-grained facies. A general description of the mineralogy of the sand-size fraction of the host rock

indicated a composition of 60% quartz and 40% mixed feldspars, with some muscovite, biotite, and other minerals (Anderson, 1969). This member of the Wind River Formation contains only about 10-15% clay matrix overall. Fine-grained sediments, such as silty sandstone and mudstone, which are present in the upper and lower transition zones,are more unfavorable to concentration of large amounts of uranium ore, although some is found in the lens sands of the upper transition sediments. The decrease in uranium concentration from coarse to fine grained sediments is usually attributed to lower permeability.

The uranium ore bodies themselves are crescent-shaped in cross section and irregularly sinuous in plan view. The upper and lower tails of the crescent thin out, with the greatest thickness of ore at the front of the roll. In the Gas Hills, on the concave side of the crescent is cream-colored to yellow host rock which has been altered, presumably by the fluids which have deposited the ore. The contact between this and the ore-bearing zone is sharp, the transition taking three inches or less. On the convex side of the crescent, the host rock has been left unaltered and has a greenish-gray color. The contact between the ore and this unaltered zone is gradational and irregular. In some places, there is no intervening ore and the bleached zone of the host rock contacts the unaltered, colored zone. Individual rolls are often bound by

mudstone interlayers in the sandstone. There are many variations of this general geometry, including multiple deposits stacked en echelon through vertical section (Houston, 1969). Figure 2 shows a diagrammatic cross section of roll-type deposits as they are found in the Gas Hills district (Armstrong, 1970).

Unoxidized ore of uranium is generally dark and fine grained. In the Gas Hills the chief ore mineral is uraninite, accompanied by some coffinite. Pyrite and marcasite are also found in close association with the ore in the ore-bearing zone. Alteration of the host rock causing bleaching or yellow coloring has chiefly been achieved by oxidation. Feldspar fragments in the arkosic sandstone have been kaolinized and pyrite has been removed or converted to limonite.

As in the Gas Hills, ore occurrences in the Crooks Gap Mining district are bound by alteration zones in which feldspar of the arkosic material has been kaolinized and pyrite has been large removed or converted to limonite. Downdip from the uranium deposits, the sandstones are light to medium gray, unoxidized, and unbleached. This occurrence also supports the interpretation that these oxidized areas adjacent to the ore are interrelated with the ore emplacement process. In this and the Green Mountain area, the Battle Springs formation is the host rock, in which present oxidation and one or more later Tertiary or Pleistocene oxidation levels seem to be

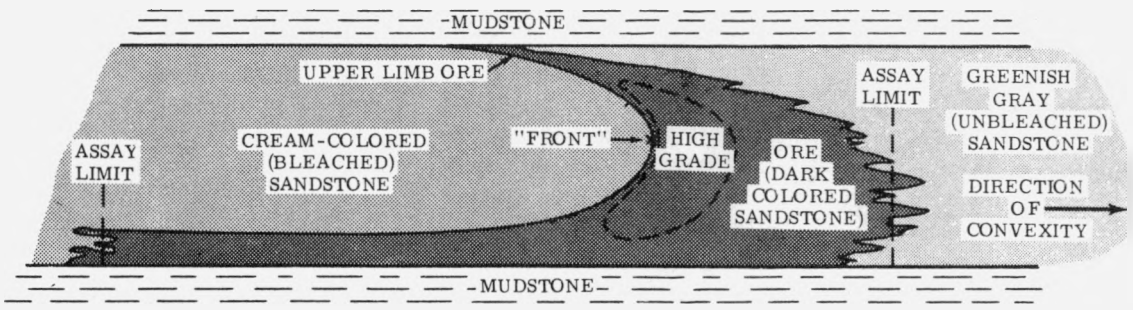

FIGURE 2. DIAGRAMMATIC CROSS SECTION THROUGH A "ROLL" (CRESCENT-SHAPED) ORE BODY. From Armstrong, 1970.

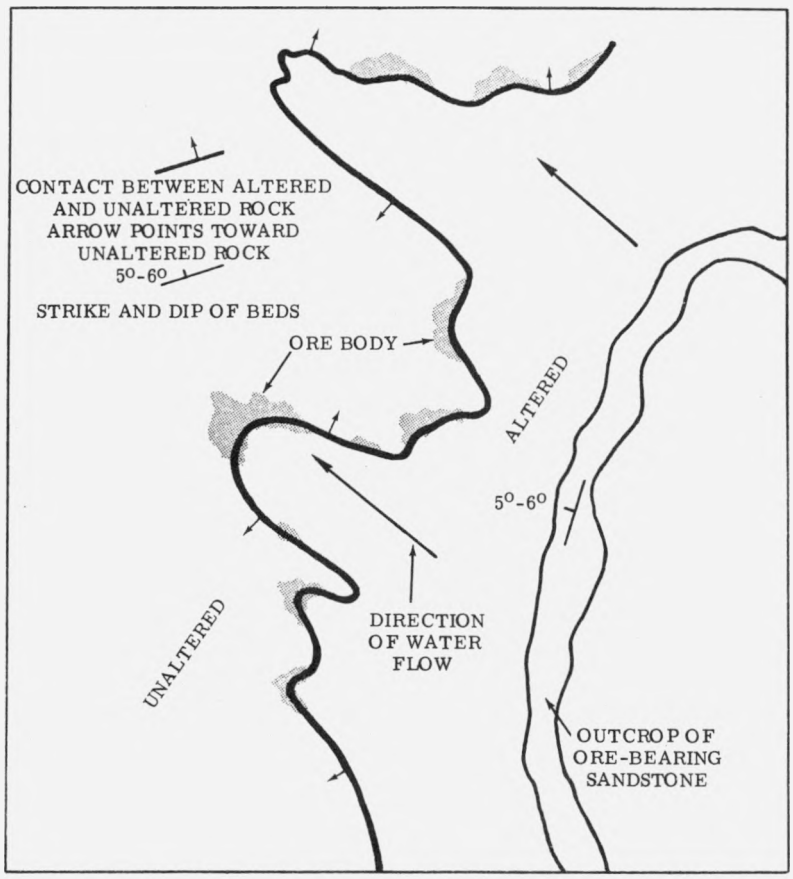

FIGURE 3. SANDSTONE TYPE URANIUM DEPOSIT IN U.S.S.R. From Germanov, 1960.

present. Noteably, one of the features of this area that first encouraged exploration efforts was the limonitic staining which could be seen at the surface.

Geometry, as well as chemistry, is an important consideration for possible detection of roll-type deposits by remote sensing techniques. It is necessary that the region of oxidation is intersected by the topography in a manner such that the geometry can be recognized. Although the ideal shape for the contact between altered and unaltered sandstone would be curvilinear, in practice the contact is often much more irregular. Armstrong (1970) presents a schematic given by Germanov of the contact between altered and unaltered rocks of a sandstone type uranium deposit in the U.S.S.R. which has been reproduced here. Only at precise stages of denudation would the actual geometry of the ore body be obvious at the surface. More often as implied by Figure 3, the outcrop pattern of the altered sandstone would be the feature of geometric importance.

3.3 SPECTRAL PROPERTIES OF ALTERATION MINERALS

Ore deposits with associated iron-oxide alteration occurring at the surface are promising remote sensing targets because of the prominent spectral features in the visible and reflected infrared wavelength regions of these minerals. Both limonite and hematite are known to be associated with certain roll-type uranium deposits, and their particular influence on coloring and spectra of the surface

materials, even when present in relatively minor amounts, may be useful for exploration by multispectral remote sensing. The relationship of these minerals in particular concentrations and associations with the color they impart to soil or rock is not unambiguous. Consideration of natural occurrences of these and the wide variety of situations in which they occur is essential for evaluation of the strength of remote sensing as an exploration technique.

Krishna Murti and Satyanarayana (1971) assessed the relative importance of individual factors in soil color with a partial regression analysis. They determined that for a number of soil profile samples from the reddish-brown soils of the Malwa Plateau, India, which were developed on basic rocks, there were statistically significant correlations with Munsell designations and chemical constituents. Color hue (over value or chroma) seemed to correlate best with percent iron or titanium. Value of soil color seemed to depend on the percent clay or organic content. In these soils manganese was present in sufficient quantity to also influence the value, or "light to darkness." No significant correlation was observed between chroma and any of the soil characteristics above. The correlation analysis also indicated that percent ferrous iron correlated better with hue than did ferric; they indicated that hue could be predicted by knowing ferrous and titanium alone for 95% of their trials, with ferrous iron more important to color determination than titanium.

In a study on soil types collected in Pennyslvania, Mathews et al. (1972), concluded that in the spectral region between 0.4 and 2.6 μm diffuse reflectance was affected by percent organic matter, free iron oxides present, and silt influence. Organic matter and free iron oxides influence reflectance in the 0.5 to 1.2 μm region most, while clay type influenced curve shape and intensity over the entire range. Silt had the greatest influence on reflectance in the infrared region. In an interesting experiment, the Hagerstown silt loam containing 4.2% initial Fe_2O_3 was washed of its free iron oxide. Comparison of the spectral curve of the material before and after the leaching process showed the strong influence of iron in the spectral region below 1.0 (Figure 4). This finding supports our assumption of the importance of the influence on iron oxides on spectral reflectance in the LANDSAT band region, even in small percentages.

The importance of iron oxides in the color of sedimentary rocks in the western United States is cited by High and Picard (1965). Analysis of the "purple" and "ochrous" units of the Popo Agie Member of the Triassic Chugwater Formation resulted in their generalization that the ochrous rocks were high in analcime with minor amounts of montmorillonite and were probably colored by iron oxides, apparently yellowish and yellowish-brown goethite. Similarly, the red coloration of the purple unit, which has little or no analcime but is usually high in montmorillonite, is probably colored by small amounts of hematite or reddish goethite. X-ray diffraction

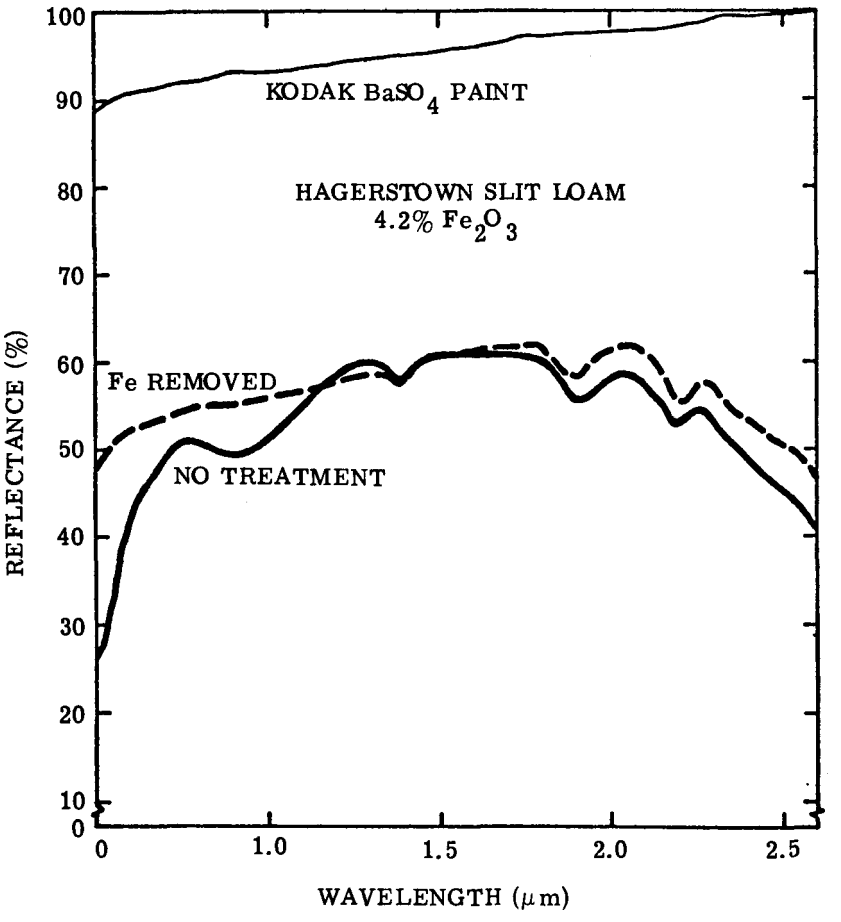

FIGURE 4. SPECTRAL REFLECTANCE CURVES ILLUSTRATING THE EFFECT OF FREE IRON OXIDE ON REFLECTANCE INTENSITY. From Mathews, 1972.

confirmed that small amounts of hematite were present in the purple units.

Color differences thought to be caused by iron-oxides particularly have been important as indicators of uranium deposits. The updip oxidation characteristic of roll-type deposits is most often described macroscopically as a color difference between the oxidized area and the unaltered sandstone downdip of the ore. In the field, contacts between the altered and unaltered material are often sought initially on the basis of color alone. The cause of these color differences is important to understand. It must be identified that features sensed as multispectral features, either as differences associated with color in the visible or other differences in the infrared, are features of importance for exploration. Color differences detected by the scanner might be due to variable vegetation cover, variations in concentration of pigment minerals, grain size variation, or increased mixing with minerals which quench the spectral properties of minerals of interest.

Assuming the finding of workers quoted previously and other geochemical studies is correct, that iron oxides are important pigment minerals, the use of their spectral properties must be carefully analyzed in remote sensing applications. It is not necessarily true that those soils or rocks showing strongest iron-related colors are those with largest percent iron present. Other

properties, such as dissemination of iron, grain size, etc. are just as important in determining the "influence," or "dominance," of iron on the perceived color.

The spectral features of iron oxides in the wavelength region below approximately 2.0 μm are caused by electronic transitions of the Fe^{3+} ion at 0.87 μm, 0.70 μm, and 0.40 μm. These electronic transitions produce spectral reflectance minima, the most prominent of which is the 0.87 μm absorption. Sample spectra of iron oxide minerals from the ERSIS* library are presented here for reference (Figures 5 and 6). The reflectance minima of ferric oxides are preceded on the short wavelength side by a spectral curve of positive slope (Vincent, 1973). A feature that can be seen both on the spectra reported in the ERSIS data bank on individual minerals and those samples measured in the course of this study presumed to include hematite and limonite can be seen at wavelengths near 0.50 μm. A slope steepening beginning near 0.5 μm seems to appear on all those strongly colored yellow or red samples. The often touted absorption band in the vicinity of 0.87 μm for ferric iron varies in strength, being seen sometimes as a dip in reflectance and other times

*ERSIS is a compilation of laboratory spectral data housed at the Johnson Space Center in Houston, Texas, and the Environmental Research Institute of Michigan (ERIM) in Ann Arbor, Michigan (Leeman, V., et al., 1971, 1972; Vincent, R. K., 1973).

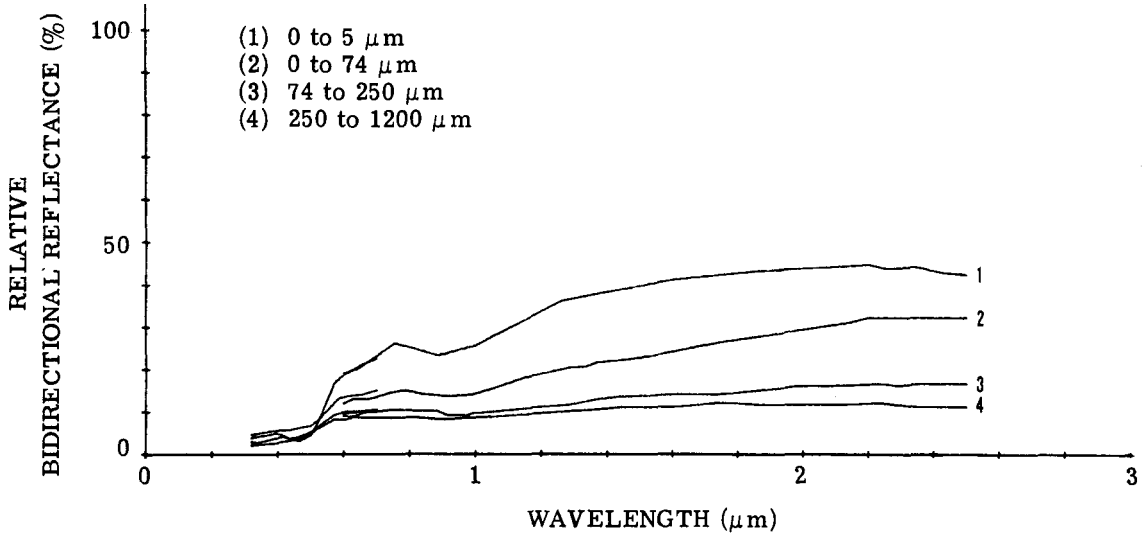

(a) Goethite (Biwabik, Minnesota)

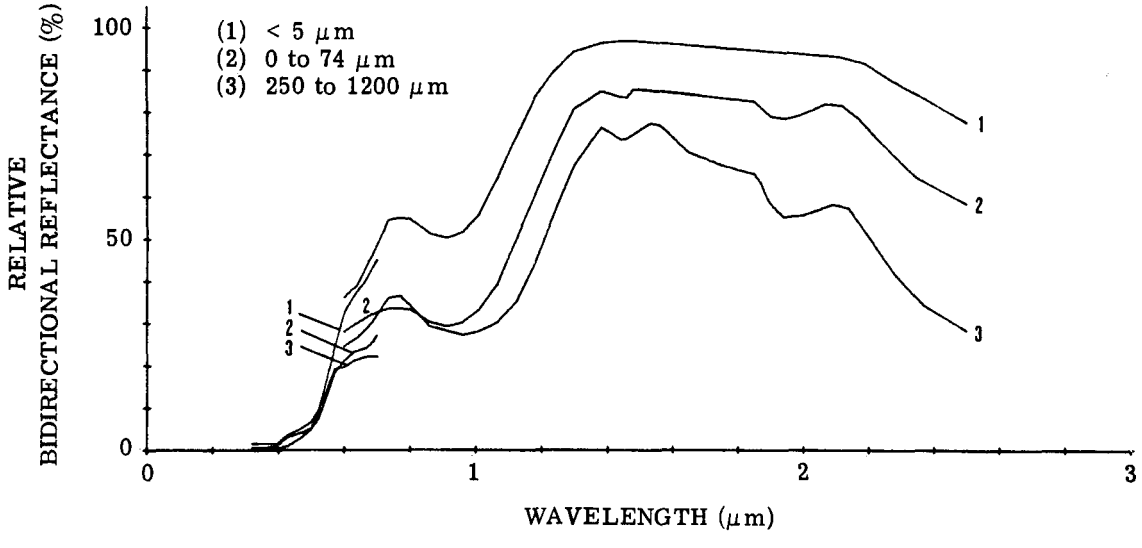

(b) Limonite (Tuscaloosa County, Alabama)

FIGURE 5. RELATIVE REFLECTANCE VS. WAVELENGTH. From Leeman, 1972.

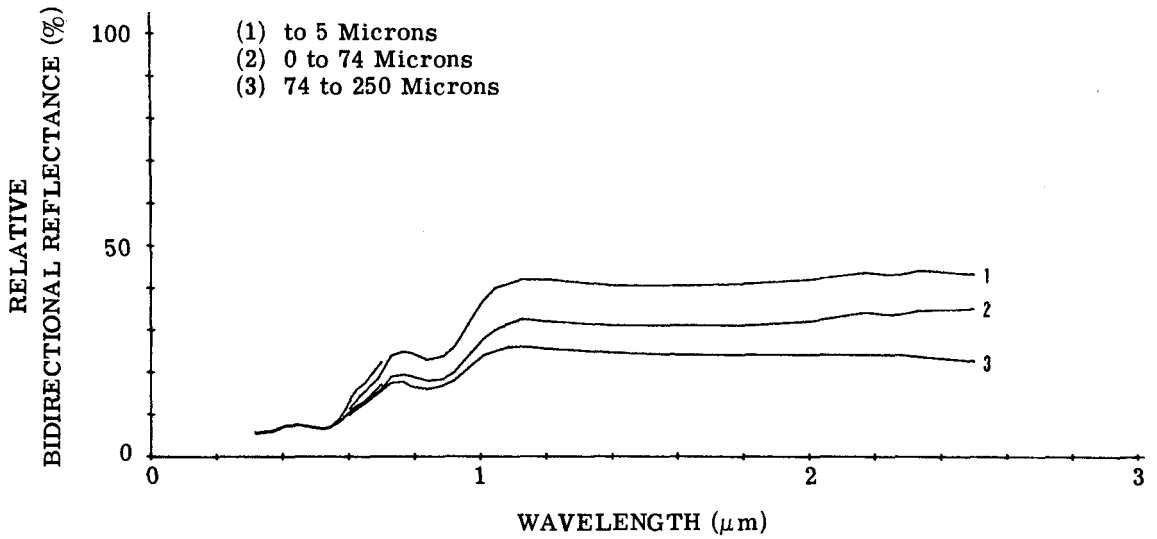

(a) Hematite (Irontown, Minnesota)

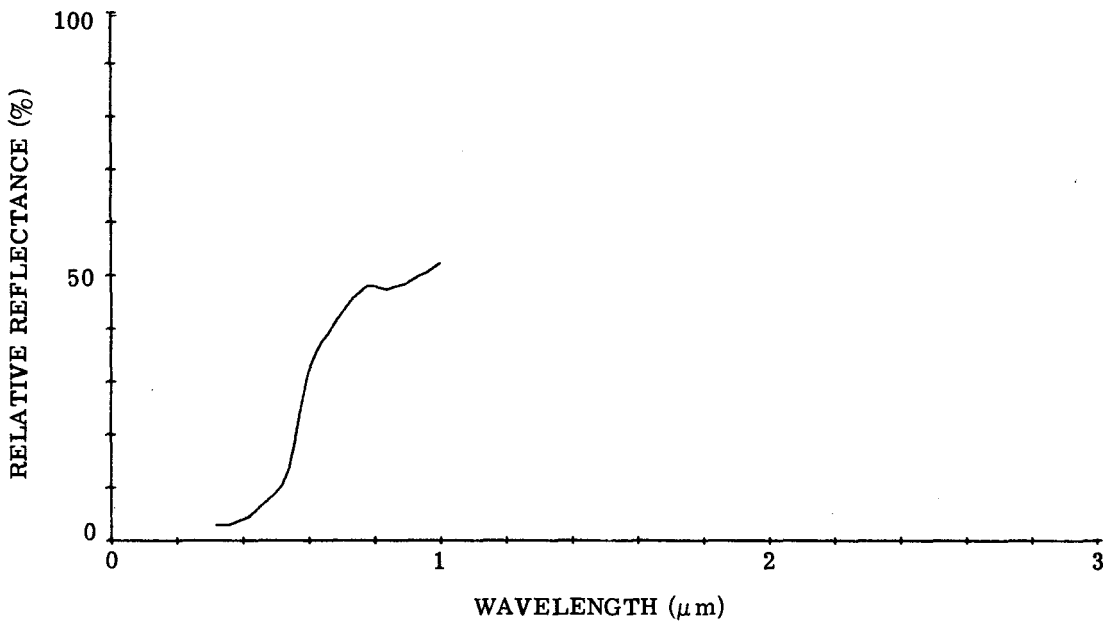

(b) Quartz Sand with a Hematite Satin (Bok Tower, Florida)

FIGURE 6. RELATIVE REFLECTANCE VS. WAVELENGTH. From Leeman, 1972.

as merely a reduction of slope. In the visible and near-infrared regions there is room for improvement over the LANDSAT configuration in the use of more selective, narrow spectral bands.

It is important to determine the spectral regions which are most useful in separating iron absorptions from the spectral characteristics of other materials. Mathews et al. (1972) reported that a divergence analysis computer program published by the Agricultural Experimental Station of Purdue University was used to select the five optimal bands from The University of Michigan M7 scanner data for recognizing bare soil on training fields in Southeastern Pennsylvania. Since these soils are not necessarily related to those soils developed in the western United States, the spectral bands chosen by these criteria may not be the best for differention in semiarid climates. However, the presence of free iron oxide, clays such as illite, and the occurrence of organic material, if they are the dominant features of these eastern soils, may well provide information pertinent to band selection for other soils.

The spectral bands chosen from the thirteen available were: 0.44-0.46 μm, 0.58-0.62 μm, 0.66-0.72 μm, 1.00-1.40 μm, and 2.00.2.60 μm. Four of these (omitting 0.66-0.72 μm) were the same choices made by West for categorizing soil types, as referenced by Mathews et al., (1972). These band selections were based on the scanner band configurations available, and therefore, only indicate optimal selection for

that sensor. Although this will have bearing on other optimal band studies, these particular bands are not necessarily optimal in general. Mathews' study is pertinent to this LANDSAT study only in that two of the bands he selected, 0.58-0.62 μm and 0.66-0.72 μm, are somewhat correlative with LANDSAT bands 4 and 5.

4

ANALYTICAL MEASUREMENTS

4.1 LABORATORY SPECTRAL MEASUREMENTS

There has been, historically, some disagreement among investigators as to whether field spectra or laboratory spectra are most appropriate for comparison with remote sensing data. Field spectra have the advantage of being collected in situ so that textures, surface dust, impurities, etc., are intact and representative of the scene. However, field spectrometers are not as accurate as laboratory instruments and variations in illumination, etc., can add significant errors to the data. Laboratory spectra, although more accurate and collected under more stable conditions, have the disadvantage of being collected on samples that are unlikely to be identical to those exposed to the satellite sensor.

The variety of uses for spectra and the variation in their collection make generalities made from general collections of laboratory spectra tenuous for remote sensing. Many of the minerals for which the most spectral data is available, such as hornblende, are unlikely to appear in great quantity exposed to a passing satellite. Much of the spectral data have been collected on fine powders, sieved into uniform size ranges. These data are of interest in grain size dependent studies, but are improbable samples for extrapolation to surface materials. Soils, exposed sedimentary rocks, weathered igneous rocks, etc., are not so well sorted nor so homogeneous.

Diffuse reflectance measurements were collected in the 0.36 to 2.5 μm spectral region for twenty samples collected from the surface of the Wind River Basin. All samples measured for this study were disaggregates of surface materials which had not been sorted into size fractions and were, therefore, subject to some textural and spectral variation within the sample. Preparation in this manner was thought to be advantageous, for the samples were then more representative of natural variation. Each sample was mounted in a sample holder which had been sprayed with crylon flat black to prevent spurious reflections from surrounding surfaces.

Measurements were taken on a Cary-14 spectrometer with an integrating reflectance hemisphere. Barium sulfate was used as a reflectance standard. The scan rate for all measurements was 7.5 angstroms/second. Slit width variation is plotted in Figure 7 with curves superimposed to show the maximum variation occurring among measurements. Stability of response was shown to be good to within a few percent. Detectors were changed at the 0.7 μm wavelength and yet responses in that region were well matched; note that in most cases the curves shown have little discontinuity at this wavelength (see Appendix I).

Reflectance readings were taken every 0.2 μm wavelength and recorded automatically on punched tape to eliminate the inaccuracies of extrapolation by hand. These tapes were later corrected to the

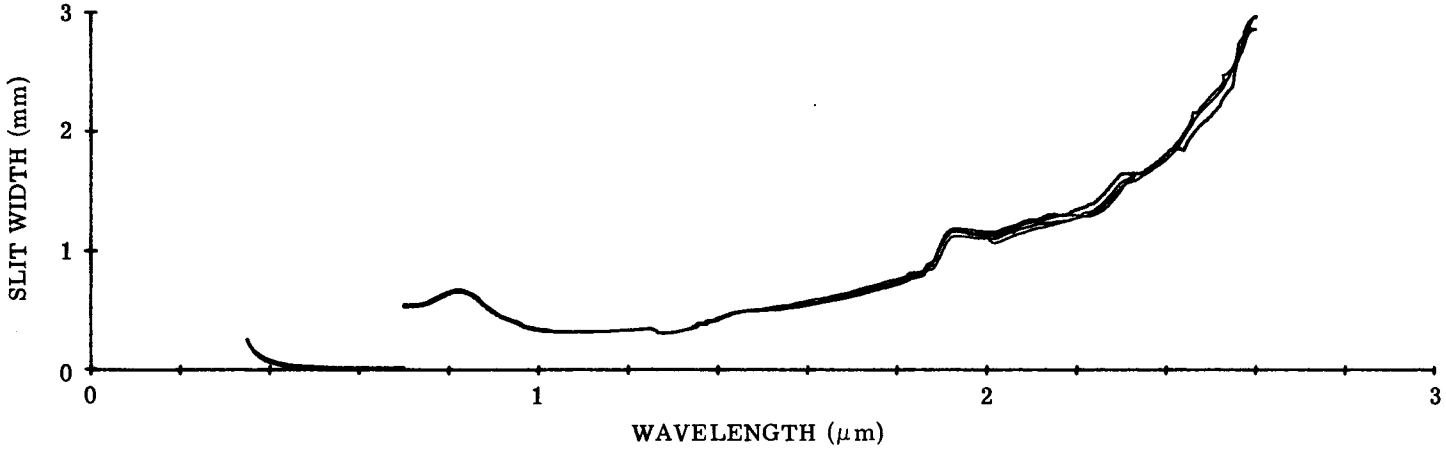

FIGURE 7. SLIT WIDTH VS. WAVELENGTH AS MEASURED DURING THE COLLECTION OF REFLECTANCE SPECTRA FOR THIS STUDY. Representative curves are superimposed to show maximum variation among measurements.

reflectance of the barium sulfate standard to produce relative reflectances. Curves of the spectra were plotted on a computer at the same time so that all values were recorded throughout automatically.

Spectral data collected by aircraft or satellite scanners are subject to the bandwidth configuration and response of the instrument. Therefore, laboratory spectral data must be corrected before comparison with data collected by a remote sensor. A sine filter, assumed to approximate the spectral response of the LANDSAT MSS bands, was used to correct the laboratory values to LANDSAT response-weighted reflectances for spectra of samples collected in the Wind River Basin. Spectral band cutoffs were assumed to be the 50% points of 0.5 μm and 0.6 μm for band 4, 0.6 μm and 0.7 μm for band 5, 0.7 μm and 0.8 μm for band 6, and 0.8 μm and 1.1 μm for band 7. Integration of each spectral curve over these intervals results in an average reflectance value per band which should more nearly correspond to that expected from the LANDSAT scanner.

4.2 COLOR ANALYSIS

Disaggregated samples of soils and rocks collected at the surface were described according to the Munsell color system. None of the samples were ground or sorted to uniform size, but were chosen to best represent the characteristics of the surface from

which they were collected. Materials were mounted in round sample holders and wet to simulate natural packing and reduce light scattering effects. Each was allowed to dry thoroughly before color determination, as it was known that the test site was dry at the time of data collection by LANDSAT. The standard medium gray background was used and samples were viewed in natural sunlight near midday.

Where colors were heterogeneous due to compositional variation and grain size, the most dominant color was specified. Most often, variations were in value (lightness) rather than in hue or chroma. Color assignments were checked three times for consistency. 10 YR colors were most difficult to describe accurately. In some cases, differences which were evident by eye could not be separated with the available Munsell designations.

Sample number and Munsell designation for all seventy three samples can be found in Appendix II.

4.3 MINERALOGICAL AND CHEMICAL ANALYSES

The minerals in each sample were identified by powder x-ray diffraction. The relative percents were qualitatively determined based on the heights of the characteristic diffraction peaks for each phase. The minerals identified include:

quartz

plagioclase

potassium feldspar

montmorillonite

illite

calcite

gypsum

dolomite

kaolinite or chlorite

Another phase, identified in Table 1 as the 35° 2θ phase, gives a characteristic peak at approximately 35° 2θ but could not be identified. In some cases, however, this peak may correspond to a feldspar. "Tr" indicates a trace amount of that mineral was found. A question mark indicates that a small amount of this phase may be present but its characteristic peaks are either masked by peaks of another phase, or so weak as to be questionably present. All other phases are present in amounts too small to be detected.

The mineralogical analysis as reported here on samples collected for this project was not adequate for recognizing small percentages of iron oxide phases present. Unfortunately these results do not allow us to correlate colors or spectra with the determined oxide mineralogy. The results were of importance, however, in indicating the general mineralogy of the samples and for recognition that few,

TABLE 1. MINERALOGY RESULTS
(PERCENT OF EACH MINERAL)

SAMPLE NO.	QUARTZ	PLAGIO-CLASE FELDSPAR	POTASH FELDSPAR	MONTMORIL-LONITE	ILLITE	CALCITE	GYPSUM	DOLOMITE	KAOLINITE CHLORITE	35°2θ
1	60	8	?	8	4	13			4	3
4	35	54	?	5	4					2
12	63	5	6	tr		18		2	3	3
14	59	26	12	3	tr		?	?	?	
15	57	20	9	6	?	tr	8	?	?	?
25	51	7	8	14	2	11		?		7
31	57	6	5	3	?	14		12		3
32	53	27	12	5	3			?		?
33	57	23	15	5						
34	32	28	12	5	5		9	?	6	3
41	60	15	15	4	2	2		?	2	
45	40	21	18	6	5			?	8	2
61	28	40	?	27	3	?	?	?	2	tr
63	45	7	10	12	3	13		6	2	2
64	83	?	6	7				2		2
66	78	9	?	7				6		
69	36	41	?	21				?		2
70	35	30	21	10	2	?		?		2
72	44	28	10	9	2				3	4
73	42	29	12	8	2			2	2	3

if any, heavy minerals or Fe-bearing phases were present in large quantities.

Inspection under the binocular microscope concurred with findings from the x-ray diffraction study that there were few heavy minerals present in any of the samples. This implies that most of the iron present was present as free iron oxide or as a chemical constituent of chlorite or clay minerals.

Chemical determinations were made by a combination of analytical techniques. Total iron and uranium were first determined by neutron activation analysis.

Analyses for uranium were done on five yellow samples to test the hypothesis that limonitic alteration was uniquely associated with uranium deposits. The results of this test are given in Table 2. Although it is true that limonitic stain is often found in association with uranium deposits, this occurrence is not unique. Four of the five samples do not show high uranium contents. The fifth sample (no. 33) was collected at the Lucky Mc Mine.

TABLE 2. URANIUM CONCENTRATION RESULTS
(parts per million)

SAMPLE	URANIUM
4	1.11
70	3.82
61	0.26
69	0.75
33	63.60

After total iron was determined for eighteen of the twenty samples which had been measured spectrally, ferrous iron was determined by the Wilson Method. The Wilson Method is a wet chemistry procedure which uses excess V^{5+} in solution to reduce ferrous ion present in the sample. The remaining unreduced vanadium is then determined by titration with a standard ferrous ammonium sulphate solution (Bowman, 1975). Ferric iron concentration was then determined as the difference between total iron and ferrous iron. It became evident during this procedure that some of the results were incongruous. Ferric ion concentrations for some samples were unexpectedly low. Total iron was rerun by atomic absorption for eight samples with seemingly much more reasonable results.* The results for chemical determinations are given in Table 3. The first of these are most dependable, as indicated.

4.4 TOPOGRAPHY AND VEGETATIVE COVERAGE

In the basin proper, vegetation is relatively sparse except for areas of agriculture along waterways and chiefly underlain by Quaternary sediments. In general, sagebrush, bunch grass, and low rabbitbrush were the main vegetation. Estimates of cover averaged

---

* It is believed that the geochemical subcontractor did not fractionate the original samples according to standard procedure.

TABLE 3. IRON CONCENTRATION RESULTS (PERCENT)

SAMPLE NO.	TOTAL IRON	FERROUS	FERRIC
25	2.53	0.68	1.85
31	2.60	1.09	1.51
32	0.72	0.48	0.24
33	2.81	0.81	2.00
41	1.40	0.82	0.58
61	4.17	0.44	3.73
63	1.93	0.20	1.73
69	3.39	0.34	3.05
1	2.32*	0.92	1.40*
4	3.95*	0.18	3.77*
12	1.53*	0.42	1.11*
14	1.18*	0.38	0.80*
15	1.76*	0.68	1.08*
64	0.35*	0.19	0.16*
66	0.13*	0.02	0.11*
70	3.52*	0.14	3.38*
72	0.73*	0.31	0.42*
73	2.47*	0.90	1.57*

*Questionable Accuracy

about the same all over the area, although locally there could be considerable variation due to the size of sagebrush, etc. Grasses at this time of year were generally brown.

It must be recognized that relatively high $R_{5,4}$ values could result from very highly colored red material, or from a reduced percent of vegetation cover. Likewise, low values could obscure a small, highly colored area associated with dense vegetation in the rest of the pixel. For this reason, consideration of these areas which can be compared in the scene — those with relatively uniform vegetation — is most meaningful in this study.

The ratio technique is used explicitly to help diminish the effects of topography and sun angle on the data values. For this reason, features which are prominent on single channel images are often subdued in ratio images. Features of structural importance which can be seen due to topographic expression rather than spectral contrast sometimes become faded in a ratio. However, a lineation separating compositionally different materials should become more evident.

5
DATA PROCESSING

5.1 LANDSAT DATA CONFIGURATIONS

The Earth Resource Technology Satellite (ERTS), now LANDSAT, was designed specifically for monitoring natural resources. The satellite was launched in July, 1972, into a sun synchronous polar orbit giving it the capability of repetitative coverage on a cycle of 18 days. The satellite revolves around the earth every 103 minutes in a circular orbit 914 kilometers above sea level and gives generally consistent coverage for any one place on earth. It is repetitive coverage, providing passes at the same time of day and with the same lighting, that gives LANDSAT its great potential for monitoring time dependent changes in surface features.

The multispectral scanner of LANDSAT is a line-scanning device operating with bands in four spectral regions. Bandwidths are defined at the fifty percent response points of each detector. Band configuration is as shown below.

BAND	WAVELENGTH	SPECTRUM
1	0.5-0.6 μm	green-yellow
2	0.6-0.7 μm	red
3	0.7-0.8 μm	red-infrared
4	0.8-1.1 μm	near infrared

A four by six array of detectors is used for collection of complete data, six detectors for each spectral band scanning at one

time to cover the field as the satellite travels across the scene. Miscalibration of these six detectors can sometimes cause a periodic variation in levels of data, informally called "the every-sixth-line effect". To a limited extent, this effect is present in the Wind River data. It is sometimes enhanced by ratioing of two bands, a disadvantage of ratioing data of poor quality.

The instantaneous field of view for each detector of LANDSAT is 79 meters. The spatial resolution reported has actually been better than expected. LANDSAT images maintain detail of features without loss of definition at a scale of 1:250,000, and features with high spectral contrast with their background have been seen to scales of 1:30,000. Sometimes major highways and smaller roads can be identified on the data, although they are only fifteen feet wide (Maugh, 1973).

A definite advantage of LANDSAT data for exploration is the wide area coverage provided by one pass. One frame of data covers a region approximately 185 kilometers square, or approximately 10,000 square miles. Structural geologists have been very successful at recognizing linear features of importance to mineral exploration and regional structural trends which are not obvious on low altitude aircraft coverage and very difficult to detect from ground surveillance. In fact, it is in structural geology, with use of LANDSAT MSS images as aerial photographs, that many contributions with LANDSAT data have been made.

Another advantage of LANDSAT data over some satellite coverage is the repetitive coverage which allows choice of data collected when weather and atmospheric or vegetative characteristics were optimal for a specific study. The data chosen for this study was collected early in the life of LANDSAT — August 5, 1972. The frame used, E-1013-17294, was centered at north 43°10' west 108°17'.

5.2 PLANIMETRIC CORRECTION AND SCALING

LANDSAT images of two types are produced by the National Data Processing Facility at NASA/Goddard: system-corrected images and precision-processed images. They both represent photo maps, but with different degrees of accuracy. The system-corrected images are corrected for the major geometric distortions introduced by spacecraft orientation, sensor characteristics, and Earth's rotation. Precision-processed images include additional adjustments based on a number of in-scene ground-control points in each frame.

The bulk digital computer-compatible-tape (CCT) data are not corrected for any of these distortions. Bulk data are, however, preferred to precision CCT data for recognition processing because radiometric accuracy is degraded by rescanning in the latter. When displayed on a line-printer gray-tone map or CRT, substantial geometric distortions are evident in bulk CCT data. Square sections are displayed as parallelelograms. Such distortions increase the

difficulty of assigning pixels to specific ground areas during processing and in comparing output products with maps and photographs.

Some investigators have studied the cartographic aspects of ERTS data, digitally correcting to match an Earth coordinate system using spacecraft attitude information and/or ground control points spread throughout a frame. Other studies have dealt with the spatial registration of data from two or more frames that cover the same scene, using ground control points and/or image correlation techniques. Techniques for both cartographic correction and spatial registration of LANDSAT data move pixels from their original positions to an overlying grid by nearest-neighbor or interpolation rules. Nearest-neighbor operations increase the uncertainty of true field boundary locations, while interpolation degrades radiometric fidelity.

The procedure employed here to apply planimetric correction to LANDSAT computer-compatible tape data relied on an empirical map transformation derived by least squares calculations from a local network of control points located on topographic maps and used a nearest-neighbor algorithm for selecting data values. The transformation produced rotations to account for the slightly non-polar orbit aspect of LANDSAT and the difference in orientation between Earth and LANDSAT data coordinates. It also corrected for the effect of the Earth's rotation. The inverse of a procedure developed for computer-

aided assignment of pixels (Malila, et al., 1973), the transformation applied was a simple one which allowed only for translation, rotation, and scaling of the axes. There are additional distortions, such as the variable pixel size caused by non-constant scan mirror velocity, that could be corrected by refinements of the procedure.

Twenty nine distinguishable points from throughout the LANDSAT frame were selected as control points and an estimate of their LANDSAT line and point numbers was made by inspection of preliminary graymaps. Inaccuracy introduced by using an average latitude would have resulted in an error of no less than $\pm$ 10 pixels at the extreme north and south latitudes, or 4.6 mm. on a map of 1:250,000. The data site is in a suture of UTM coordinates, making this system unavailable also. Therefore, an arbitrary coordinate system was imposed by overlaying a 1:250,000 topographic map of the area with high quality graph paper and reading the orthogonal grid to the nearest 0.01 inch. This was more accurate than using latitude and longitude because it involved fitting an orthogonal grid to an orthogonal grid, rather than fitting an orthogonal grid to converging longitude lines. A least-squares fit of the superimposed grid points to LANDSAT coordinates (lines and points) reduced the error in the estimated location of each control point and produced a map transformation:

$$\begin{bmatrix} P \\ L \end{bmatrix} = \begin{bmatrix} a_{11} & a_{12} \\ a_{21} & a_{22} \end{bmatrix} \begin{bmatrix} X \\ Y \end{bmatrix} + \begin{bmatrix} b_1 \\ b_2 \end{bmatrix}$$

where P and L are the LANDSAT data lines and point numbers resprectively, and

(a_{ij}) are the empirical transformation coefficients,

X and Y are the arbitrary grid points to be transformed, and

b_1 and b_2 are the offset parameters to account for different origins.

At the same time the transformation was produced, a scaling matrix was used to scale the data for the given output requirements. It was decided in advance that the final product would be produced at 1 pixel to 0.14 mm.. To produce a map at 1:250,000, each pixel must then represent an area 88.19 meters square. The LANDSAT configuration of data results in one pixel representing an area approximately 57 m. x 79 m. on the initial data. Fitting the data to a smaller-scale grid resulted in omission of some pixels in order to comply with scaling requirements. Since the instantaneous field of view of the LANDSAT scanner was, in actuality, 79 m. x 79 m. overlap of spectral information in the initial data prevented an inordinant data loss, although approximately 1/3 of the points were dropped.

Cartographers have found that LANDSAT bulk imagery is suitable for accurate mapping up to the 1:250,000 scale, a world-wide standard for medium scale maps (Bylinsky, 1975). National Map Accuracy Standards require that 90% of the points be within 125 m. ($\pm$ 1 pixels) of true, at this scale. This is statistically equivalent

to 75 m. (∿.6 pixels) rms. A least squares regression of twenty nine points distributed around the test site resulted in an accuracy estimate of ± 4.45 pixels. By the root mean squares method, an accuracy of 2.94 pixels was indicated. In either case, using only the corrections presently available to us with non-optimal coordinate systems, we were not able to meet National Map Accuracy Standards. A major portion of the inaccuracy is probably due to the aforementioned scanner mirror velocity for which we were unable to correct.

5.3 THEORETICAL DEVELOPMENT OF RATIO PROCESSING

The two major purposes of the spectral ratioing method described below are to suppress spectral effects not related to the chemical or mineralogical composition of geologic targets and to enhance the appearance of selected geologic materials relative to "background" targets, which can include other geologic materials, vegetation and water. The ultimate classification of these materials, using spectral ratioing, is based on the premise that ratio spectra of known materials are representative of that material throughout the scene. We seek to minimize environmental variations in ratios in order to satisfy this premise, so that accurate classification can be performed.

Consider first the 0.4-2.5 μm spectral region (LANDSAT includes only the 0.5-1.1 μm region), in which most of the radiation emanating

from a target on the earth's surface is reflected solar radiation. The spectral radiance of a target measured by a multispectral scanner can be expressed as (Turner et al., 1971; Vincent, 1972):

$$L_\lambda = \frac{1}{\pi}\left[\frac{SE_\lambda\ (\text{direct})}{\cos\ \theta} + E_\lambda(\text{diffuse})\right]\tau(\lambda)\rho(\lambda) + L_\lambda(\text{path}) \qquad (1)$$

where L_λ = measured spectral radiance

S = the fraction of the instantaneous field of view covered by shadow

θ = angle between the surface and the line connecting the sun and the earth center

$E_\lambda(\text{direct})$ = direct spectral irradiance of the sun (impinging upon target)

$E_\lambda(\text{diffuse})$ = diffuse spectral irradiance of solar radiation incident on the target from directions other than sun-target direction

$\tau(\lambda)$ = atmospheric transmittance

$\rho(\lambda)$ = spectral reflectance of target

$L_\lambda(\text{path})$ = spectral path radiance (caused by atmospheric scattering)

In Eq. (1) the target is assumed to approximate a quasi-Lambertian reflector, with the angular (slope-angle) dependence of the bidirectional reflectance approximately the same for all wavelengths, (i.e.,shadow and slope factor (S) is independent of wavelength). The $L_\lambda(\text{path})$ term represents path radiance caused when light that has not encountered the target is scattered into the beam between target and detector.

Whenever the L_λ(path) term is negligible, as it can be with low altitude aircraft scanner data on a clear, dry day, all of the environmental factors are multiplicative. From satellite altitudes, however, L_λ(path) cannot generally be neglected. To eliminate most of this term under high visibility conditions, one can take the purely empirical approach of dark object subtraction. A dark material in shadow will have signal levels resulting from L_λ(path) and reflected diffuse irradiance, approximating the lowest possible radiance in the scene. For a given spectral channel, the value of the lowest radiance measured within the scene can be subtracted from all other spatial resolution elements to approximately correct for path radiance. If all multispectral channels are assumed to be spectrally narrow in the 0.4-2.5 μm wavelength region, the radiance in the i-th channel can be given by

$$L(i) \approx L_{\lambda_i} \Delta\lambda_i \tag{2}$$

where λ_i is the median wavelength and $\Delta\lambda_i$ is the spectral width (at 50% response points) of the i-th channel. After dark object subtraction, the ratio of the i-th and j-th channels will be approximately equal (Turner, et al., 1971; Thomson, 1973) to

$$R_{i,j} = \frac{L(i)}{L(j)} \approx \frac{[SE(\text{direct},i) + E(\text{diffuse},i)]\tau(i)\rho(i)}{[SE(\text{direct},j) + E(\text{diffuse},j)]\tau(j)\rho(j)} = \frac{E(\text{sun},i)\,\tau(i)\rho(i)}{E(\text{sun},j)\,\tau(j)\rho(j)}, \tag{3}$$

where E(sun,i) = SE(direct,i) + E(diffuse,i). In Eq. (3) the only terms which should vary widely over most geological test sites are S, cos θ, and $\rho(i)/\rho(j)$, the spectral reflectance ratio of the target. On a clear day of 23 km visibility at 0.55 μm (Turner, et al., 1971), E(direct,i) is approximately 73% of the total downwelling irradiance. For longer wavelengths, particularly those greater than 0.7 μm, the direct irradiance term is a much larger fraction of the total irradiance. The smaller the diffuse irradiance term, the less the S and cos θ factors, controlled primarily by topographic variations, affects $R_{i,j}$. When the diffuse term is negligible, as it can be for reflective infrared and sometimes for red spectral channels, the S-factor is essentially cancelled from the $R_{i,j}$ expression in Eq. (3). The $R_{i,j}$ ratio, therefore, is much more independent of topographic variations across the scene than is the single-channel radiance of Eq. (2).

Although $R_{i,j}$ should be relatively invariant with topographic changes across the scene, it still may not be invariant for a given type in two data sets collected at different times in different places. For a further suppression of environmental factors [E(sun, i), τ(i) and L(path, i)], one can use the spectral ratio of a known target to normalize to an area within the scene:

$$(R_{i,j})_{ref.} = \frac{E(sun,i)}{E(sun,j)} \frac{\tau(i)}{\tau(j)} \left[\frac{\rho(i)}{\rho(j)}\right]_{ref} \qquad (4)$$

Division of Eq. (3) by Eq. (4) yields, after rearrangement, the corrected ratio:

$$R^{c}_{i,j} \simeq \frac{R_{i,j}}{(R_{i,j})_{ref.}} \left(\frac{\rho_i}{\rho_j}\right)_{ref.} \simeq \frac{\rho_i}{\rho_j} \tag{5}$$

which is equal to the spectral reflectance ratio of the target, almost independently of environmental factors. The "almost" is included in the foregoing statement because the degree of environmental independence is a function of how well the dark object subtraction succeeds in suppressing the path radiance term. If shadows are present over materials of varying brightness, a more rigorous determination of L_λ(path) can be made, but with greater difficulty (Piech and Walker, 1974).

The use of a known reflectance value for calibration of a particular data set is described herein as ratio normalization. This procedure does not help discrimination among targets on a relative basis within a single data set, but it is useful for extending recognition results in time and space. Normalization is necessary for any absolute value determinations using reflectance values from laboratory spectra as training sets. In the future, improved atmospheric models allowing more accurate determination of multiplicative atmospheric terms (see Eq. 4) may alleviate the necessity for in-scene references (see Eq. 5).

5.4 DEVELOPMENT OF THE $R_{5,4}$ RATIO AND DENSITY SLICING

LANDSAT data was converted from the LANDSAT-CCT format to a 9 bit data format with a digital range of 0 to 511. In accord with the processing procedures described in Section 4.1, dark level subtraction and ratio processing were performed on the data to form a corrected $R_{5,4}$ ratio. Determination of the darkest values in the scene for each band of data was performed by searching bodies of water and cloud shadow that were seen on positive transparencies to be the darkest areas in the scene. Dark levels for each tape were assumed to be the best estimate of the voltage representing path radiance (see Section 4.1) and were subtracted from all the points in the scene. These levels had been determined for this data previously, and therefore, were already available for all bands. Digital values for each can be found below.

	LANDSAT MSS BANDS			
	4	5	6	7
Tape 1 (west)	12	6	4	0
Tape 2 (center west)	12	6	4	0
Tape 3 (center east)	16	11	9	2
Tape 4 (east)	16	11	8	1

In spite of different scaling constants relating digital counts to radiance in each band, these dark levels are consistent with expectations that path radiance would be greatest in the green band

and decrease to the longest wavelength infrared band. Also, it appears that there was some atmospheric variation across the scene, but that a degree of correction was allowed by dark level subtraction. Within one band, dark level determinations were smaller over higher elevations in the scene, i.e., west to east in each basin.

After these values were subtracted from the data, band 5 was divided into band 4 and the resulting digital values were scaled by multiplication to produce a new set of data representing the relative reflectance of each point in the red and green bands. This single ratio tape was used for analysis and is referred to as the LANDSAT $R_{5,4}$.

5.5 SPECIAL PURPOSE ANALOG RECOGNITION COMPUTER (SPARC) PROCESSING

Preliminary analog processing allowed a qualitative preview of results which could be used in the field and for planning research activities. Analog tapes of LANDSAT data of this region were already available from a previous study (Vincent, et al., 1975). Although Figures 17 to 24 were generated on the analog recognition computer from tapes of the same data used for the digital products, and are therefore comparable in every cardinal respect, there are important differences between the two.

First, in order to completely block out the fill-bytes at the edges of these LANDSAT analog tapes, framing requirements necessitated the loss of approximately 3% of the data at the end of each scan line

of each individual tape. This produced gaps when data from the four contiguous LANDSAT tapes were abutted. Note that this omission of data is in evidence in Figures 17 to 24. In addition, analog recognition products lack planimetric correction available in the digital product. These figures contain orbital skew and may not have an accurate aspect ratio.

Another important characteristic in the analog processed data is the apparent overlap of recognition due to "blooming" of recognition dots in the photographic process. This problem tends to bias the interpretation of the visual display by indicating stronger recognition and importance than is warranted, particularly where a few dots converge. The alternative to this is to use very light recognition and lose just as much detail due to non-reproduction of dispersed recognition. Again, this biases the data by making strongly recognized areas look more unique. These products do, however, have some advantages over IBM 7094 computer processed data in that they can be produced quickly, can display large amounts of data at reasonable expense, and are output directly onto photographic film for convenience of handling and reproduction.

A simple method for level slicing one channel of data on the Special Purpose Analog Recognition Computer (SPARC) was established. The initial step is the determination of the mean voltage in terms of the potentiometer settings for the maximum and minimum values for the data. This established the dynamic range for the ratio being

used. A small variance level was established to give narrow voltage windows for recognition. Density slicing involved varying the mean potentiometer in equal increments, leaving the width of the variance constant and straddling the means with contiguous voltage ranges.

Figures 17 and 24 show recognition resulting from density slices of the highest levels of the dynamic range of LANDSAT MSS Band 5/Band 4. These, although they do not correspond one to one with levels in the accompanying digital product, do show the same progression in voltage and therefore, relative ratio values. Results should be approximately the same for both products. Table 4 shows the analog levels corresponding to Figures 17 to 24 and their probable relationship to the digital levels represented in the accompanying color map.

TABLE 4. RELATIONSHIP OF ANALOG DENSITY SLICE LEVELS TO DIGITAL RANGES ON ACCOMPANYING COLOR MAP

ANALOG SLICE		COLOR DIGITAL	
FIGURE NO.	SLICE NO.	SLICE NO.	DIGITAL RANGE
		1	200-255
17	1	2	176-199
18	2	3	168-175
19	3	4	158-167
20	4	5	150-157
21	5	6	144-149
22	6	7	138-143
23	7	8	128-137
24	8	9	120-127
		10	94-119
		11	80-93
		12	12-79
		13	0-11

6

ANALYSES AND RESULTS

6.1 SPECTRAL RATIOS AND ANALYTICAL RESULTS

Laboratory measurements were conducted on twenty representative samples selected from the seventy three collected (See Appendix II). Although a variety of color and texture was present in the selection, some were chosen specifically because they were similar. Response-weighted reflectances and spectral ratios were calculated for LANDSAT bands from laboratory reflectances and are presented in Table 5. These were first compared with two color criteria, Munsell designation and a general color description. The latter was initiated because color differences which are important to geologists were not obvious in Munsell designations, particularly in the 10 YR hue range. The Munsell color and general color descriptions of each sample are listed in Table 6.

Testing first the relationships of LANDSAT visible channels to color, Figure 8 shows response-weighted reflectances for bands 4 and 5 against a progression of Munsell hues. Accordingly, MSS Band 4 separates these samples on the basis of color more correctly than Band 5, although the separation is not optimal. Notice that in these figures a progression from YR to GY to Y colors is used.

TABLE 5. CALCULATED RESPONSE-WEIGHTED REFLECTANCES AND RATIO VALUES FOR LANDSAT CHANNELS OF LABORATORY SPECTRAL MEASUREMENTS ON SAMPLES FROM THE WIND RIVER BASIN, WYOMING

SAMPLE NUMBER	BAND				RATIO					
	4	5	6	7	$R_{5,4}$	$R_{6,4}$	$R_{6,5}$	$R_{7,4}$	$R_{7,5}$	$R_{7,6}$
1	13.74	20.70	24.68	27.26	1.51	1.80	1.19	1.98	1.32	1.11
4	16.50	21.78	25.20	27.92	1.32	1.53	1.16	1.69	1.28	1.11
12	11.94	19.46	23.92	25.43	1.63	2.00	1.23	2.13	1.31	1.06
14	17.96	24.09	28.32	32.34	1.34	1.58	1.18	1.80	1.34	1.14
15	22.04	24.59	27.59	31.19	1.12	1.25	1.12	1.42	1.27	1.13
25	23.24	24.07	25.17	28.13	1.04	1.08	1.05	1.21	1.17	1.12
31	16.28	25.70	32.15	36.10	1.58	1.98	1.25	2.22	1.40	1.12
32	20.25	26.08	29.52	33.81	1.29	1.46	1.13	1.67	1.30	1.15
33	14.36	19.15	23.07	25.44	1.33	1.61	1.21	1.77	1.33	1.10
34	28.24	29.45	30.27	32.65	1.04	1.07	1.03	1.16	1.11	1.08
41	16.13	21.44	26.65	33.13	1.33	1.65	1.24	2.06	1.55	1.24
45	34.37	38.70	42.71	47.85	1.13	1.24	1.10	1.39	1.24	1.12
61	17.00	23.30	27.47	27.82	1.37	1.62	1.18	1.64	1.19	1.01
63	13.42	25.88	31.65	37.28	1.93	2.36	1.22	2.78	1.44	1.18
64	16.49	30.14	36.02	43.42	1.83	2.18	1.20	2.63	1.44	1.21
66	21.70	34.85	38.70	44.69	1.61	1.78	1.11	2.06	1.28	1.16
69	19.83	27.49	33.92	36.43	1.39	1.71	1.23	1.84	1.33	1.07
70	18.28	25.95	30.55	32.94	1.42	1.67	1.18	1.80	1.27	1.08
72	30.63	33.44	36.84	39.29	1.09	1.20	1.10	1.28	1.18	1.07
73	10.44	16.58	20.14	23.76	1.59	1.93	1.22	2.28	1.43	1.18

TABLE 6. COLOR DESIGNATIONS OF SAMPLES UNDERGOING ANALYTICAL MEASUREMENTS

SAMPLE NO.	MUNSELL COLOR	GENERAL COLOR AND ABBREVIATIONS	
64	5 YR 5.5/8	Dark Orange; (Nugget ss)	[Or]
66	5 YR 7/8	Light Orange; (Nugget ss)	[Or]
63	2.5 YR 4.5/6	Bright Red; (Chugwater Fm.)	[R]
12	5 YR 4/6	Dark Red-Brown	[R]
73	5 YR 4/4	Bright Red	[R]
31	5 YR 5/6	Pale Red	[R]
1	5 YR 5/4	Pale Red	[R]
70	10 YR 5/6	Yellow	[Y]
69	10 YR 6/5.5	Yellow	[Y]
61	10 YR 4/6	Yellow	[Y]
33	10 YR 5/5	Yellow	[Y]
4	10 YR 6/6	Yellow	[Y]
14	10 YR 5/3.5	Tan	[T]
41	10 YR 5/3	Tan	[T]
32	10 YR 6/3	Tan	[T]
45	2.5 Y 8/2	White to Pale Orange	[W]
15	5 Y 6/4	Yellow-Green	[YG]
72	5 Y 6/2	Pale Yellow-Green	[YG]
34	5 GY 7/2	Blue-Green	[G]
25	5 GY 6/2	Green	[G]

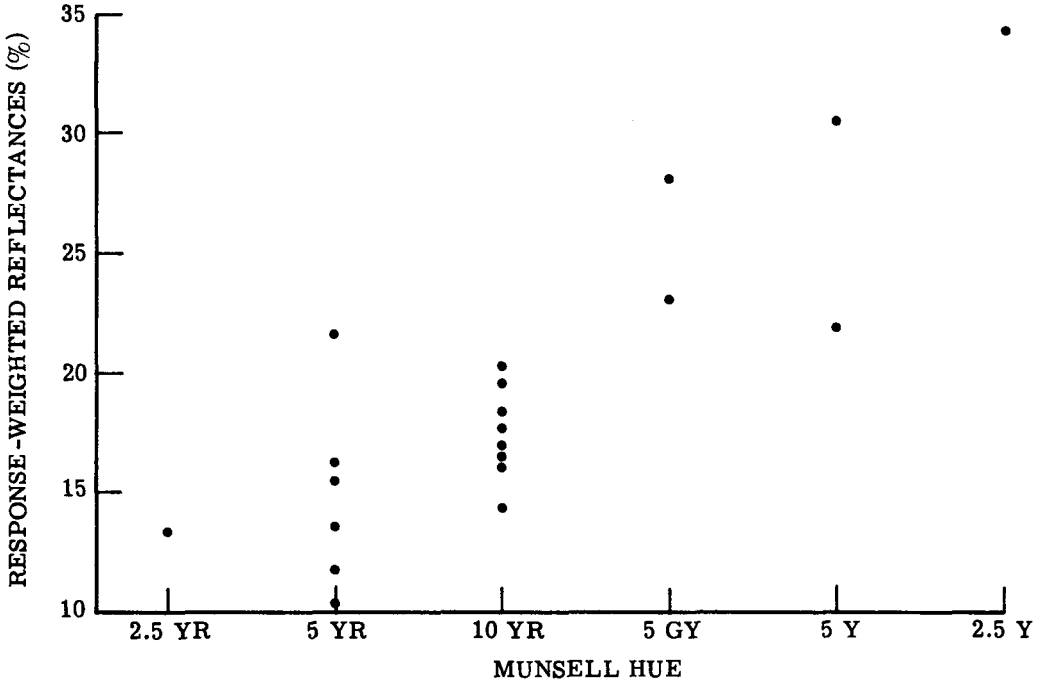

(a) Band 4 (Green)

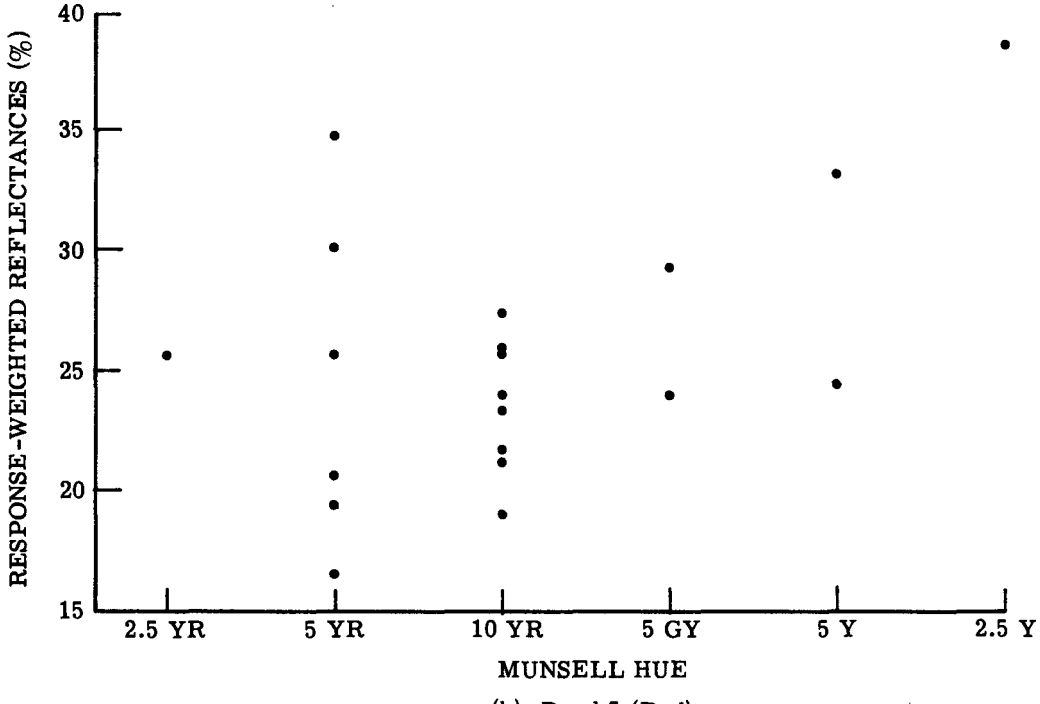

(b) Band 5 (Red)

FIGURE 8. LANDSAT RESPONSE-WEIGHTED REFLECTANCES FOR MSS BANDS 4 AND 5 VS. MUNSELL HUE FOR 20 SAMPLES OF SURFACE MATERIALS FROM WIND RIVER BASIN, WYOMING

Spectral ratio values using bands 5 and 4 were formed for each sample and plotted against full Munsell designation in the order of increasing ratio value (Figure 9). Note that unlike the single channel plots, samples having GY designations are at the end of the progression, which continues from Y to YR. The ratio values not only correlate well with Munsell hue, but show discontinuities between hue designations. This quantitative measure of differences is important for predicting LANDSAT capabilities for exploration.

Even with the differences apparent in Figure 9, which are above noise level of the LANDSAT scanner, important separations have still not been achieved. As indicated in Table 6, Munsell hue 10 YR contains samples of the general description of both tan and yellow. This is, geologically, an important distinction to make. Data points in the 10 YR range (and one other yellow sample) in Figure 9 are annotated by a small "y" indicating a yellow sample, or by a small "t" for tan. This ratio alone is unable to separate these two colors, their difference being obvious visually.

The sample spectral curves shown in Figure 10 illustrate the possible reasons for distinct color differences between these subgroups which cannot be detected by using the LANDSAT band configuration. A strong absorption feature at approximately 0.48 μm is clear in the spectra of all the yellow samples, but is not evident in those of the tan samples. Salisbury and Hunt (1970) have attributed iron absorptions in the .43 and .45 μm region to electronic transitions of

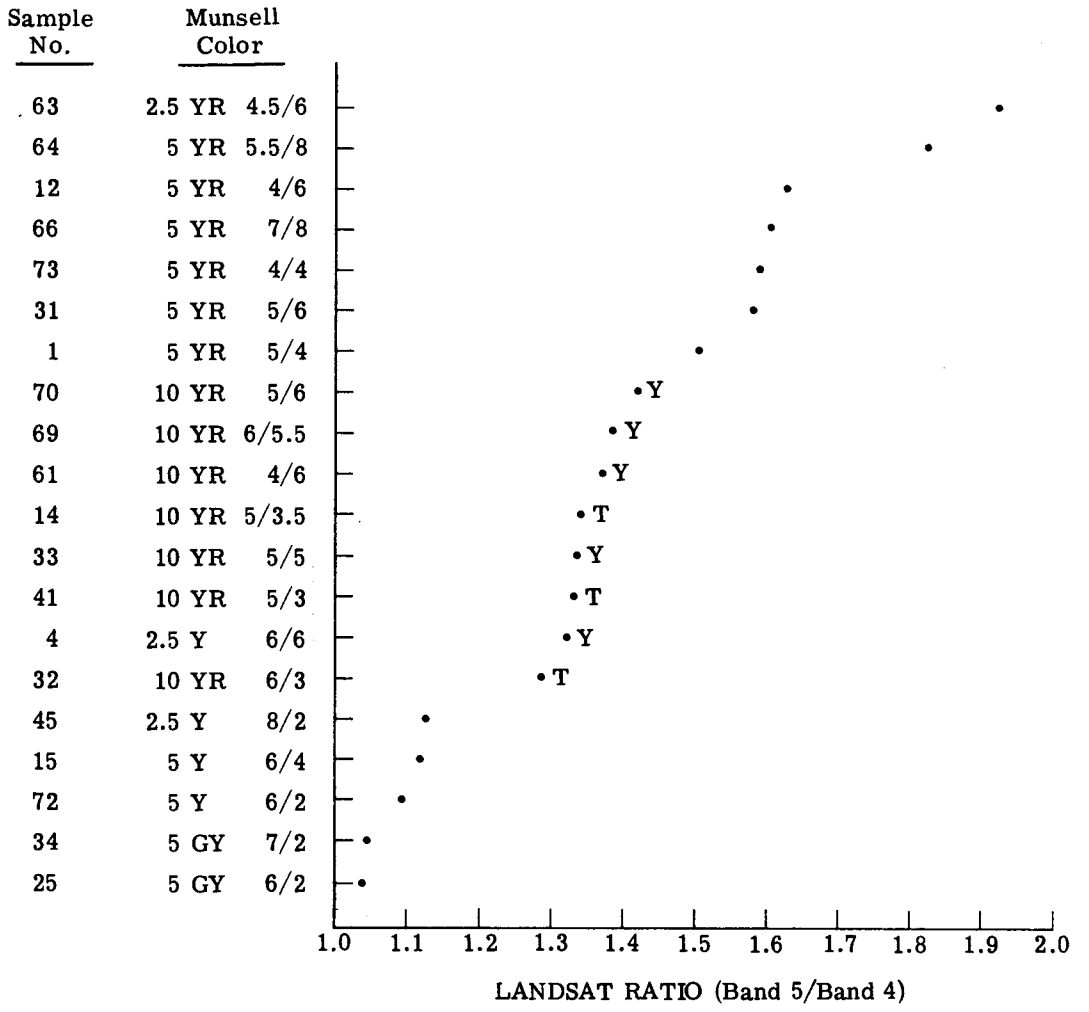

FIGURE 9. INCREASING LANDSAT $R_{5,4}$ VALUE VS. MUNSELL COLOR FOR 20 SAMPLES FROM WIND RIVER BASIN, WYOMING

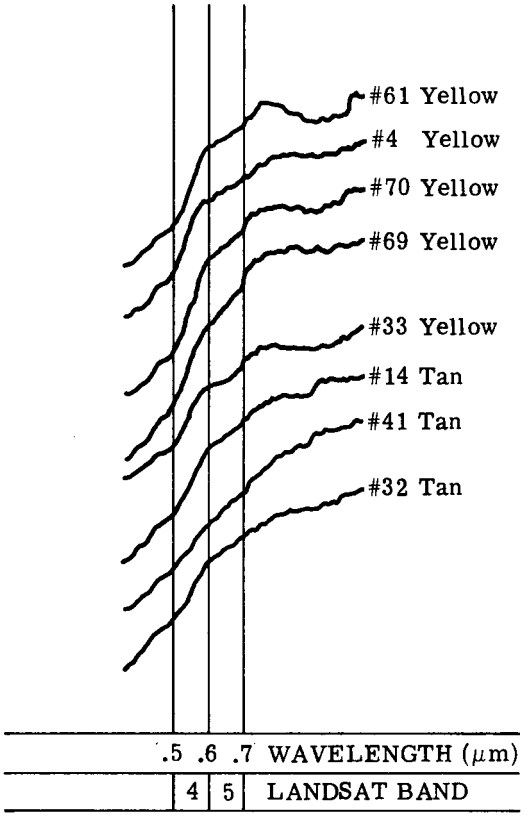

FIGURE 10. VISIBLE SPECTRAL DIFFERENCES IN SAMPLES SEPARATED INTO TAN AND YELLOW BY GENERAL COLOR

the Fe^{2+} ferrous ion. In all but two of the samples reported here, ferrous ion is less abundant than ferric, usually substantially so. In the samples in which the 0.48 μm feature is most distinct, both intuition and chemical analyses would support an Fe^{3+} ferric absorption. The solution of this problem is beyond the limits of this study; simply stated, this feature is strong in those samples high in Fe^{3+} ferric iron with a yellow color. Within band 4 there is an apparent slope difference between tan and yellow samples also. The wide band coverage of LANDSAT does not allow for use of this feature for their separation.

Spectra collected over the whole visible region show definite, promising differences between those colors of interest. The non-optimal LANDSAT configuration is unable to make use of these spectral features. As could be expected when ratioing two bands in the visible region of the spectrum, LANDSAT ratio $R_{5,4}$ is consistent with color differences as perceived visually, but not as sensitive to them as required for detecting the presence of yellow, limonitic stain. However, a degree of success with LANDSAT red to green can be achieved. This ratio is more sensitive to Munsell hue than is a single LANDSAT band even without consideration of atmospheric and topographic parameters. At least five levels of colors interesting to geologists should be separable, although these colors are likely also recognizable on aerial photography where it is available.

Having identified the $R_{5,4}$ successful direct correlation with color, the next question of importance concerns surface geochemistry. Iron determinations are plotted in Figure 11 against ratio values for the red to green $R_{5,4}$. General color determinations are annotated by letters next to the data points. Although results are partially consistent, the $R_{5,4}$ clearly does not separate the samples either on the basis of total iron (11a) or ferric iron (11b) content. More importantly, a relationship between color and iron content begins to appear and is elucidated in Figure 12 where samples are listed in the order of their ferric iron content with annotated color. In this case, the general color description correlates with iron content. The progression of colors as iron content increases is different from that correlating with the LANDSAT visual ratio, indicating that for this set of samples, $R_{5,4}$ ratio value does not correlate directly with iron content. However, relationship between that ratio and iron content is present, in that color seems to relate closely to both, albeit differently.

LANDSAT infrared bands were examined for possible geochemical information which may be apparent in the spectral data. Ratio $R_{7,6}$, dividing the 0.8-1.1 μm region by the 0.7-0.8 μm region, should result in low values where iron content is highest or most influential. Figure 13 shows $R_{7,6}$ ratio values vs. total iron and ferric iron, the two being relatively similar for these samples. Letter annotations

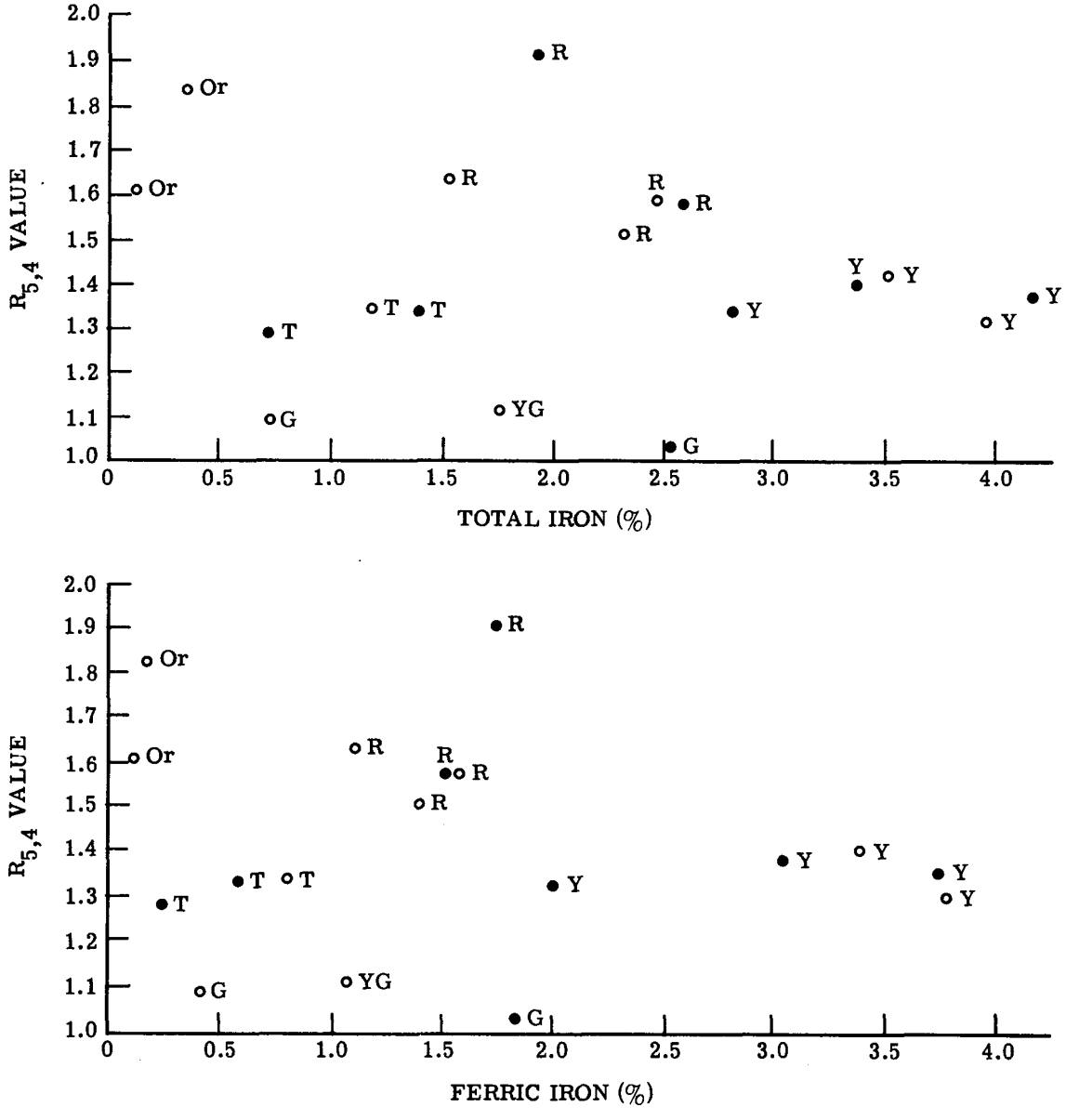

FIGURE 11. IRON CONTENT VS. LANDSAT $R_{5,4}$ VALUE FOR 20 SAMPLES FROM WIND RIVER BASIN, WYOMING

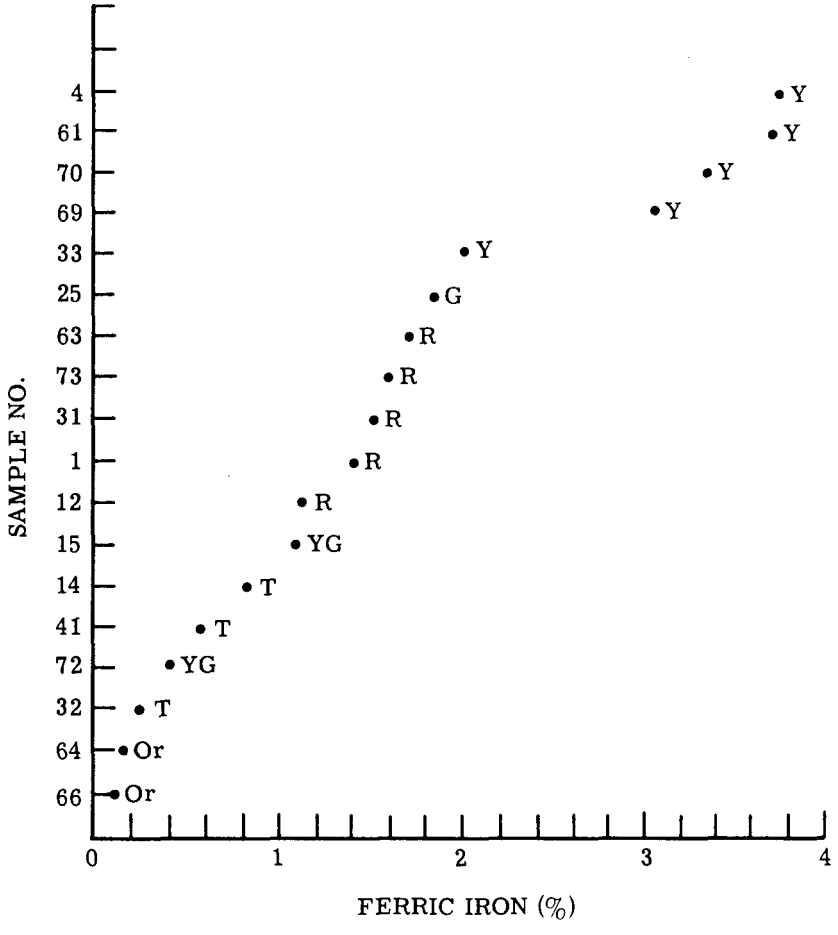

FIGURE 12. FERRIC IRON CONTENT VS. SAMPLE NUMBER.
Colors are annotated.

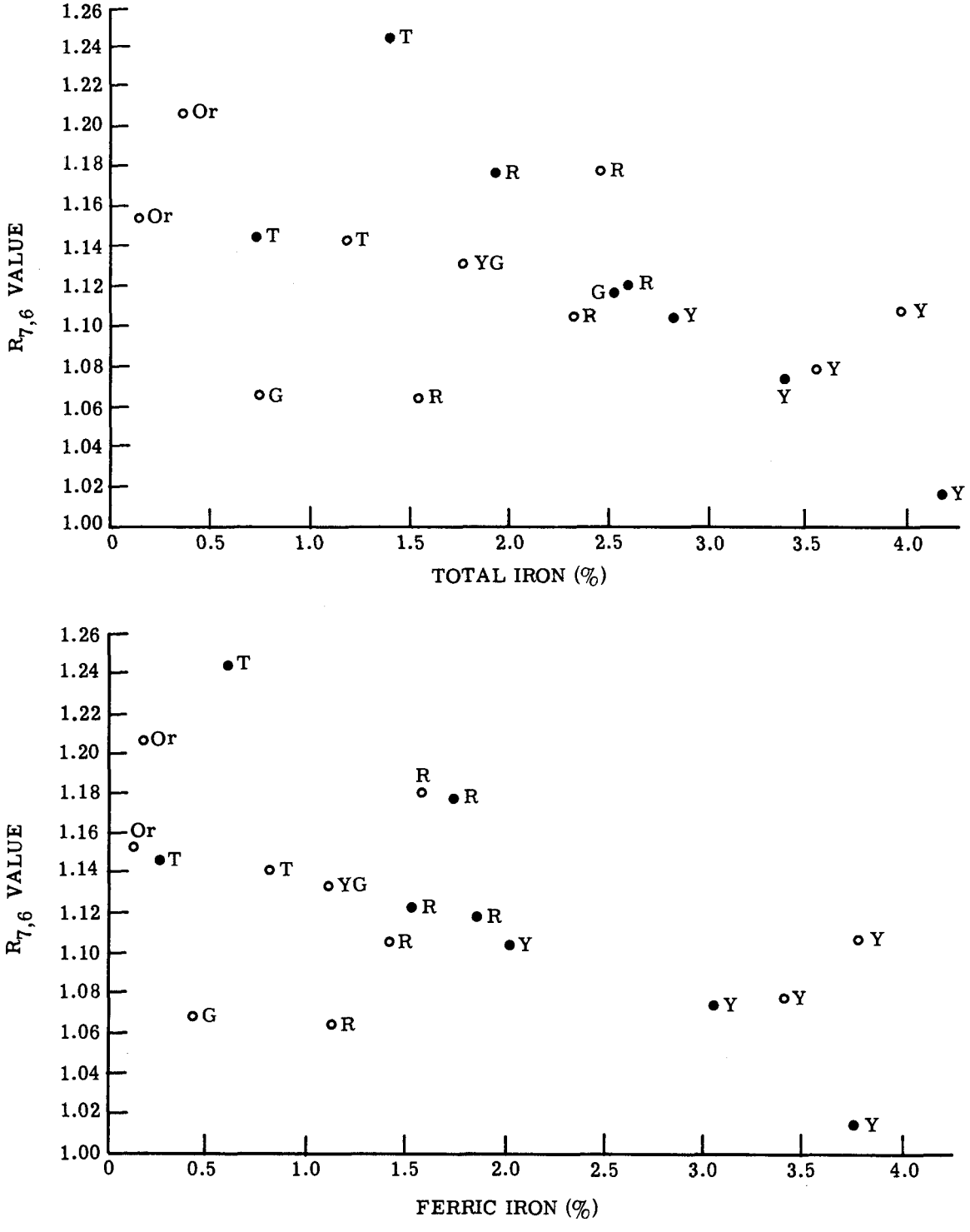

FIGURE 13. IRON CONTENT VS. LANDSAT $R_{7,6}$ VALUE FOR 20 SAMPLES FROM WIND RIVER BASIN, WYOMING

indicate general color designations. Most importantly, yellow samples, which in this case are highest in iron content (and ferric iron content), are easily separated from the tan samples. Looking at the spectra that have resulted in this trend, increased strength of a supposed iron absorption near 0.87 μm can be seen in these samples (Figure 14).

For the samples measured here, ferric iron content greater than two percent seems to result in significant absorption in the infrared. The infrared region, as it is collected by the LANDSAT satellite, is not necessarily optimal for recognition of the iron absorption bands. Increased spectral resolution may show even greater separation of this geochemical feature. It would seem, however, that recognition processing using at least the LANDSAT $R_{7,6}$ and $R_{5,4}$ ratios could do a better job of separating limonitic soils uniquely from other targets.

6.2 LANDSAT $R_{5,4}$ IN THE WIND RIVER BASIN

Interpretation of the $R_{5,4}$ ratio map of the Wind River Basin concurs with spectral information as it is presented in the previous section; limonitic stains associated with known or suspected uranium deposits were not separated using only this ratio. The colors that are enhanced using only the visible bands are not those of most importance for the alteration which is characteristic of this

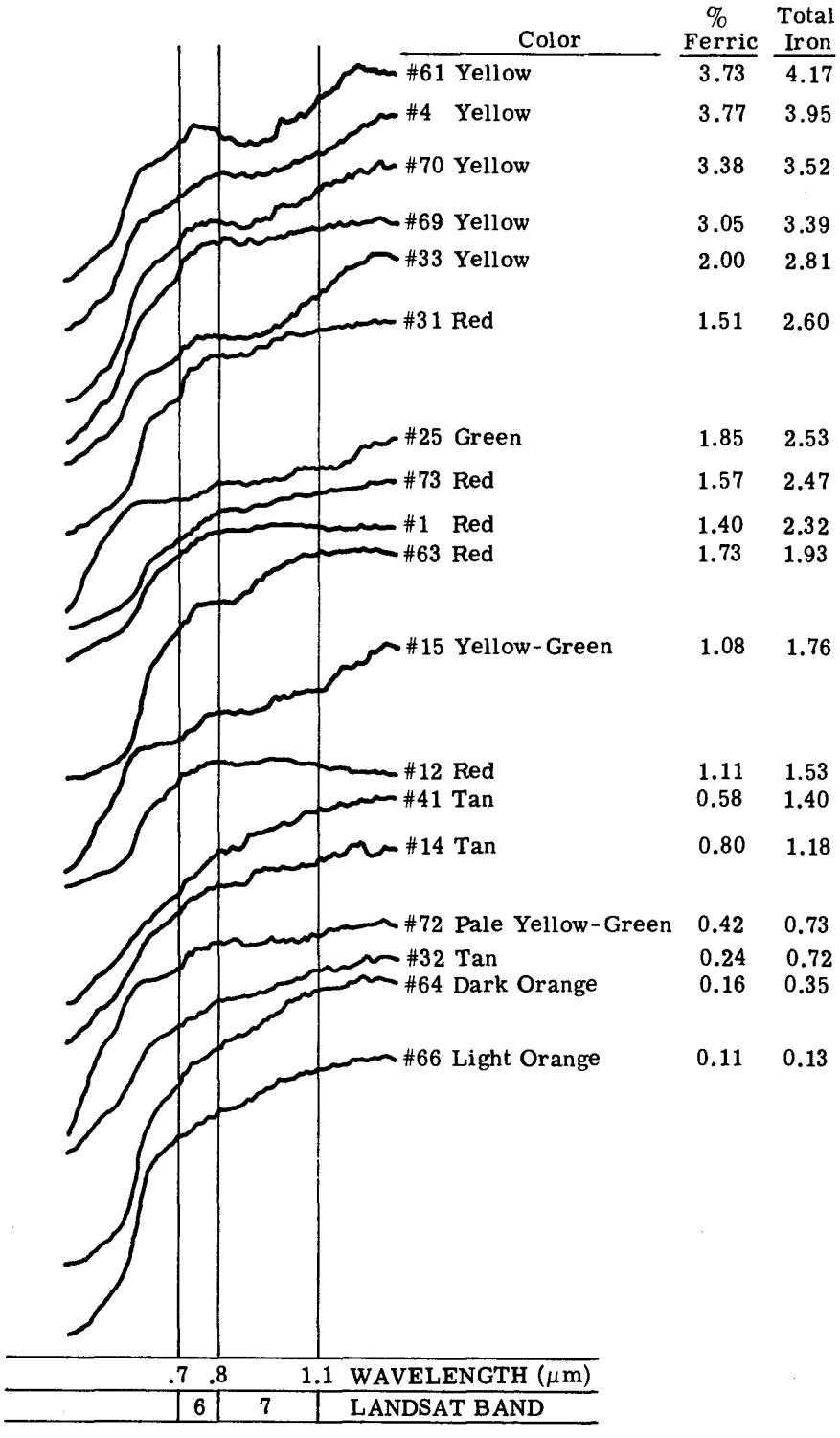

FIGURE 14. INFRARED SPECTRAL FEATURES IN ORDER OF DECREASING TOTAL IRON CONTENT. Annotated by general color.

geographical area. Moreover, the range of ratio values in which limonite-rich materials is likely to be found is also likely to be well populated with unimportant surface compositions. Figure 15 is the summary results of an airborne gamma spectrometer survey conducted in a separate study (Texas Instruments Incorporated, 1974). Neither the color digital map (provided to the sponsor only) nor the appropriate analog slices can be interpreted to have a definite correlation with these anomalies. This being the case, no recommendations for possible uranium prospects have been made.

Although the results of this specific study were not successful in locating prospective sites in the Wind River Basin, the results do warrant evaluation in the perspective of their systematic approach. Documentation substantiating the origin of specific "features" or "differences" is rare in the literature. As a result, techniques which appear to enhance "features" of importance in one application are sometimes found unreliable in the next application.

$R_{5,4}$ ratio digital map and the accompanying analog level slices apparently correlate very well with the relative values of the spectral data collected in the laboratory. The highest analog ratio slice represented in analog level slice 1 (Figure 17) clearly recognizes part of those areas mapped as Triassic Chugwater and associated formations. These are bright red, chiefly fine-grained clastic sediments which are well exposed throughout the west. Those areas

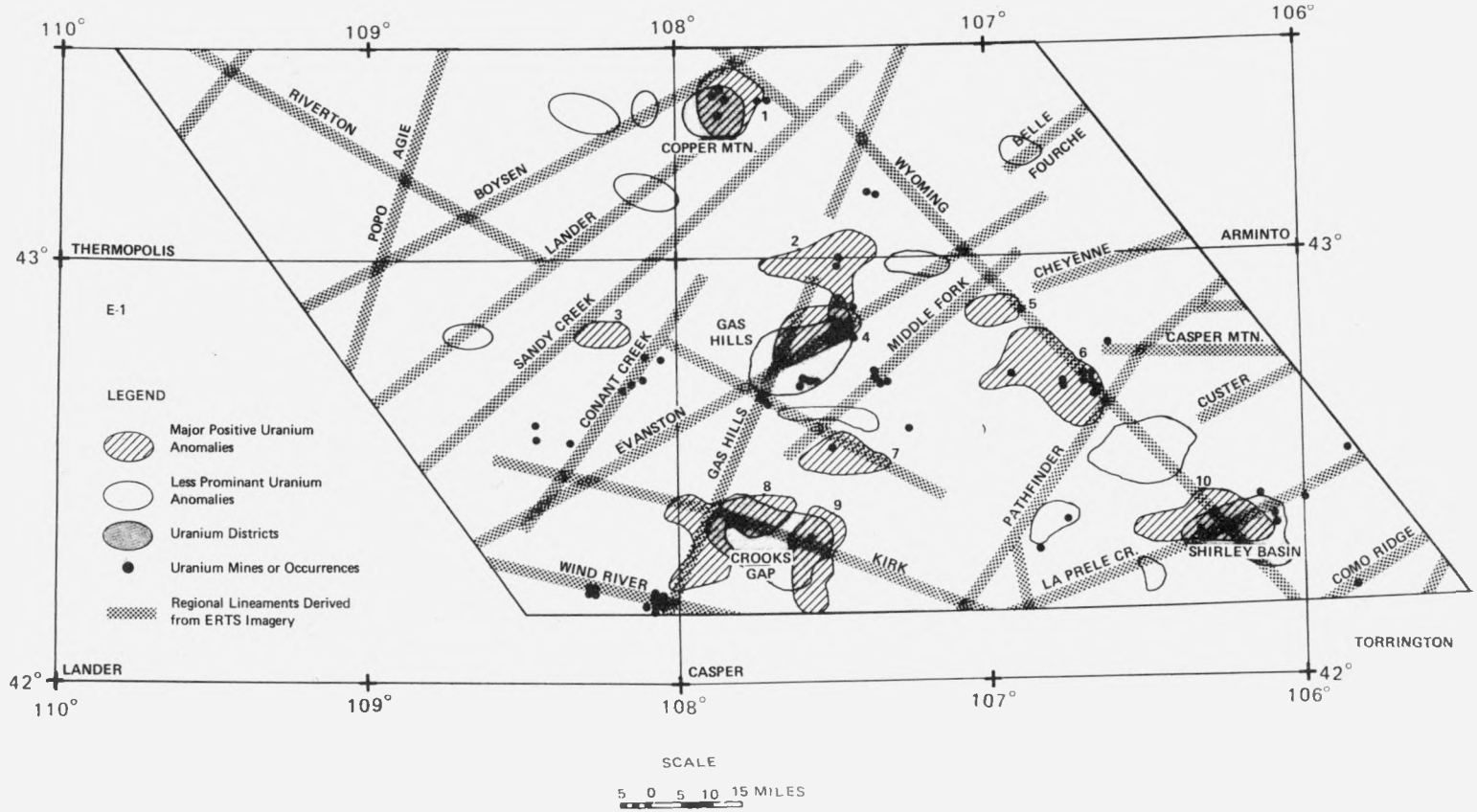

FIGURE 15. AREAS OF ANOMALOUS HIGH URANIUM GAMMA-RAY DATA. From Texas Instruments, 1974.

recognized in this highest $R_{5,4}$ slice are known in some places in the basin to be areas of very little to no vegetative cover. The next lower slice (Level Slice No. 2) still chiefly includes the Triassic redbeds, although a few other areas are recognized also (see Figure 18). Of particular interest in this slice and in slice no. 3 (Figure 19) is the recognition of areas inside the Mexican Flat and Beaver Creek oil localities. Figures 19 through 24 continue in levels of $R_{5,4}$ ratio from high values to low. Refer to Table 4 for explanation of the range of the level slice in relation to those on the digital map. Slice 4 (Figure 20) or slice 5, strongly "blooming" in Figure 21, is likely to contain those ratio values of limonitic stains which would have been important to this study. Slice 8 shows strictly areas of fairly dense, well-watered vegetation. Levels below slice 8 were not included here, as they chiefly recognized detail in large bodies of water, such as the Boysen reservoir.

Variation in vegetation cover, left unaccounted for, has the potential of influencing the results of an $R_{5,4}$ density sliced product. Improved quantitative determinations could result from an additional preprocessing technique which has been proposed for vegetation analysis. This procedure, which utilizes an infrared to red ratio relatively insensitive to soil conditions but very sensitive to vegetation cover, was actually devised for rangeland

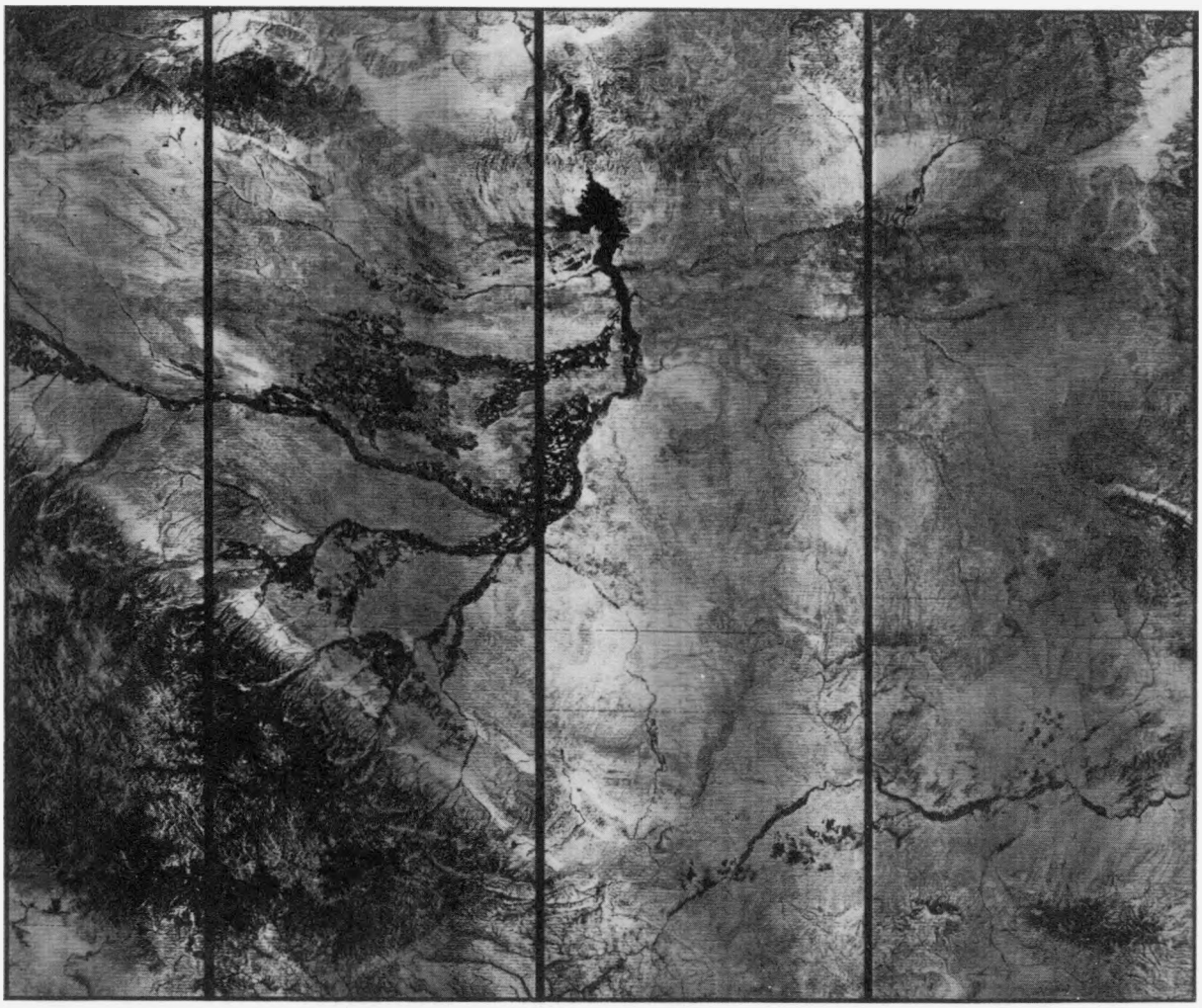

FIGURE 16. LANDSAT $R_{5,4}$ ANALOG RATIO IMAGE, WIND RIVER BASIN, WYOMING

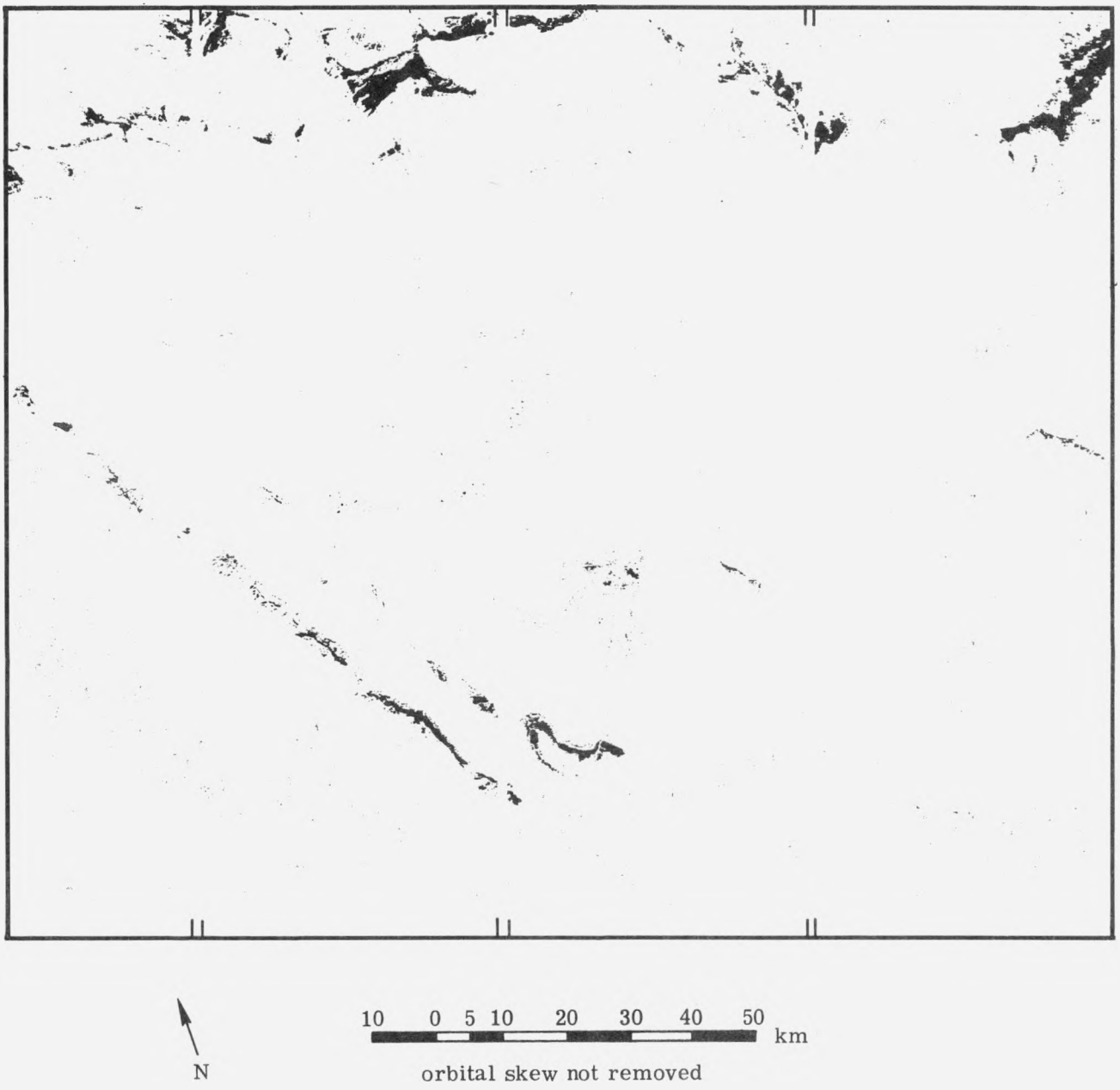

FIGURE 17. LEVEL SLICE NO. 1 OF LANDSAT $R_{5,4}$, WIND RIVER BASIN, WYOMING

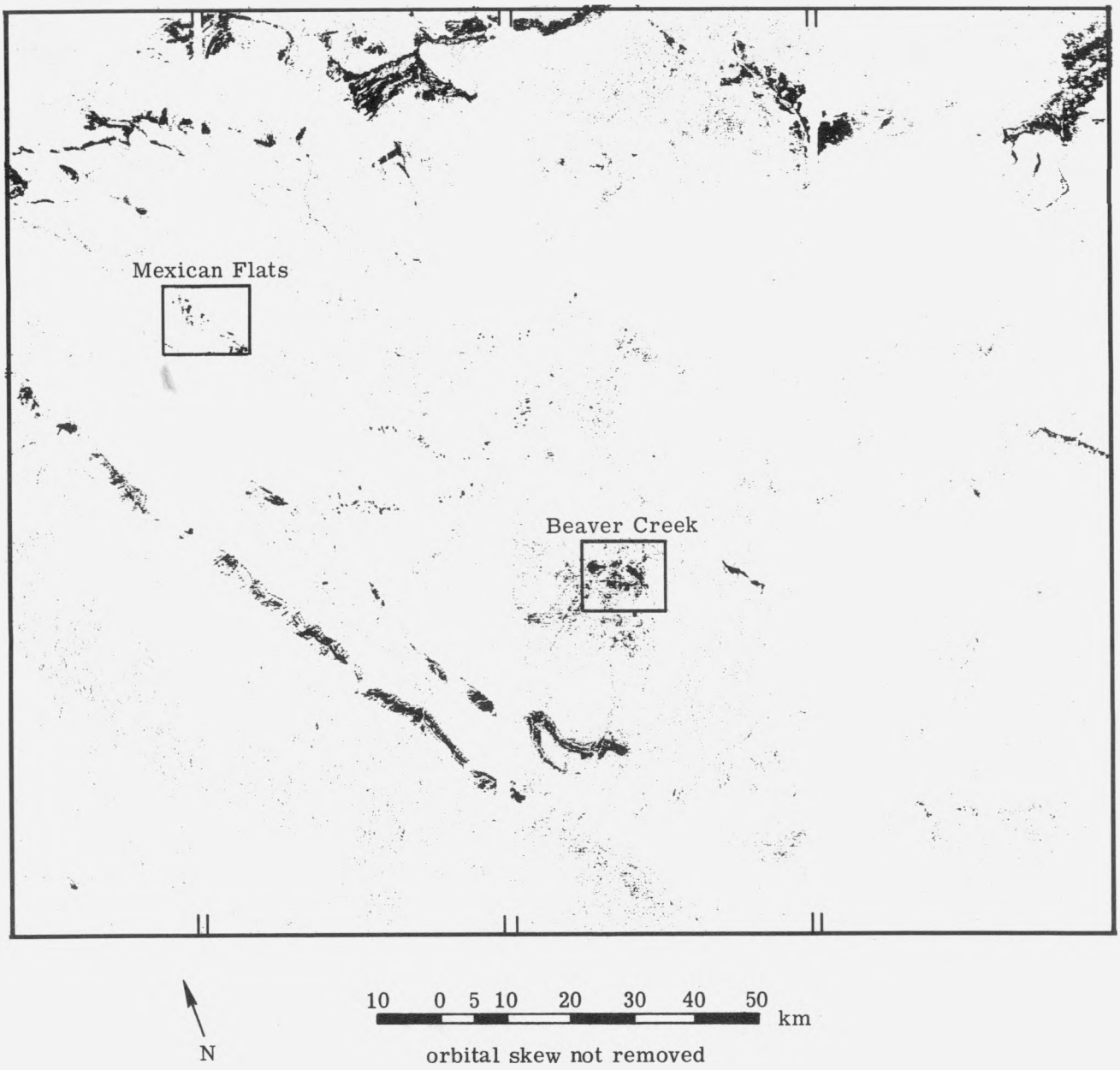

FIGURE 18. LEVEL SLICE NO. 2 OF LANDSAT $R_{5,4}$, WIND RIVER BASIN, WYOMING

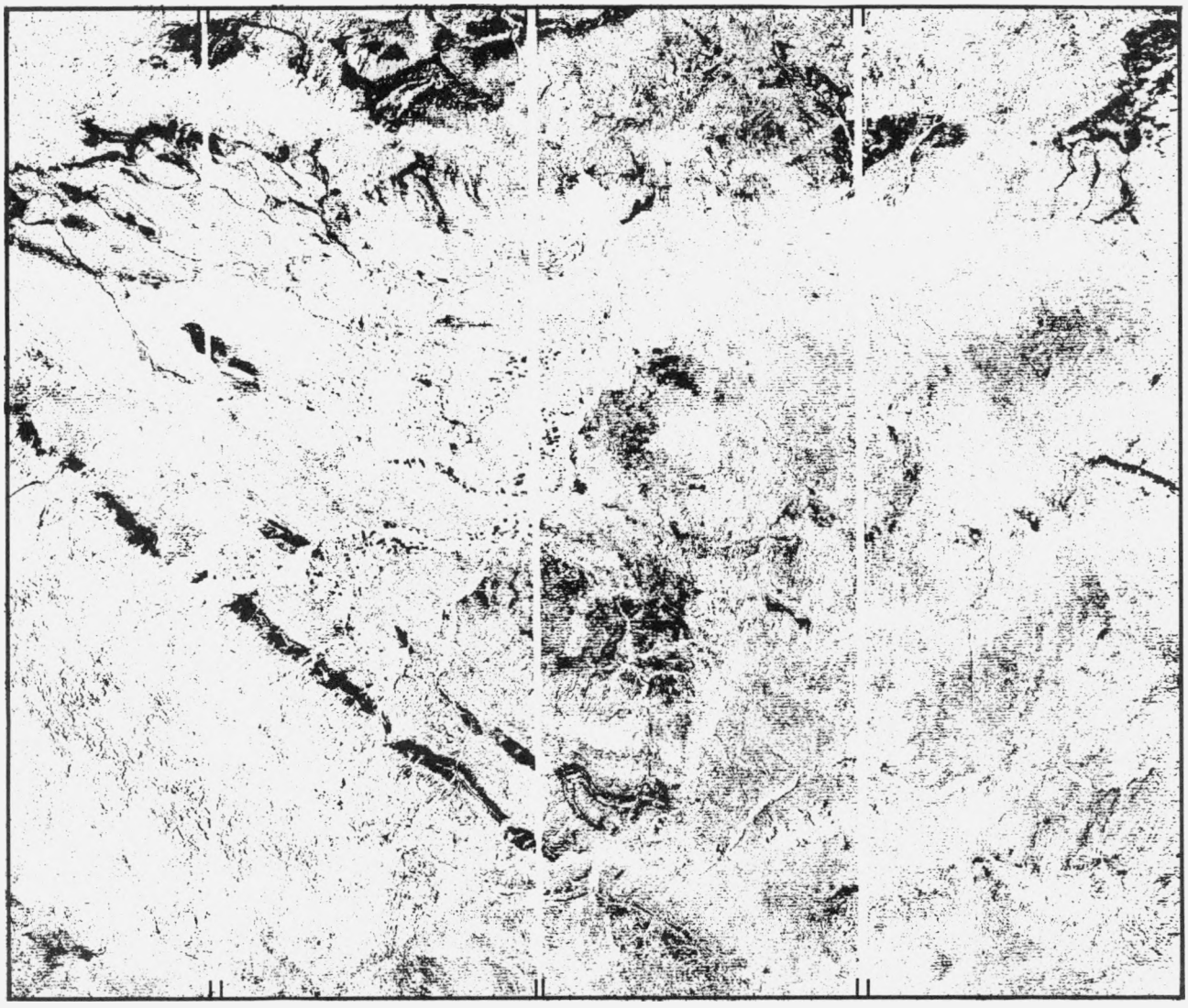

FIGURE 19. LEVEL SLICE NO. 3 OF LANDSAT $R_{5,4}$, WIND RIVER BASIN, WYOMING

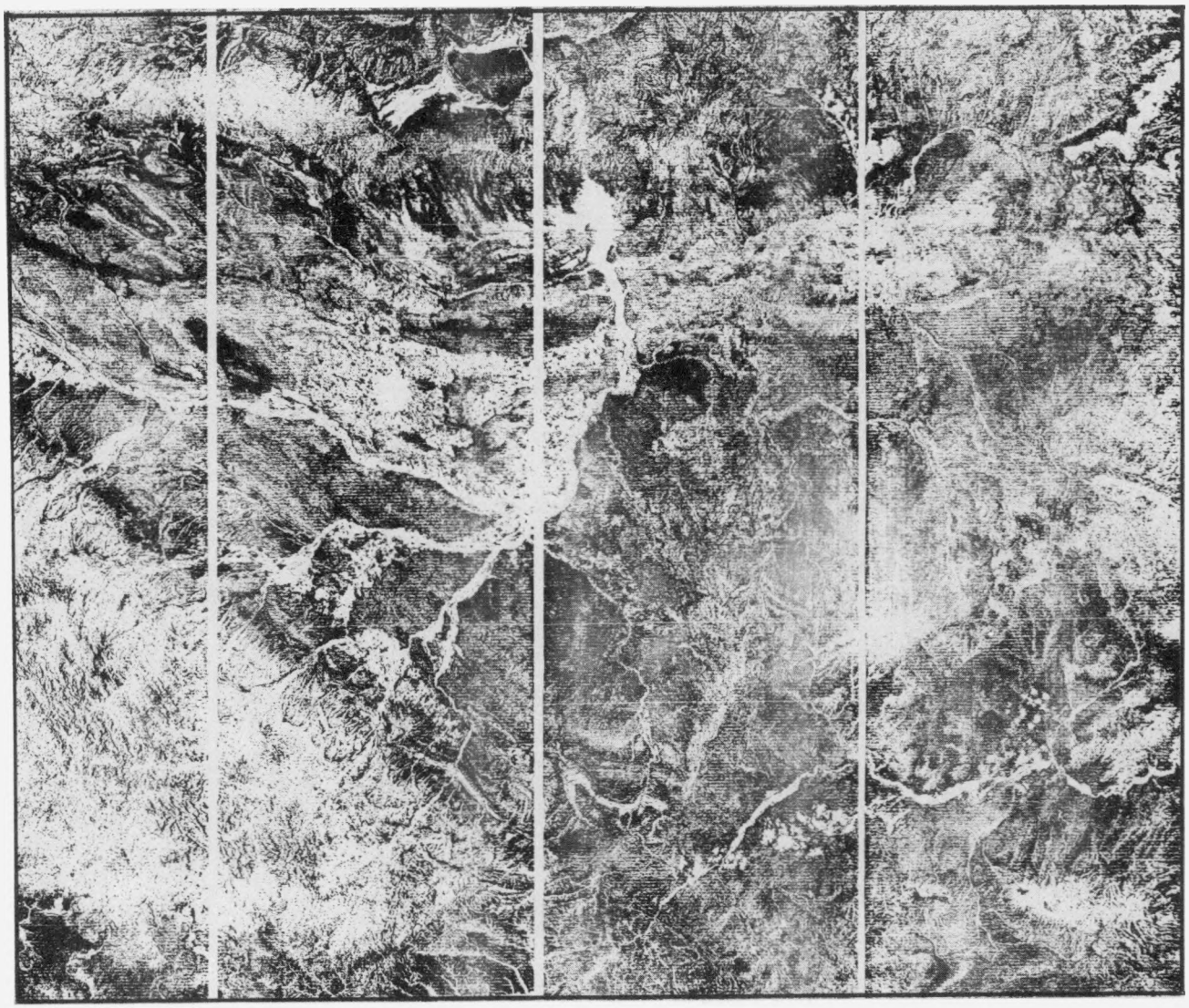

FIGURE 20. LEVEL SLICE NO. 4 OF LANDSAT $R_{5,4}$, WIND RIVER BASIN, WYOMING

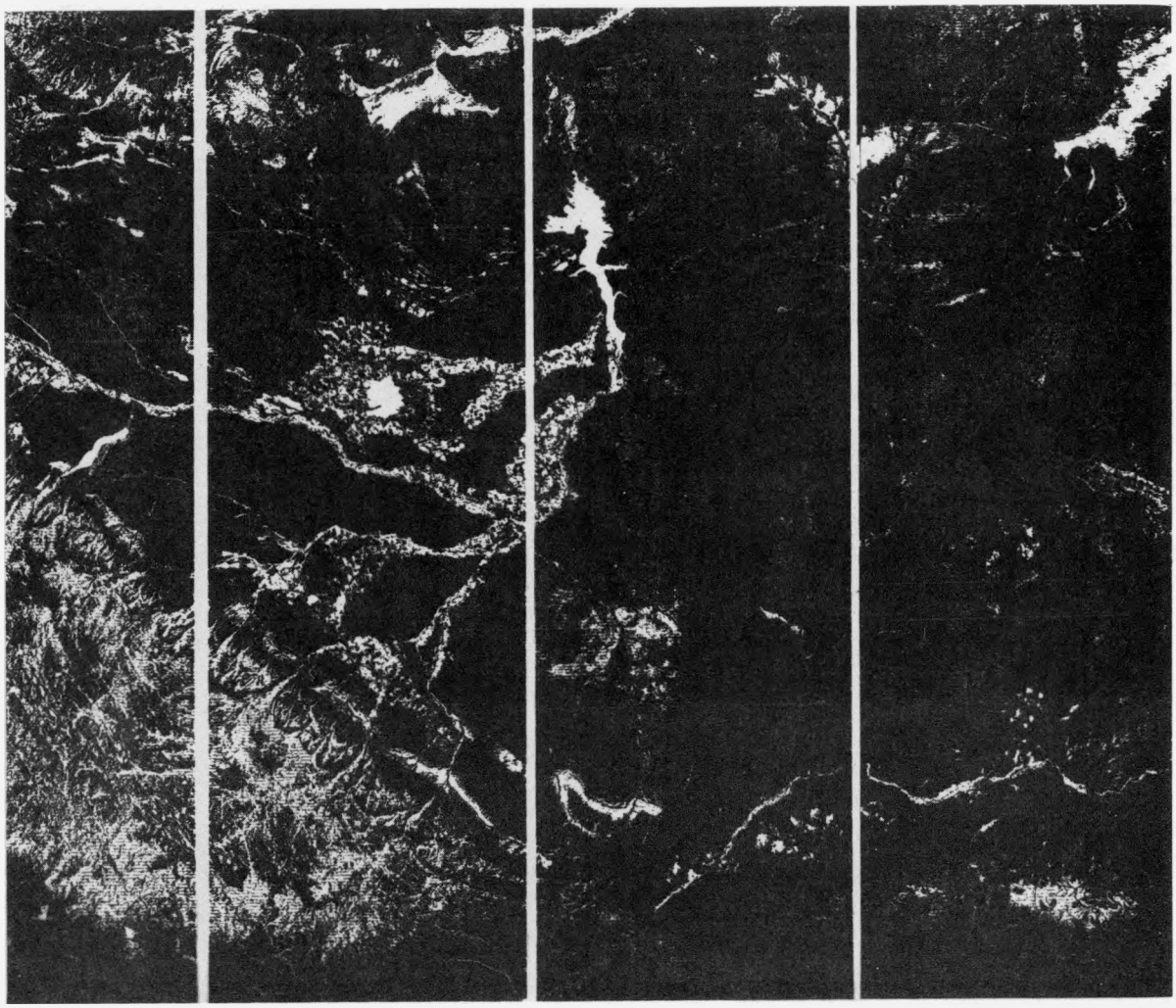

FIGURE 21. LEVEL SLICE NO. 5 OF LANDSAT $R_{5,4}$, WIND RIVER BASIN, WYOMING

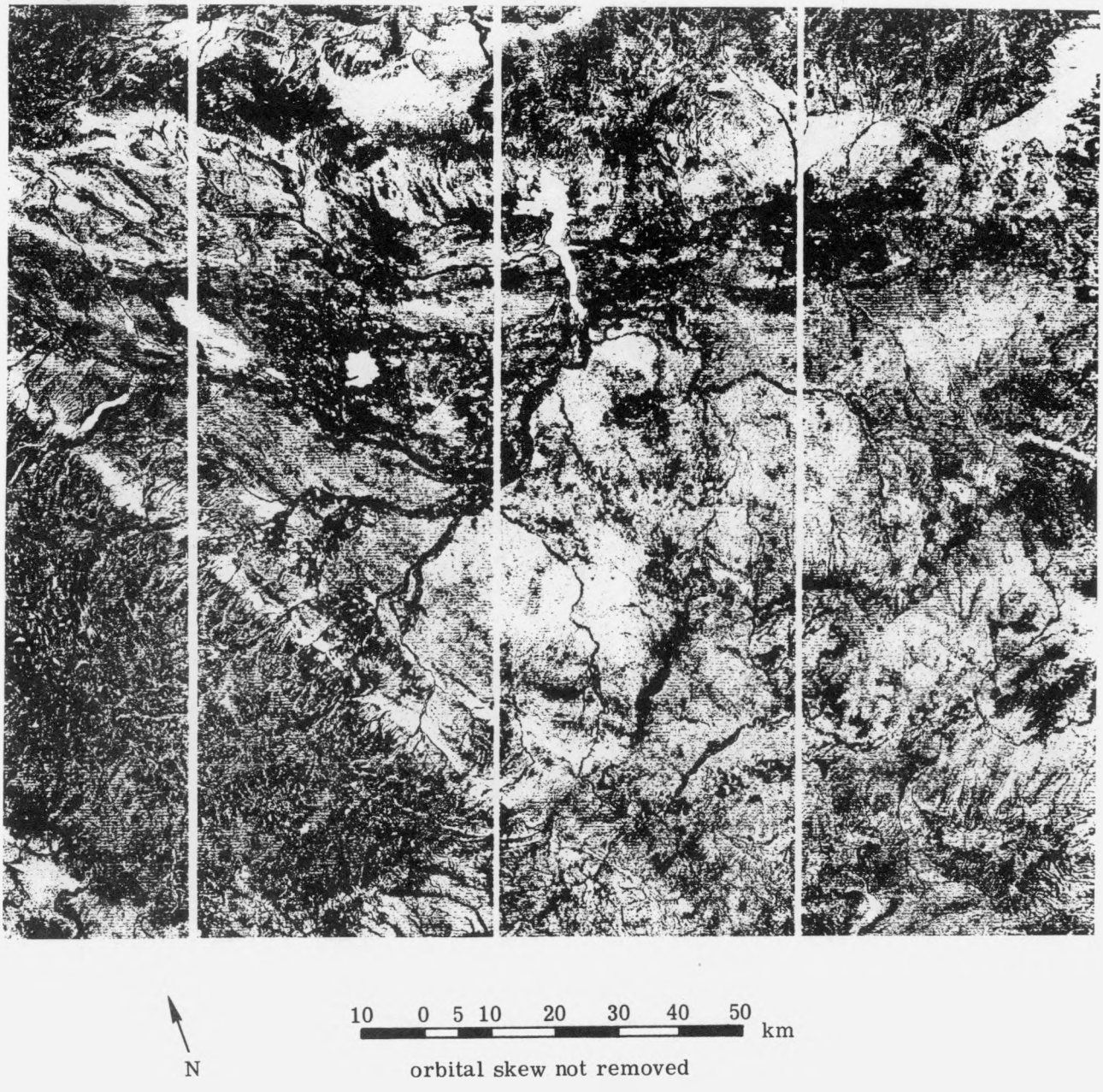

FIGURE 22. LEVEL SLICE NO. 6 OF LANDSAT $R_{5,4}$, WIND RIVER BASIN, WYOMING

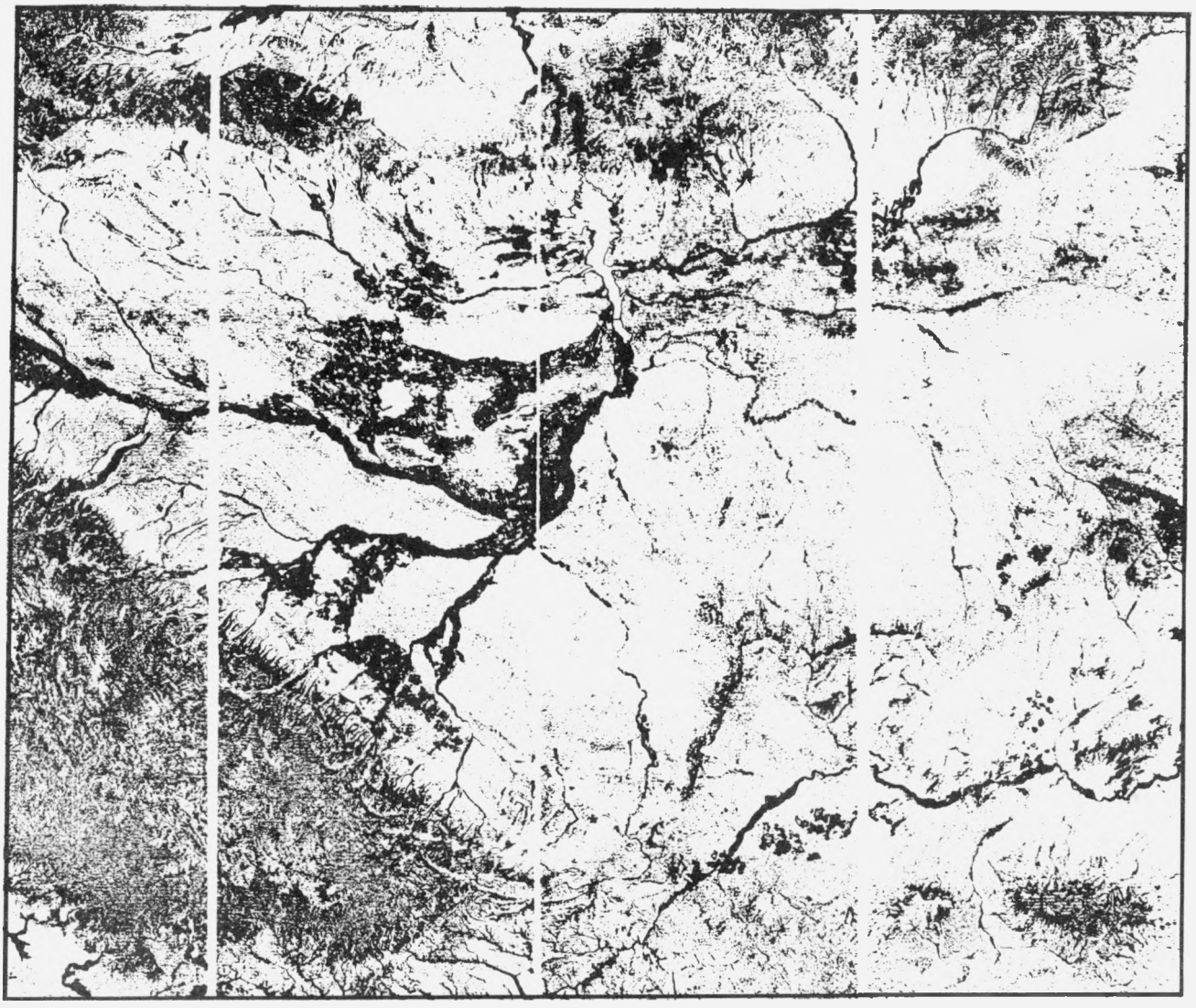

FIGURE 23. LEVEL SLICE NO. 7 OF LANDSAT $R_{5,4}$, WIND RIVER BASIN, WYOMING

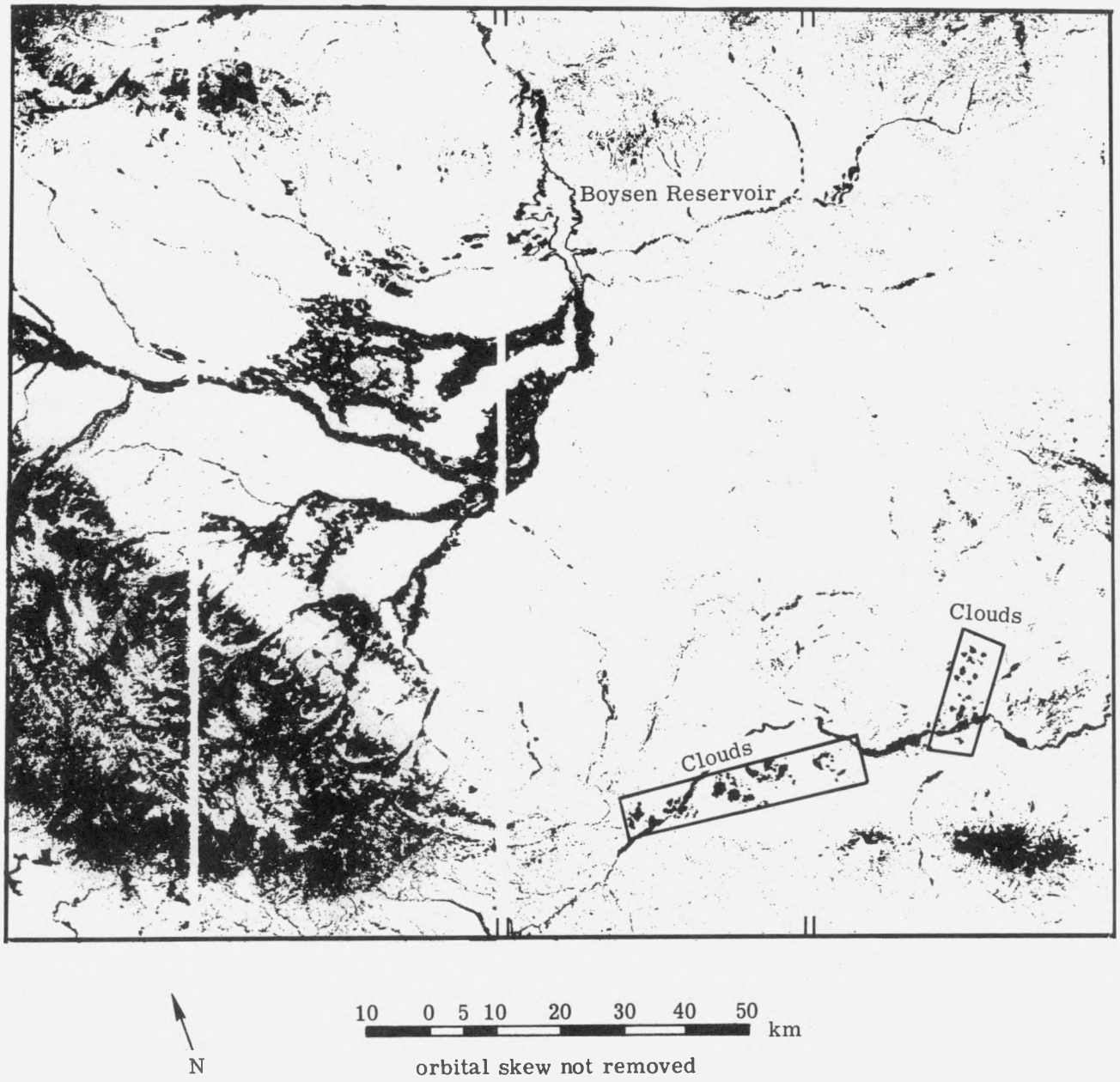

FIGURE 24. LEVEL SLICE NO. 8 OF LANDSAT $R_{5,4}$, WIND RIVER BASIN, WYOMING

evaluation. Estimates of live (green) vegetation, dead vegetation, percent shadow, and percent soil are made for control points. Normalization to these points would allow automatic correction for vegetative cover differences to reduce the number of variables in an $R_{5,4}$ determination. This correction was not performed on this data set. Without it, vegetation will always be a factor in spectral resolution.

In conclusion, it is only fair to say that the approach and procedures used herein have been shown to be internally consistent, and therefore promising. Although the desired enhancement was not effected here, much more is known now about possible future applications.

7

AUXILIARY INFORMATION AND SUGGESTED AREAS FOR CONTINUED STUDY

7.1 SKYLAB RESPONSE-WEIGHTED RELFECTANCES

The Skylab satellite was launched in April, 1973 into an orbit at an inclination of 50 degrees to the equator at approximately 235 nautical miles (435 km) altitude. The Earth Resources Experimental Package (EREP) aboard included visible-light and near-infrared photography and infrared spectrography, an electromechanical multispectral scanner, and microwave sensors. The multispectral scanner was a thirteen-band conical scan instrument with a 0.182 milliradian field of view. Scanning through 110° of the 360° scan assembly rotation, a ground swath of approximately 40 nautical miles (74 km) could be collected in one overpass. The multispectral configuration of the S-192 scanner is given in Table 7.

Response-weighted reflectances (Table 8) were generated from laboratory spectra using the Skylab band configuration for samples from the Wind River Basin (for method,see section 4.1). A comparison of Skylab red to green ratios and a look at some additional information shows that resolution of color differences geologically important was improved over LANDSAT results. Although eight samples which were divided by inspection into two groups, yellow and tan, were not separated using the LANDSAT red to green

TABLE 7. SKYLAB MULTISPECTRAL BANDS

CHANNEL	LOWER 50% POINT	UPPER 50% POINT
1	.42 μm	.45 μm
2	.45 μm	.50 μm
3	.50 μm	.55 μm
4	.54 μm	.60 μm
5	.60 μm	.65 μm
6	.65 μm	.73 μm
7	.77 μm	.89 μm
8	.93 μm	1.05 μm
9	1.03 μm	1.19 μm
10	1.15 μm	1.28 μm
11	1.55 μm	1.73 μm
12	2.10 μm	2.34 μm

TABLE 8. CALCULATED RESPONSE-WEIGHTED REFLECTANCES AND RATIO VALUES FOR SKYLAB CHANNELS OF LABORATORY SPECTRAL MEASUREMENTS ON SAMPLES FROM THE WIND RIVER BASIN, WYOMING

SAMPLE NUMBER	BAND				RATIO			
	3	4	5	6	$R_{5,3}$	$R_{5,4}$	$R_{6,3}$	$R_{6,4}$
1	11.23	14.93	18.87	22.18	1.68	1.26	1.98	1.49
4	13.18	18.24	20.20	22.77	1.53	1.11	1.73	1.25
12	9.30	13.34	17.61	21.30	1.89	1.32	2.29	1.60
14	14.96	19.31	22.24	25.50	1.49	1.15	1.71	1.32
15	19.28	23.00	23.38	25.00	1.21	1.02	1.30	1.09
25	21.62	23.19	23.01	24.02	1.06	0.99	1.11	1.04
31	12.50	18.32	23.67	27.88	1.89	1.29	2.23	1.52
32	17.30	21.43	24.24	27.21	1.40	1.13	1.57	1.27
33	11.47	15.86	17.70	20.53	1.54	1.12	1.79	1.30
34	26.41	28.07	28.06	29.30	1.06	1.00	1.11	1.04
41	13.88	16.99	19.51	23.28	1.41	1.15	1.68	1.37
45	31.34	34.79	36.36	39.72	1.16	1.05	1.27	1.14
61	13.23	19.05	21.62	24.62	1.63	1.14	1.86	1.29
63	9.68	15.60	23.23	28.19	2.40	1.49	2.91	1.81
64	11.60	19.40	27.46	32.40	2.37	1.42	2.79	1.67
66	16.12	24.86	32.26	36.20	2.00	1.30	2.25	1.46
69	16.01	21.76	24.95	30.06	1.56	1.15	1.88	1.38
70	14.08	20.60	23.93	27.74	1.70	1.16	1.97	1.35
72	27.77	31.16	31.58	34.38	1.14	1.01	1.24	1.10
73	8.13	11.66	15.06	17.80	1.85	1.29	2.19	1.53

ratio, they were separated using Skylab ratios $R_{5,3}$ and $R_{6,3}$. In Figures 25 and 26 a "y" marks any point corresponding to a yellow sample and a "t" marks any corresponding to a tan sample. Note that in each case the tans and yellows now group together in ratio values, although in $R_{5,3}$ a pale red is also included with the yellows. Sample 4 is an interesting exception to the usual smooth progression through Munsell designation, as it is visually more similar in color to the yellows of the 10 YR group. This separation is an important one for recognition of alteration associated with goethite-limonite, which lends a yellow stain to soils and rocks. It was made, however, on the slope difference of the spectral curves (Figure 10) and did not take advantage of the absorption at approximately 0.48 μm.

Graphs showing iron content and color compared to Skylab response-weighted reflectances indicate infinite possibilities for separation. However, the radiometric fidelity of the Skylab instrument would, from experience, limit the success which could be achieved. Other sensors with band configurations more specific than the relatively wide band configuration of LANDSAT may provide the answer.

7.2 URANIUM OCCURRENCE IN THE POWDER RIVER BASIN

The results of spectral reflectance data for LANDSAT band configurations mark other possibilities for uranium exploration. Although it appears that limonitic alteration is not uniquely

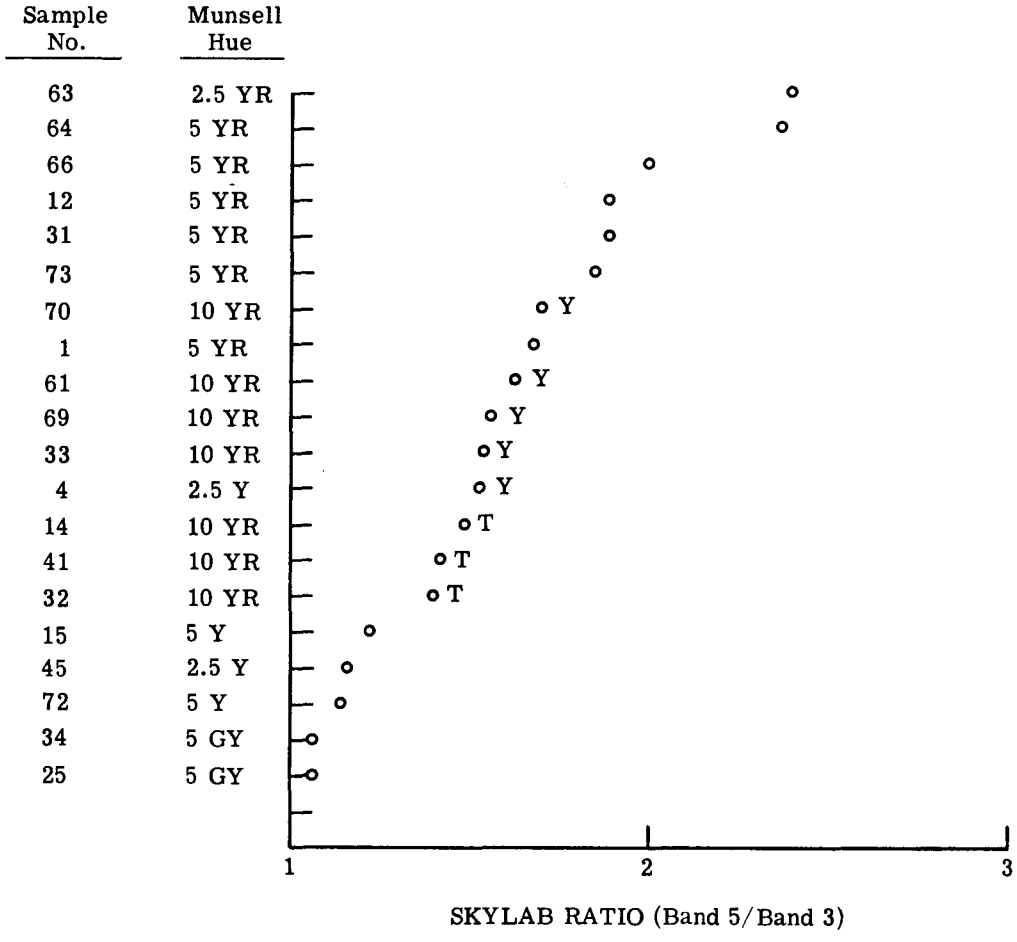

FIGURE 25. INCREASING SKYLAB $R_{5,3}$ VALUE VS. MUNSELL HUE FOR 20 SAMPLES FROM WIND RIVER BASIN, WYOMING

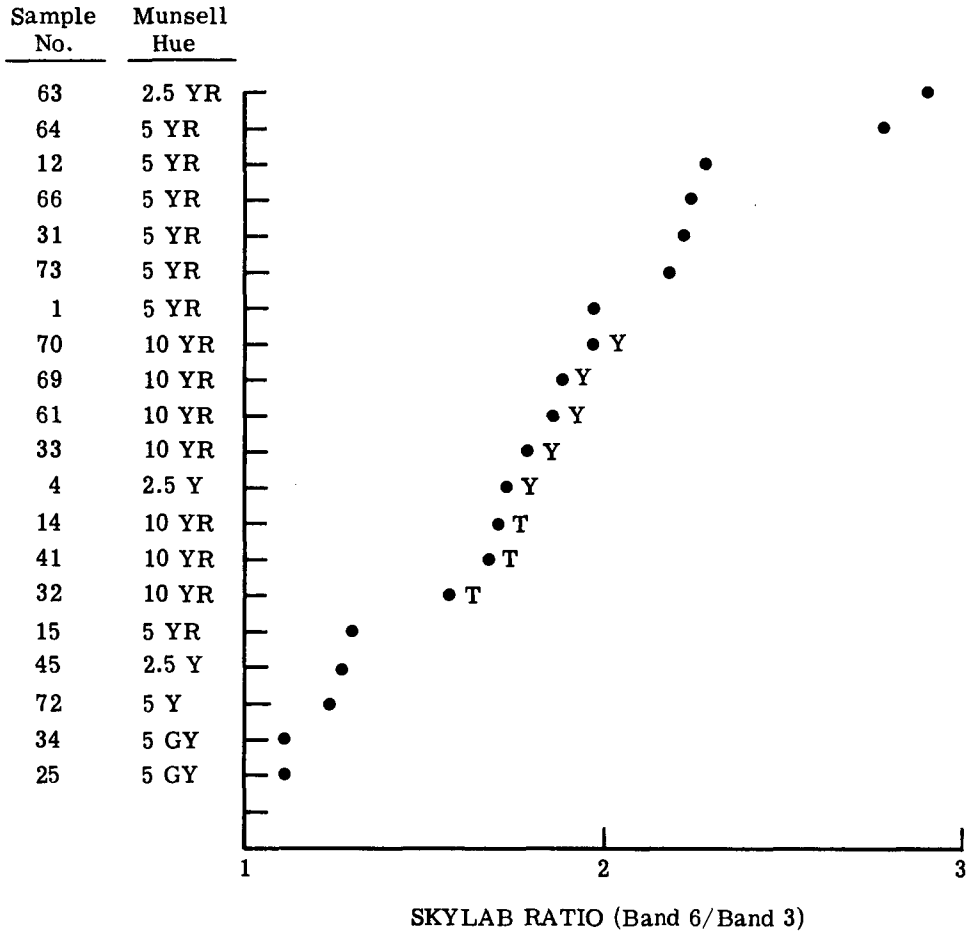

FIGURE 26. INCREASING SKYLAB $R_{6,3}$ VALUE VS. MUNSELL HUE FOR 20 SAMPLES FROM WIND RIVER BASIN, WYOMING

recognized using the single ratio approach, a single ratio procedure may be of more importance where hematite alteration is characteristic. In this light, uranium deposits such as those found in the Powder River Basin (Figure 1) are of interest as potential remote sensing targets. As indicated by the results in section 6.1, red colors produced on sandstones by hematitic stain should be easily recognized with an $R_{5,4}$ ratio alone.

The host formations in the Powder River Basin are the Fort Union and Wasatch (stratigraphically correlative to the Wind River Formation) of Early Eocene Age. Unaltered sandstones downdip of the roll-type deposits are typically gray to dark gray with humate and carbonaceous material present (Childers, M. O., 1970). Hematite stain, resulting in pale red, lavendar, and pinkish-red tones, is the pervasive and distinctive alteration updip of mineralized zones in this area. It appears that these red sands were formed by the oxidation of diagenetic pyrite at the same time groundwaters carrying mobilized uranium and vanadium deposited ore bodies at the oxidation-reduction interface.

Local reducing conditions at the ore zone are often recognized through color changes in sandstones and associated mudstones. According to Finch (1967),near the uranium there are often color changes to brown, yellow, gray, or green, and the mudstone layers immediate to the ore zone have been changed from bright red to gray

or green. Pyrite is often found in the unaltered sandstone near the alteration contact. Chemical and mineralogical studies of the altered and unaltered materials show little difference other than oxidation state of iron oxide. Rapid changes in sediment grain size, such as from coarse to fines in a scour and fill deposit, can also produce an altered-unaltered contact without concomittant mineralization.

Apart from colorful mineralogical difference, the occurrence of the roll-type deposits in this region is similar to the situation in the Wind River Basin. The origin of the uranium deposited in the Powder River Basin is postulated by Davis (1970) as the Oligocene-Pliocene tuffs which once covered the area. Hydrolysis of these tuffs producing alkaline groundwater conditions allowed the mobilization of the uranium which was later deposited in the permeable sands of the older Paleocene sediments. According to Davis, the permeability of the volcanics allowing leaching would have been good until hydrolosis produced clays from the volcanic material. Unoxidized ore bodies which are sometimes presently found were protected from weathering by caps of impervious silt and claystone overburden. This protective stratigraphic layer figures strongly into the location of oxidized or unoxidized deposits, although there is evidence that some unoxidized deposits have resulted from solution

and reconcentration of oxidized deposits. For this and similar areas, spectral studies of clays derived from volcanic material may be of additional interest.

7.3 FUTURE WORK

This program was directed toward one aspect and processing techniques of LANDSAT data and was, therefore, of limited scope. The chief purpose here was to document the basis on which a red to green ratio seemed to enhance areas of hematite and possibly limonite. Until now, there had been no definitive studies of the spectral characteristics, color, and composition showing clear correlation with actual LANDSAT data. Although only a minimum of compositional and spectral information could be collected for this study, to the limited extent it was applied the results indicate many promising areas for continued work.

Recommendations for continued multispectral work are as follows:

1. Continue and improve the implementation of response-weighted reflectances for LANDSAT and other multispectral configurations. Response-weighted reflectances should be recalculated using the actual response curves of the LANDSAT multispectral scanner. The University of Michigan M7 scanner and/or other appropriate responses should be used to generate comparable response-weighted reflectances for those samples already measured in the laboratory.

2. Measure the spectral reflectivities of more natural materials with continued study of their significant differences. The twenty samples cited here are the bare minimum for consideration. Some additional pertinent measurements are available in the literature, although adequate documentation of these samples is rarely provided. Color determination and spectral measurement, preferably accompanied with compositional information, are imperative.

3. Implement processing procedures which minimize or negate the effects of variable vegetation cover on spectral response. Differences in spectral reflectivities are only the first step in a feasibility study. Although in isolated cases negligible vegetative interference may be a good assumption, such an approach will be highly restrictive in an operational exploration effort. The reliability of data processing in the visible and near-infrared will always depend on variability afforded by different degrees of vegetative cover. As mentioned, interest in measuring biomass as a parameter for rangeland evaluation has led to the development of the algorithms necessary for vegetation correction. Before the application of more sophisticated processing for geologic purposes without accounting for vegetative differences, collaboration with experts in the remote sensing of vegetation is advisable.

4. Use to advantage the improved band selection available in existing scanners other than LANDSAT MSS. LANDSAT multispectral bands

are relatively broad and were never expected to be optimal for mineral exploration. The presence in the Wind River Basin of surface concentrations of both limonite and hematite provided an opportunity to test LANDSAT sensitivity to these two colorful iron oxides as they occur naturally. This effort was partially hindered by mineralogical determinations of inadequate sensitivity. Systematic results, however, based on color designations assuming red pigmentation to come chiefly from hematite and yellow chiefly from goethite-limonite, have allowed a measure of success.

It can be seen from these results that there are prevalent spectral features which are not adequately cultivated by LANDSAT MSS configuration. Other band configurations, such as those narrow bands available on some existing aircraft scanners, may allow more sophisticated separation of spectral differences.

5. Use multi-ratio processing of LANDSAT data to explore for uranium deposits associated with limonite.

6. Use single ratio processing (if uniform vegetation cover is assumed) of LANDSAT $R_{5,4}$ for uranium deposits in areas such as the Powder River Basin where hematite is the important alteration iron oxide.

7. Investigate whether or not the spectral properties of other alteration products, such as kaolinite and sericite, contribute spectral properties which are measurable separately from the strong

influence of iron oxides. Processing techniques which most effectively recognize iron oxides may not be appropriate for enhancing the spectral contributions of these products.

8. Try other methods of processing for enhancement of color or other spectral differences. Ratio processing, although chosen here on sound basis for suppressing environmental factors, must be recognized as a one-dimensional system. As expected, any single ratio cannot account for all color differences, as color is a multi-dimensional feature. More complex approaches could be taken to any specific color question. Such approaches, however, carry the implicit requirement that the significance of the color feature in question be recognized as pertinent in the task confronted, i.e., exploration for uranium.

APPENDIX I

SPECTRAL CURVES FOR MATERIALS COLLECTED IN THE WIND RIVER BASIN, WYOMING, 1974

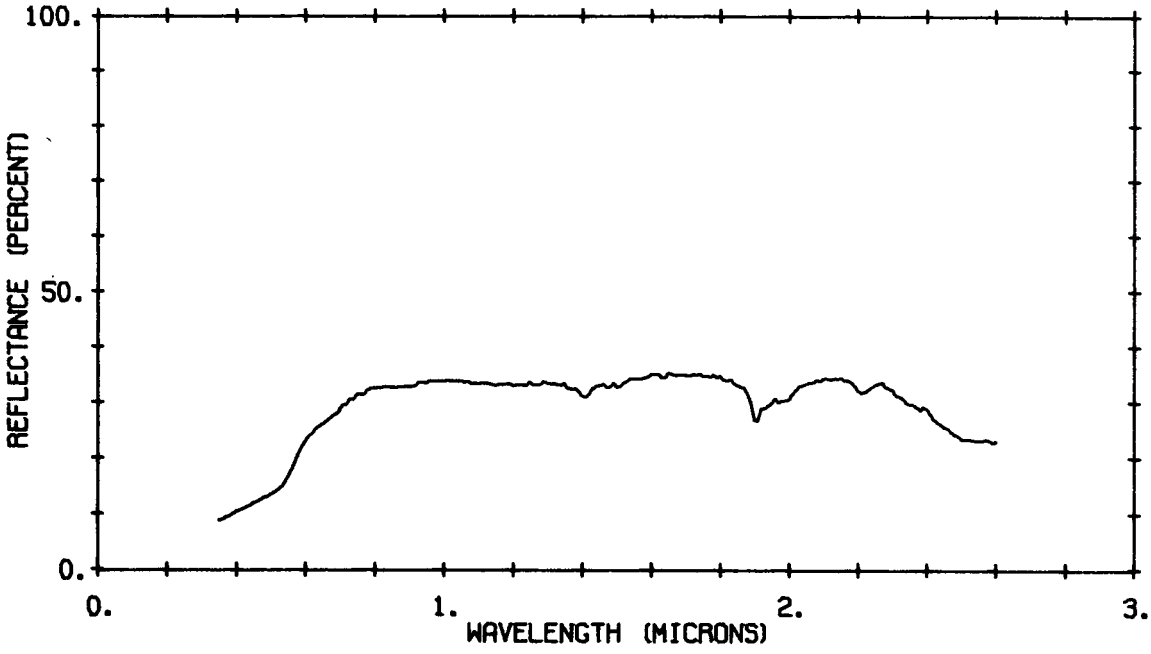

SAMPLE 1 COLOR: 5 YR 5/4

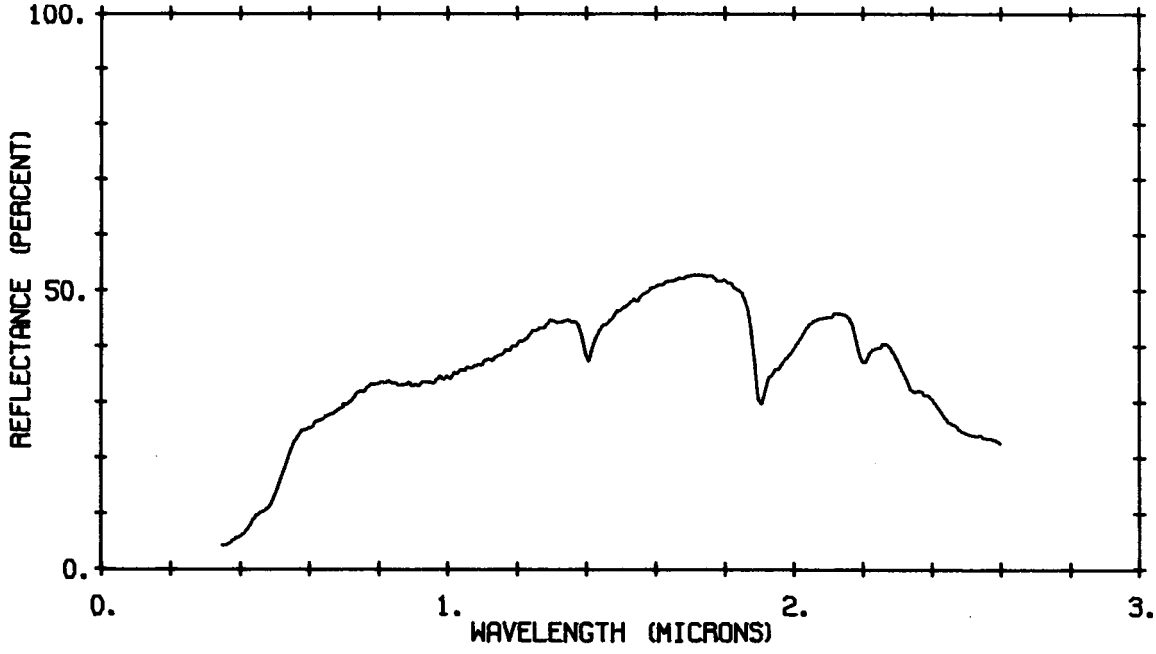

SAMPLE 4 COLOR: 2.5 Y 6/6

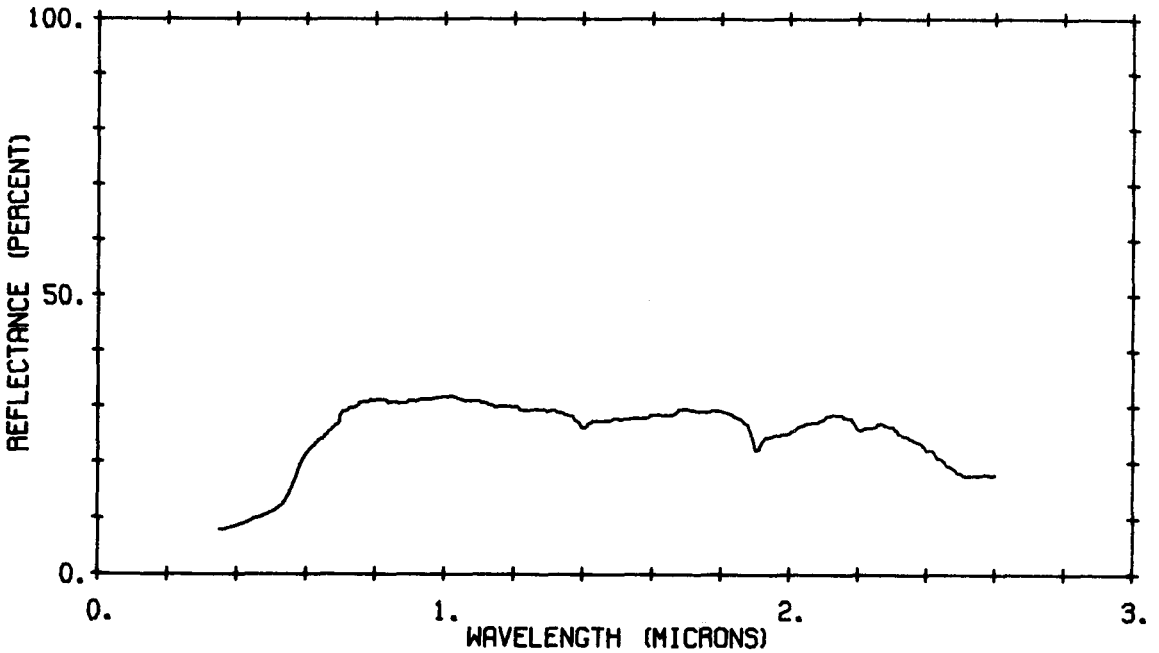

SAMPLE 12 COLOR: 5 YR 4/6

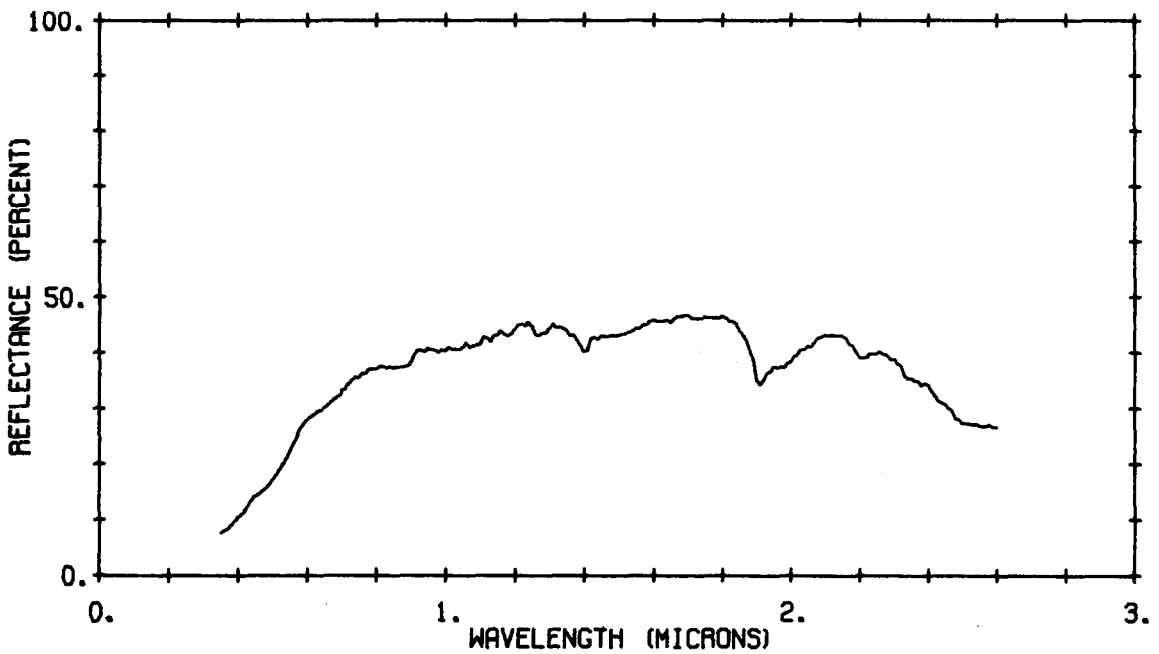

SAMPLE 14 COLOR: 10 YR 5/3.5

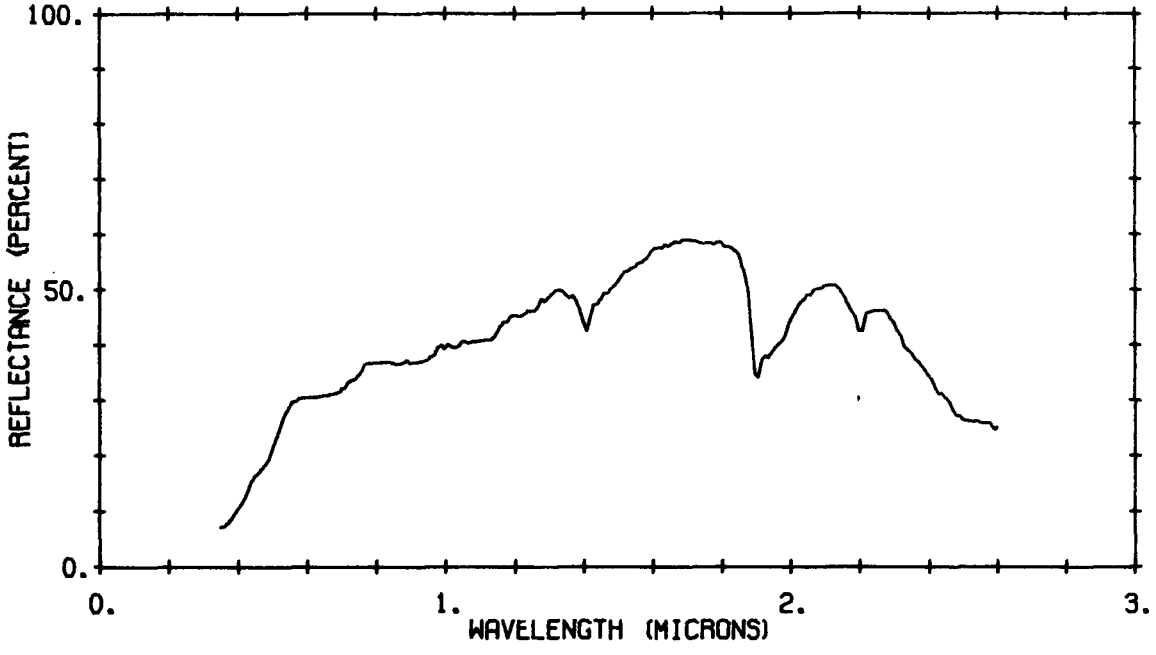

SAMPLE 15 COLOR: 5 Y 6/4

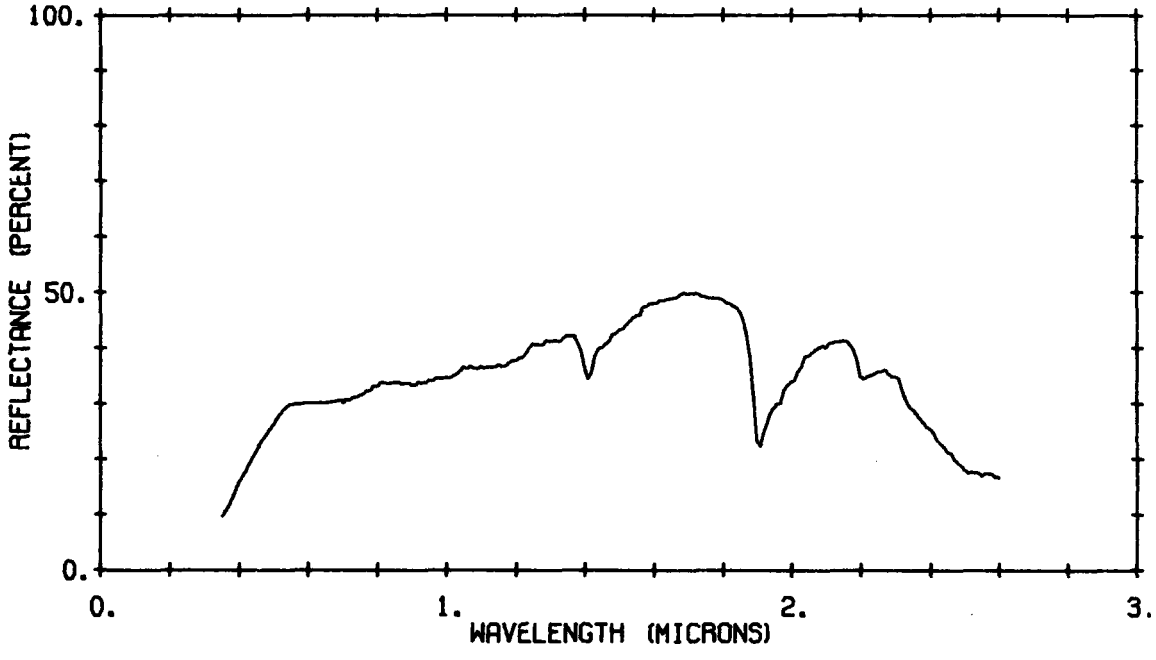

SAMPLE 25 COLOR: 5 GY 6/2

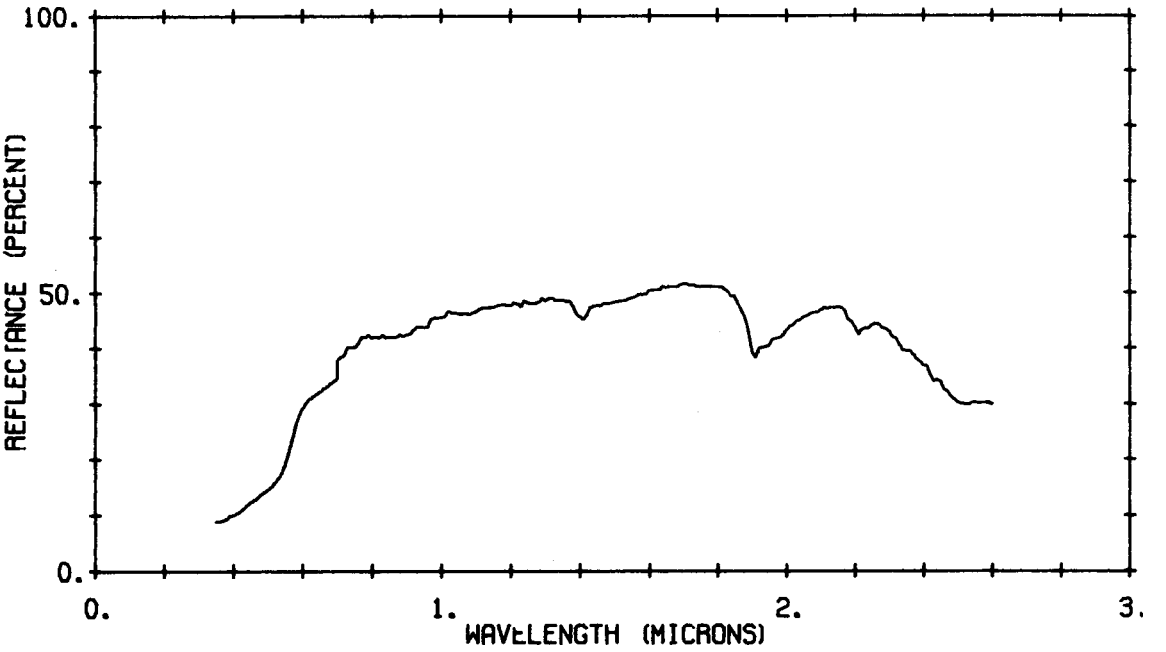

FIGURE. SAMPLE 31 COLOR: 5 YR 5/6

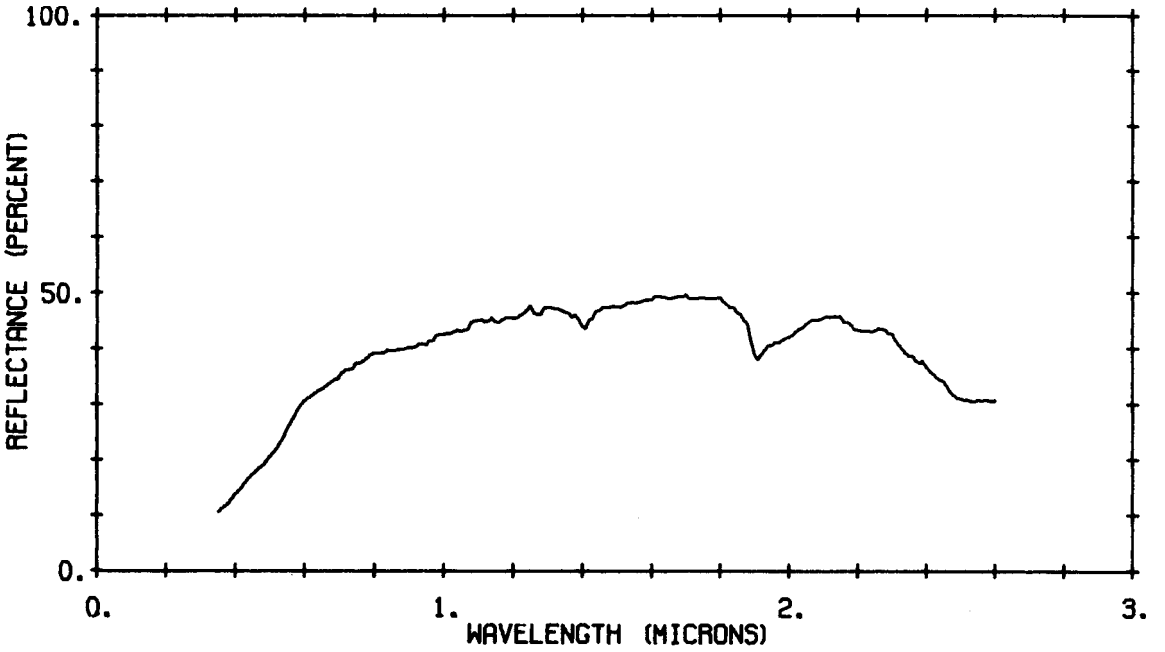

SAMPLE 32 COLOR: 10 YR 6/3

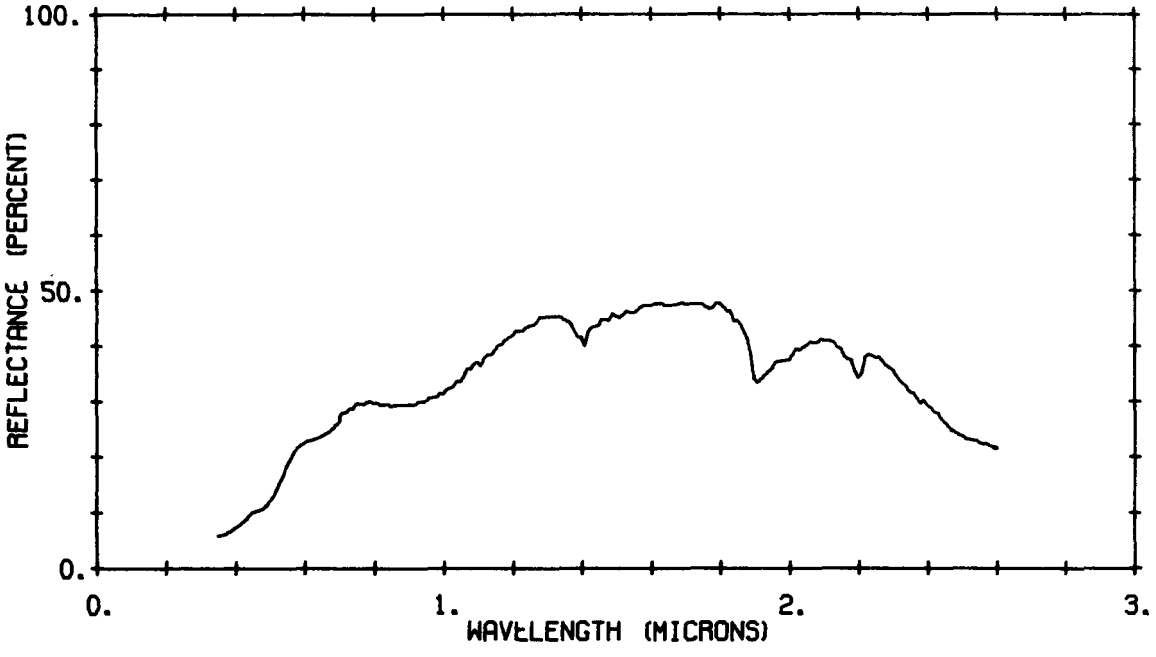

SAMPLE 33 COLOR: 10 YR 5/5

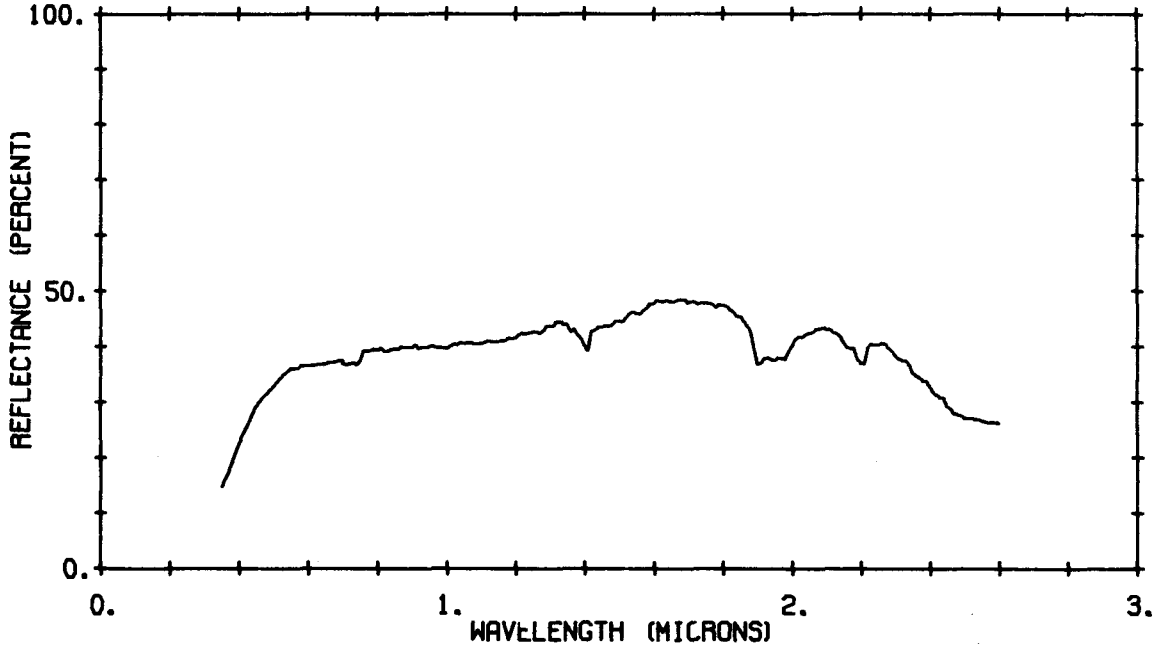

SAMPLE 34 COLOR: 5 GY 7/2

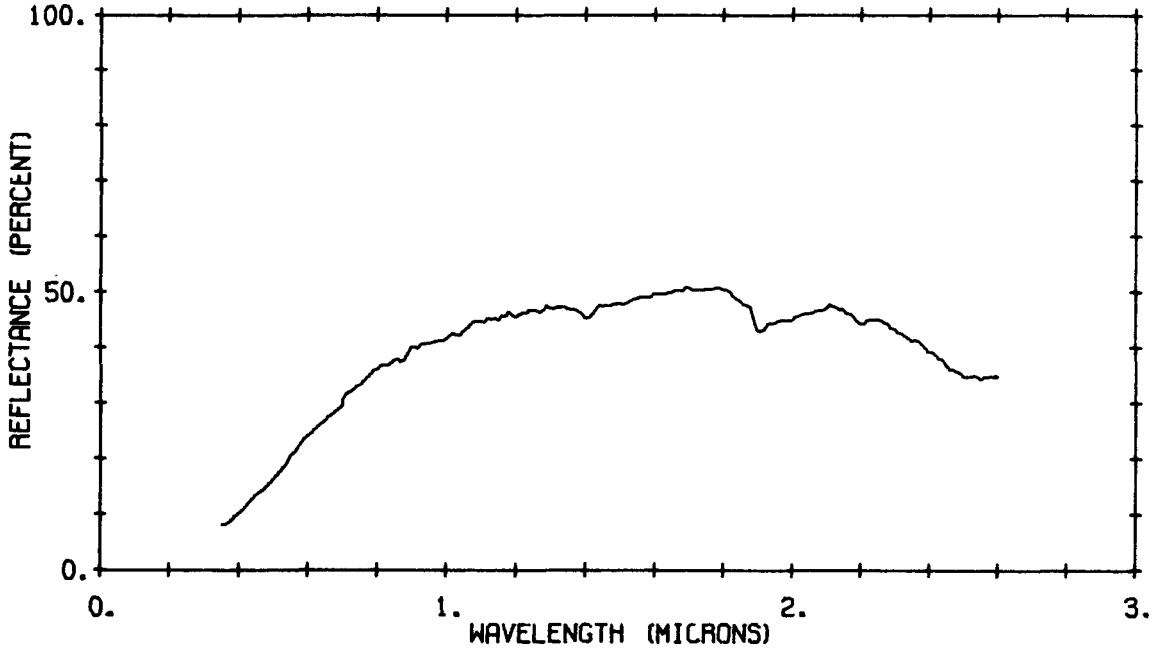

SAMPLE 41 COLOR: 10 YR 5/3

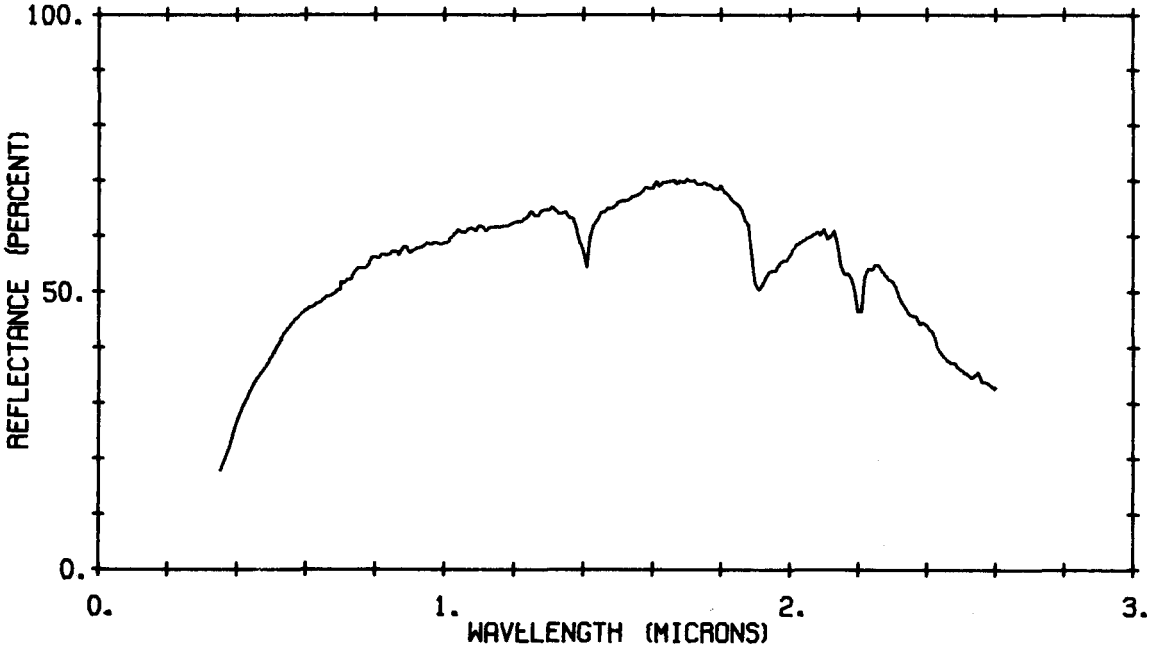

SAMPLE 45 COLOR: 2.5 Y 8/2

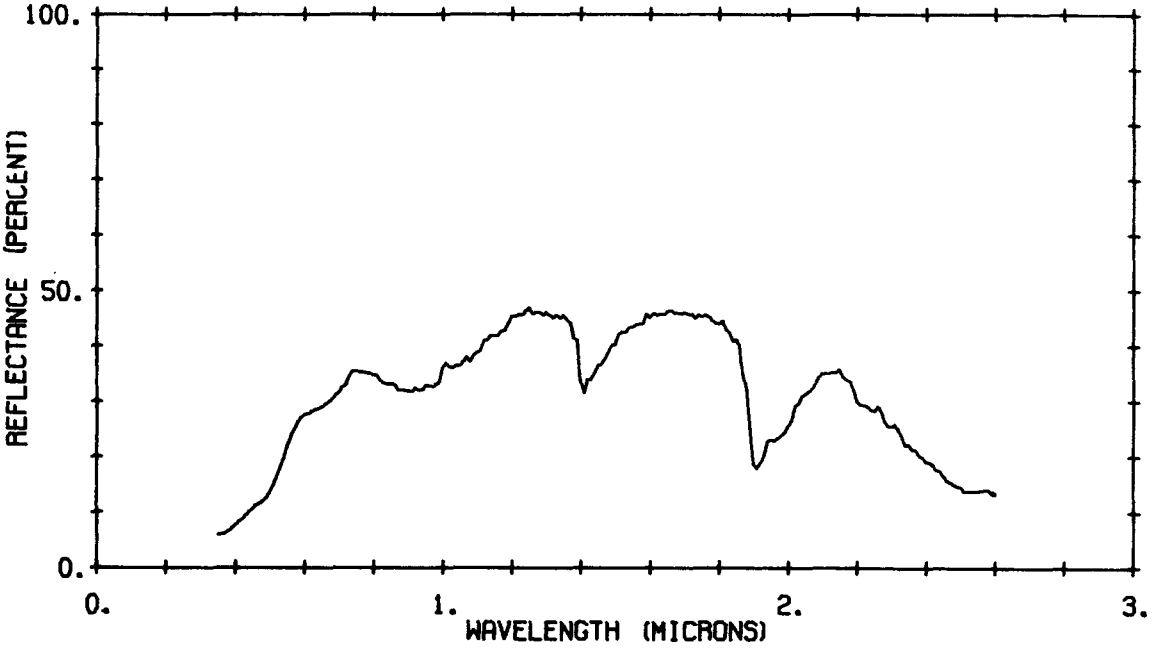

SAMPLE 61 COLOR: 10 YR 4/6

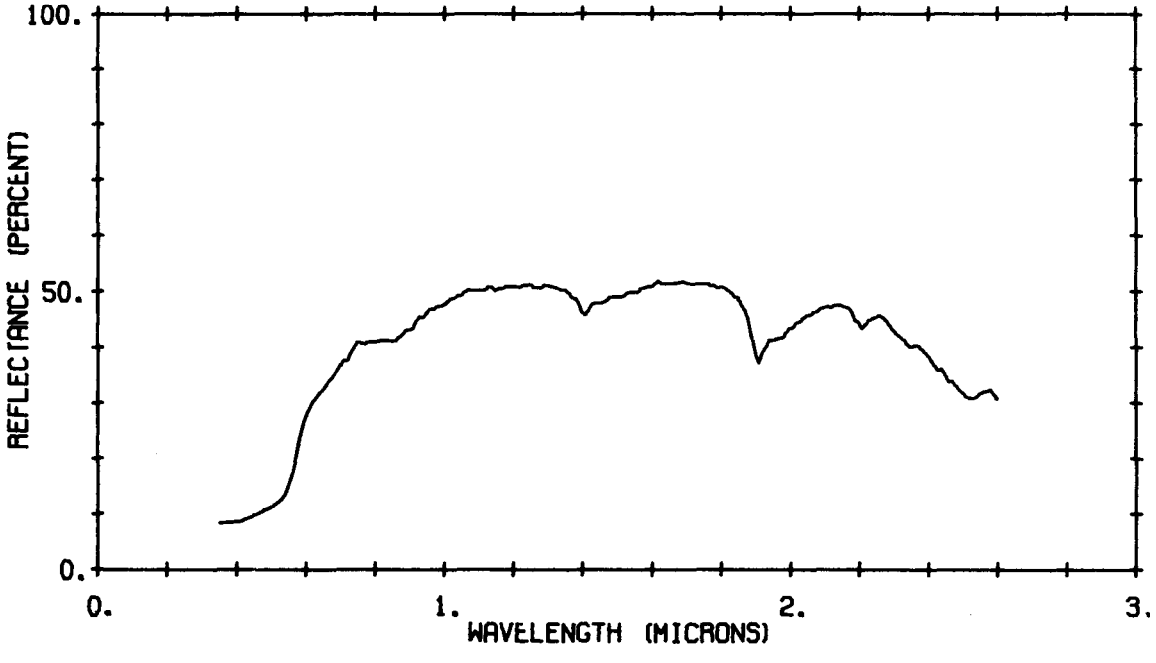

SAMPLE 63 COLOR: 2.5 YR 4.5/6

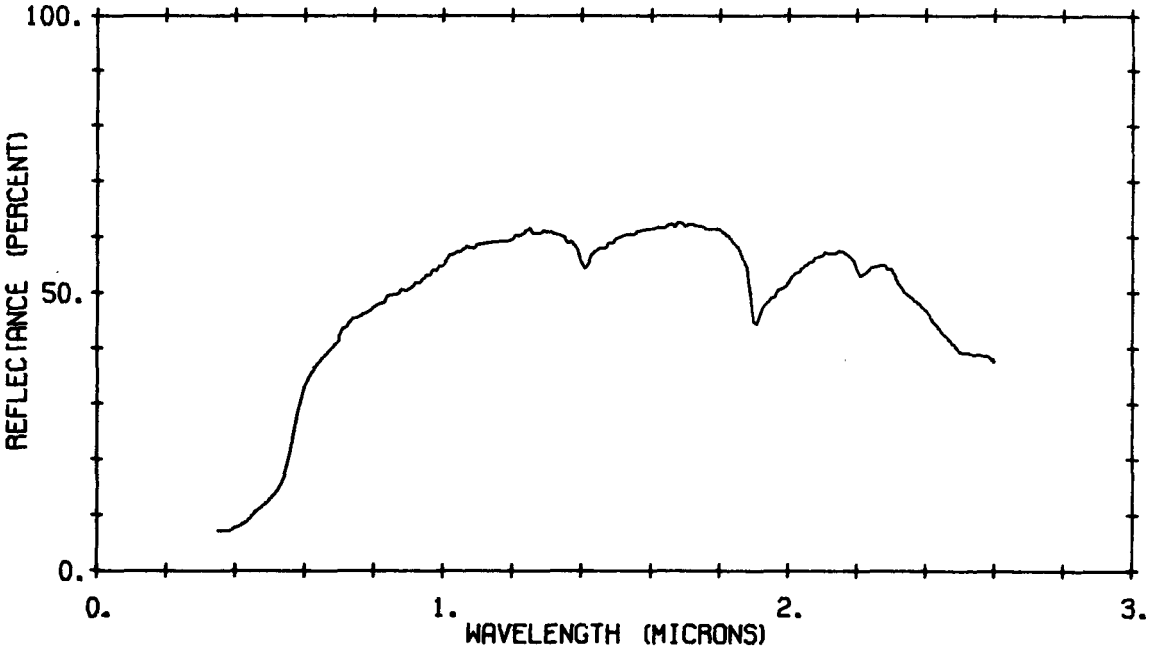

SAMPLE 64 COLOR: 5 YR 5.5/8

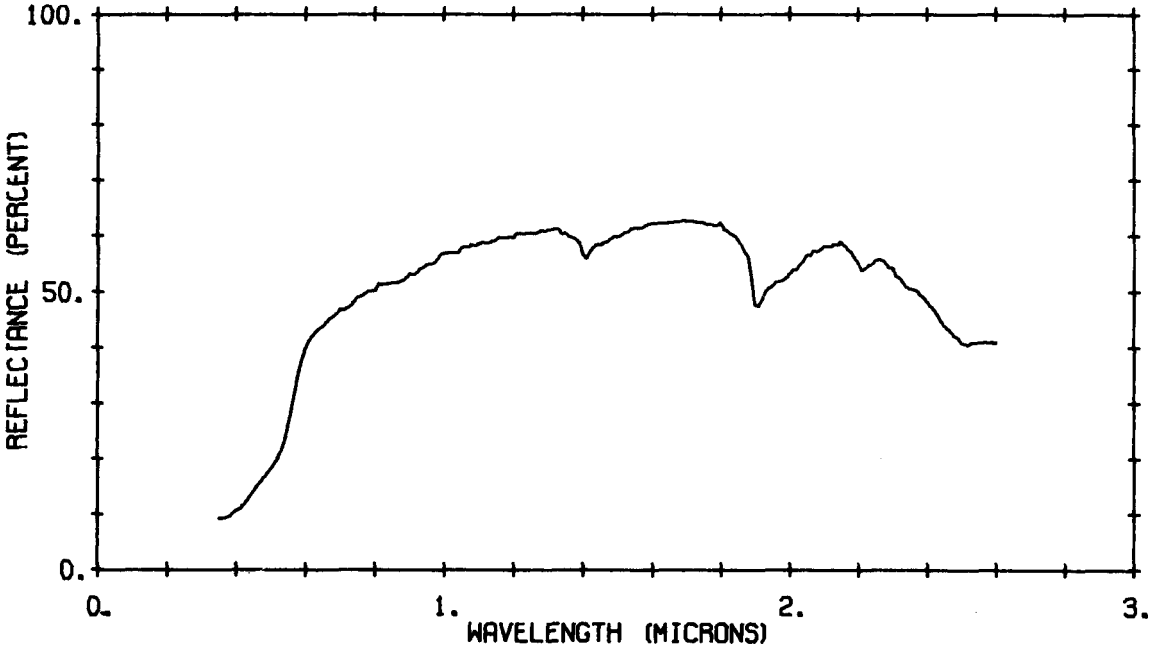

SAMPLE 66 COLOR: 5 YR 7/8

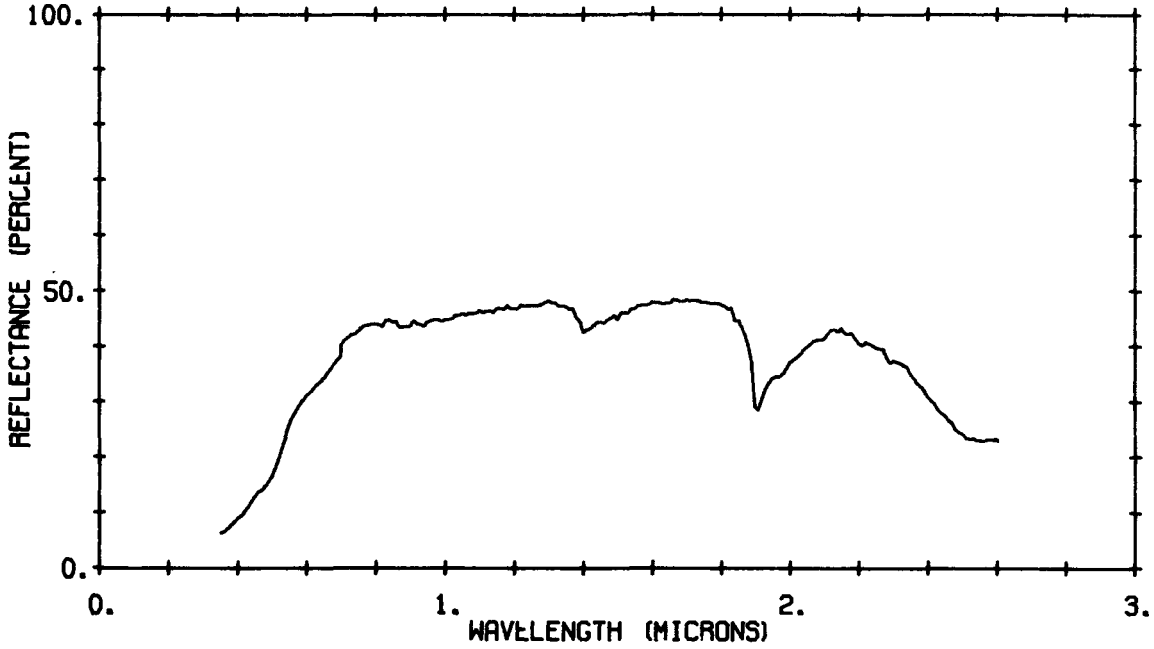

SAMPLE 69 COLOR: 10 YR 6/5.5

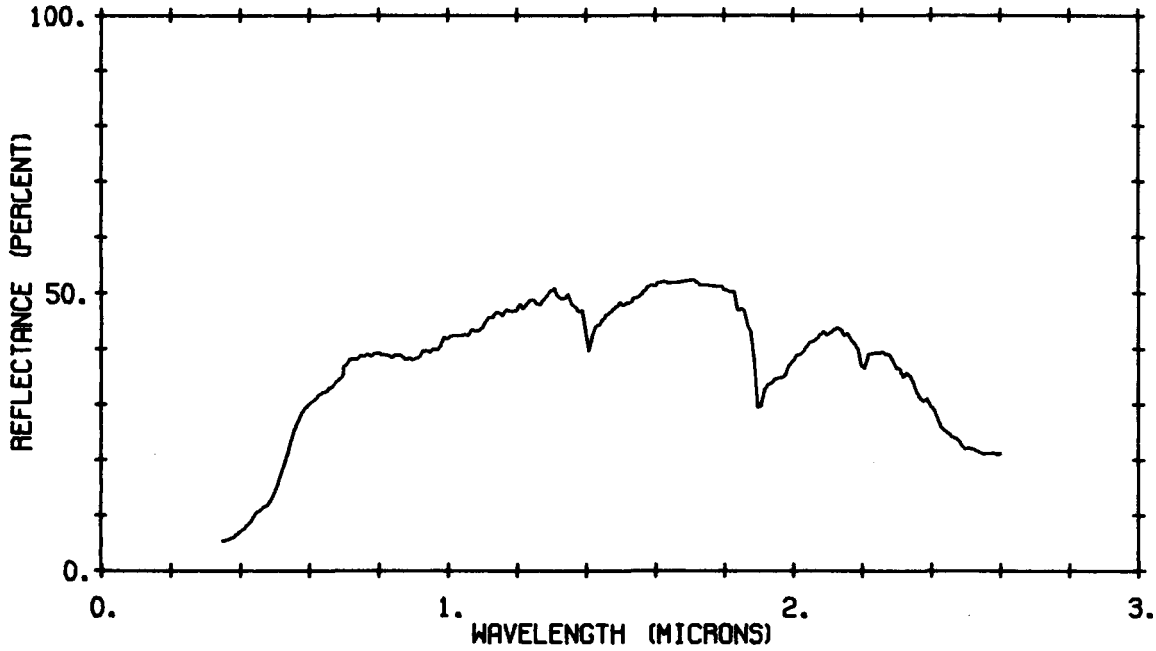

SAMPLE 70 COLOR: 10 YR 5/6

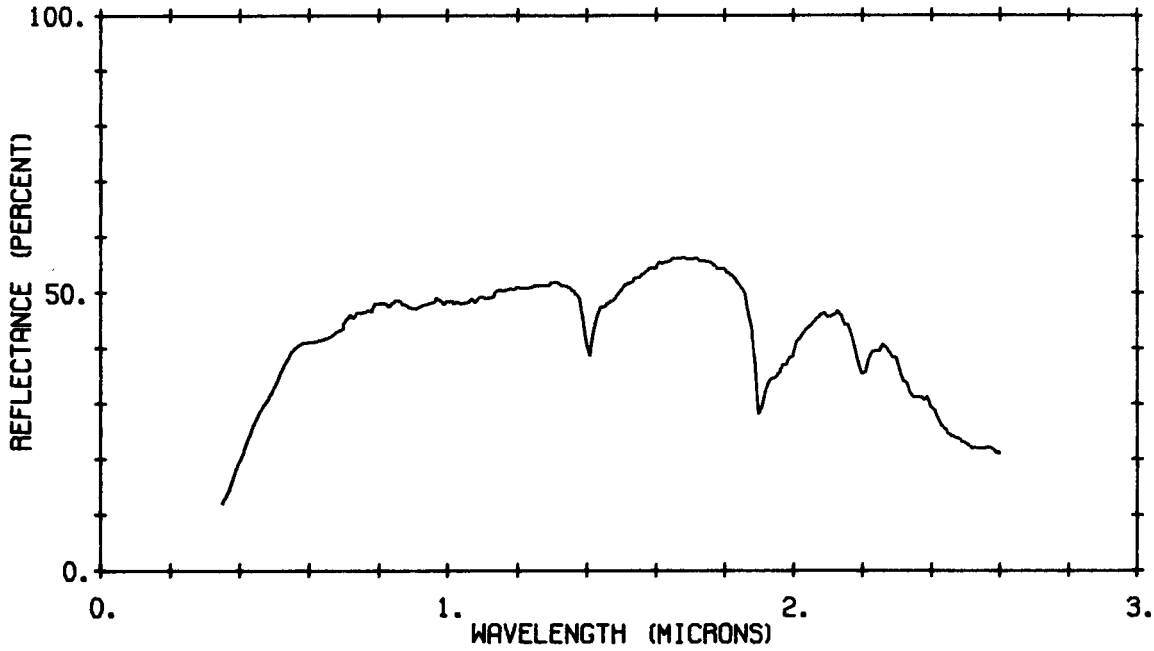

SAMPLE 72 COLOR: 5 Y 6/2

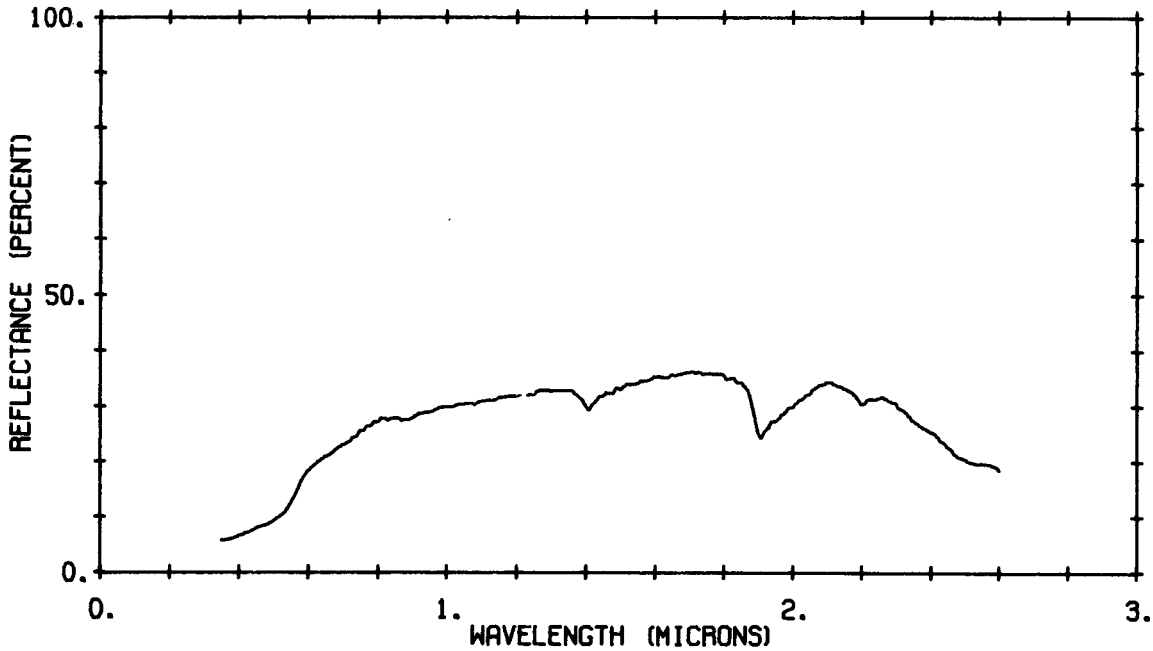

SAMPLE 73 COLOR: 5 YR 4/4

APPENDIX II

INDEX TO SAMPLE NUMBER AND MUNSELL COLOR FOR MATERIALS COLLECTED IN THE WIND RIVER BASIN, WYOMING, 1974

SAMPLE	COLOR	MEASURED
1	5 YR 5/4	*
2	5 Y 5/2	
3	5 Y 6/2	
4	2.5 Y 6/6	*
5	5 Y 6/2	
6	10 Y 5/2	
7	2.5 Y 6/4	
8	5 YR 5/3	
9	10 YR 5/4	
10	2.5 Y 5/2	
11	2.5 YR 3/6	
12	5 YR 4/6	*
13	10 YR 5/3.5	
14	10 YR 5/3.5	*
15	5 Y 6/4	*
16	10 YR 5/4	
17	5 YR 4/4	
18	10 YR 7/4	
19	5 YR 4/8	
20	10 YR 6/6	
21	7.5 YR 5/8	
22	5 Y 8/1	
23	2.5 Y 7/4	
24	7.5 YR 5/4	
25	5 GY 6/2	*
26	5 YR 5/1	
27	5 YR 6/2	
28	5 Y 6/1	
29	10 YR 6/6	
30	10 YR 6/4	
31	5 YR 5/6	*
32	10 YR 6/3	*
33	10 YR 5/5	*
34	5 GY 7/2	*
35	5 Y 4/1	
36	5 Y 7/5	
37	10 YR 6/3	
38	10 YR 6/6	
39	10 YR 5/3	
40	2.5 Y 7/6	

SAMPLE	COLOR	MEASURED
41	10 YR 5/3	*
42	10 YR 6/3	
43	2.5 Y 8/4	
44	2.5 Y 6/8	
45	2.5 Y 8/2	*
46	10 YR 5/2	
47	2.5 Y 7.5/2	
48	10 YR 4/2	
49	10 YR 4/2	
50	10 YR 6/4	
51	7.5 YR 6/4	
52	10 Y 5/3	
53	N 3	
54	2.5 Y 4/6	
55	5 Y 4/1	
56	10 Y 5/3	
57	2.5 YR 3/4	
58	10 YR 7/4	
59	10 YR 4/3	
60	5 Y 7/2	
61	10 YR 4/6	*
62	2.5 YR 5.5/6	
63	2.5 YR 4.5/6	*
64	5 YR 5.5/8	
65	5 YR 6.6/7	
66	5 YR 7/8	*
67	2.5 Y 4.5/4	
68	2.5 Y 6/2	
69	10 YR 6/5.5	*
70	10 YR 5/6	*
71	5 Y 7/2	
72	5 Y 6/2	*
73	5 YR 4/6	*

BIBLIOGRAPHY

Adams, J.B., 1974, Visible and near-infrared diffuse reflectance spectra of pyroxenes as applied to remote sensing of solid objects in the solar system, Journal of Geophysical Research, v. 79, no. 32, pp. 4829-4836.

Adler, H.H., 1970, Interpretation of colour relations in sandstone as a guide to uranium exploration and ore genesis, in Uranium Exploration Geology; Proceedings of a panel, I.A.E.A., Vienna, Austria, pp. 331-344.

Anderson, D.C., 1969, Uranium deposits of the Gas Hills, in Contributions to Geology, Wyoming uranium issue, v. 8, no. 2, pp. 93-103.

Armstrong, Frank C., 1970, Geologic factors controlling uranium resources in the Gas Hills District, Wyoming, in Wyoming Geological Association Guidebook-1970, Wyoming Sandstone Symposium, pp. 31-44.

Bowman, J., 1975, personal communication.

Bylinsky, G., 1975, ERTS puts the whole earth under a microscope, Fortune, February, pp. 116-130.

Charette, M.P., McCord, T.B., Pieters, C., and Adams, J.B., 1974, Application of remote spectral reflectance measurements to lunar geology classification and determination of titanium content of lunar soils, Journal of Geophysical Research, v. 79, no. 11, pp. 1605-1613.

Childers, M.O., 1970, Uranium geology of the Kaycee area, Johnson County, Wyoming, in Twenty Second Annual Field Conference - 1970, Wyoming Geological Association Guidebook, pp. 13-20.

Davis, J.F., 1969, Uranium deposits of the Powder River Basin, in Wyoming uranium issue: Wyoming Univ. Contr. Geology, v. 8, no. 2, pt. 1, p. 131-141.

Dillman, R.D. and Vincent, R.K., 1974, Unsupervised mapping of geologic features and soils in California, Proceedings of the Ninth International Symposium on Remote Sensing of Environment, the Environmental Research Institute of Michigan, Ann Arbor, pp. 2013-2025.

Germanov, A.N., 1960, Main genetic features of some infiltration-type hydrothermal uranium deposits (English translation): Akad. Nauk SSSR Izv. Ser. Geol., no. 8, p. 60-71.

Groth, F.A., 1970, New sandstone uranium deposit in the Battle Spring Formation, Lost Soldier - Green Mountain area, Sweetwater County, Wyoming, in Twenty Second Annual Field Conference - 1970, Wyoming Geological Association Guidebook, pp. 9-12.

Hellinger, T., 1971, unpublished paper.

High, L.R. and Picard, J.D., 1965, Sedimentary petrology and origin of analcime-rich Popo Agie Member, Chugwater (Tr) Formation, west-central Wyoming, Journal of Sedimentary Petrology, v. 35, pp. 49-70.

Houston, R.S., 1969, Aspects of the geologic history of Wyoming related to the formation of uranium deposits, in Contributions to Geology: Wyoming uranium issue, v. 8, no. 2, pp. 67-79.

Hunt, G.R. and Salisbury, J.W., 1970a, Visible and near-infrared spectra of minerals and rocks: I. Silicate minerals, Modern Geology, v. 1, no. 4, pp. 238-300.

Hunt, G.R. and Salisbury, J.W., 1970b, Visible and near-infrared spectra of minerals and rocks: II. Carbonates, Modern Geology, v. 2, pp. 23-30.

Hunt, G.R., Salisbury, J.W., and Lenhoff, C.J., 1971a, Visible and near-infrared spectra of minerals and rocks: III. Oxides and hydroxides, Modern Geology, v. 2, no. 3, pp. 195-205.

Hunt, G.R., Salisbury, J.W., and Lenhoff, C.J., 1971b, Visible and near-infrared spectra of minerals and rocks: IV. Sulfides and sulphates, Modern Geology, v. 3, pp. 1-14.

Hunt, G.R., Salisbury, J.W., and Lenhoff, C.J., 1972a, Visible and near-infrared spectra of minerals and rocks: V. Halides, phosphates, arsenates, vanadates and borates, Modern Geology, v. 3, pp. 121-132.

Hunt, G.R., Salisbury, J.W., and Lenhoff, C.J., 1973a, Visible and near-infrared spectra of minerals and rocks: VI. Additional silicates, Modern Geology, v. 4, pp. 85-106.

Hunt, G.R., Salisbury, J.W., and Lenhoff, C.J., 1973b, Visible and near-infrared spectra of minerals and rocks: VII. Acidic igneous rocks, Modern Geology, v. 4, pp. 217-224.

Hunt, G.R., Salisbury, J.W., and Lenhoff, C.J., 1973c, Visible and near-infrared spectra of minerals and rocks: VIII. Intermediate igneous rocks, Modern Geology, v. 4, pp. 237-244.

Hunt, G.R., Salisbury, J.W., and Lenhoff, C.J., 1974, Visible and near-infrared spectra of minerals and rocks: IX. Basic and ultrabasic igneous rocks, Modern Geology, v. 5, pp. 15-22.

Krishna Murti, G.S.R., and Satyanarayana, K.V.S., 1971, Influence of chemical characteristics in the development of soil colour, Geoderma, v. 5, pp. 243-248.

Leeman, V., Earing, D., Vincent, R.K., and Ladd, S., 1971, The NASA Earth Resources Spectral Information System: A Compilation, Report No. NASA CR-31650-24-T, Willow Run Laboratories of the Institute of Science and Technology, The University of Michigan, Ann Arbor.

Leeman, V., 1972, The NASA Earth Resources Spectral Information System: A Compilation, First Supplement, Report No. NASA-CR-WRL-31650-69-T, Willow Run Laboratories of the Institute of Science and Technology, The University of Michigan, Ann Arbor.

Love, J.D., 1954, Preliminary report on uranium in the Gas Hills area, Fremont and Natrona counties, Wyoming, U.S. Geological Survey Circular 352, 11 p.

Malila, W.A., Hieber, R.H., McCleer, A.P., 1973, Correlation of ERTS MSS data and earth coordinate systems, Report No. 193300-18-SA/J, for Purdue Conference on Machine Processing of Remotely Sensed Data, October 16-18, the Environmental Research Institute of Michigan, Ann Arbor, 14 p.

Mathews, H.L., 1972, Application of multispectral remote sensing and spectral reflectance patterns to soil survey research, The University of Pennsylvania, University Park, Ph.D. thesis.

Mathews, H.L., Cunningham, R.L., Cipra, J.E., and West, T.R., 1972, Application of multispectral remote sensing to soil survey research in southeastern Pennsylvania, Journal Series on Pennsylvania Agriculture Experimental Station, paper no. 4204, University Park, 16 p.

Mathews, H.L., Cunningham, R.L., and Petersen, G.W., 1973, Spectral reflectance of selected Pennsylvania soils, Soil Science Society of America Proceedings, v. 37, pp. 421-424.

Maugh, T.B., 1973, ERTS: Surveying earth's resources from space, Science, v. 180, 6 April, pp. 49-51.

Picard, M.D., 1965, Iron oxides and fine-grained rocks of Red Peak and Crow Mountain Sandstone Members, Chugwater (Triassic) Formation, Wyoming, Journal of Sedimentary Petrology, v. 35, no. 2, pp. 464-479.

Picard, M.D., 1967, Stratigraphy and depositional environments of the Red Peak Member of the Chugwater Formation (Triassic), west-central Wyoming, Wyoming University Contributions to Geology, v. 6, no. 1, pp. 39-67.

Piech, K.R. and Walker, J.E., 1974, Interpretation of soils, Photogrammetric Engineering, v. XL, pp. 84-94.

Pohn, H.A., 1974, Near-infrared reflectance anomalies of andesite and basalt in southern California and Nevada, Geology, v. 2, no. 11, pp. 547-550.

Reinhardt, E.V., 1952, Practical guides to uranium ores on the Colorado Plateau RMO-1027, U.S. Atomic Energy Commission Technical Information Service, Oak Ridge, Tennessee, 13 p.

Roadifer, R.E., 1957, Catalog of formation names for southwestern Wind River Basin, in Wyoming Geological Association Guidebook: Southwest Wind River Basin.

Rowan, L.C., 1972, Near infrared iron absorption bands: applications to geologic mapping and mineral exploration, Fourth Annual Earth Resources Program Review, v. III, sec. 60.

Rowan, L.C, Wetlaufer, P.H., Goetz, A.F.H., Billingsley, R.C., and Stewart, J.H., 1974, Discrimination of rock types and detection of hydrothermally altered areas in south-central Nevada by the use of computer-enhanced ERTS images, U.S.G.S. Professional Paper 883, 35 p.

Salisbury, J.W., and Hunt, G.R., 1974, Remote sensing of rock type in the visible and near-infrared, Proceedings of the Ninth International Symposium on Remote Sensing of Environment, The Environmental Research Institute of Michigan, Ann Arbor, pp. 1953-1958.

Salmon, B.C. and Vincent, R.K., 1974, Surface compositional mapping in the Wind River Range and Basin, Wyoming, by multispectral techniques applied to ERTS-1 data, Proceedings of the Ninth International Symposium on Remote Sensing of Environment, the Environmental Research Institute of Michigan, Ann Arbor, pp. 2005-2012.

Soister, P.E., 1968, Stratigraphy of the Wind River Formation in south-central Wind River Basin, Wyoming: U.S.G.S. Professional Paper 594-A, 50 p.

Thomson, F.J., 1973, ERIM Progress Report on Use of ERTS-1 Data, Summary of Ten Tasks, Type I, Report No. NASA-CR-ERIM 193300-24-L, Environmental Research Institute of Michigan, Ann Arbor.

Thomson, F.J., 1973, ERIM Progress Report on Use of ERTS-1 Data, Summary of Ten Tasks, Type II Progress Report, Report No. NASA-CR-133556, NTIS No. E73-10899/WR, Environmental Research Institute of Michigan, Ann Arbor.

Turner, R., Malila, W.A., and Nalepka, R.F., 1971, Importance of atmospheric scattering on remote sensing, or, everything you've wanted to know about remote sensing but were afraid to ask, Proceedings, Seventh International Symposium on Remote Sensing of Environment, Report No. 10259-1-X, Willow Run Laboratories of the Institute of Science and Technology, The University of Michigan, Ann Arbor.

Van Houten, F.B., 1965, Tertiary geology of the Beaver Rim area, Freemont and Natrona Counties, Wyoming: U.S. Geol. Survey Bull. 1164, 99 p.

Van Houten, F.B., 1969, Tertiary rocks of the southern Wind River Basin area, central Wyoming, Wyoming Geological Association Guidebook, pp. 79-88.

Vickers, R.C., 1957, Alteration of sandstone as a guide to uranium deposits and their origin, northern Black Hills, S. Dakota, Economic Geology, v. 52, no. 6, pp. 599-611.

Vincent, R.K. and Thomson, F.J. 1972, Spectral compositional imaging of silicate rocks, Journal of Geophysical Research, v. 77, no. 14, pp. 2465-2472.

Vincent, R.K., Thomson, F.J., and Watson, K., 1972, Recognition of exposed quartz sand and sandstone by two-channel infrared imagery, Journal of Geophysical Research, v. 77, no. 14, pp. 2473-2477.

Vincent, R.K., and Thomson, F.J., 1972, Rock-type discrimination from ratioed infrared scanner images of Pisgah Crater, California, Science, v. 175, pp. 986-988.

Vincent, R.K., 1972, An ERTS multispectral scanner experiment for mapping iron compounds, Proceedings Eighth International Symposium on Remote Sensing of Environment, Report No. 195600-1-X, Willow Run Laboratories of the Institute of Science and Technology, The University of Michigan, Ann Arbor, pp. 1239-1247.

Vincent, R.K., 1973, Mapping exposed silicate rock types and exposed ferric and ferrous compounds from a space platform, EREP investigation 444M, NASA, Houston, Texas.

Vincent, R.K., Wagner, T.W., Drake, B., and Jackson, P., 1973, Geologic reconnaissance and lithologic identification by remote sensing, Report No. 191700-8-F, Environmental Research Institute of Michigan, Ann Arbor.

Vincent, R.K., 1973, The NASA Earth Resources Spectral Information System: A compilation, second supplement, Report No. NASA-CR-ERIM-31650-156T, the Environmental Research Institute of Michigan, Ann Arbor.

Vincent, R.K., 1973, A thermal infrared ratio imaging method for mapping compositional variations among silicate rock types, Ph.D. Dissertation, Department of Geology and Mineralogy, The University of Michigan, Ann Arbor.

Vincent, R.K., 1974, New theoretical models and ratio imaging techniques associated with the NASA Earth Resources Spectral Information System, Technical Document 190100-30-T, the Environmental Institute of Michigan, Ann Arbor.

Vincent, R.K., Salmon, B.C., Pillars, W.W., and Harris, J.E., 1975, Surface compositional mapping by spectral ratioing of ERTS-1 MSS data in the Wind River Basin and Range, Wyoming, Report No. NASA CR-ERIM 193300-32-F, the Environmental Research Institute of Michigan, Ann Arbor, 73 p.

Vine, J.D., and Tourtelot, E.B., 1970, Preliminary geochemical and pertrographic analysis of Lower Eocene fluvial sandstones in the Rocky Mountain Region, in Wyoming Geologic Association Guidebook: Wyoming Sandstones Symposium, pp. 251-263.

Watson, R.D., 1972, Spectral reflectance and photometric properties of selected rocks, Remote Sensing of Environment, v. 2, pp. 95-100.